

UNIVERSIDADE FEDERAL DE MINAS GERAIS
PROGRAMA DE PÓS-GRADUAÇÃO EM FÍSICA

Sheilla de Oliveira Marques

Quantum Darwinism

BELO HORIZONTE
2020

Sheilla de Oliveira Marques

Quantum Darwinism

Tese apresentada ao Programa de Pós-Graduação em Física do Instituto de Ciências Exatas da Universidade Federal de Minas Gerais como requisito parcial para obtenção do título de Doutor em Física.

Supervisor: Rapahel Campos Drumond

Belo Horizonte

2020

Dados Internacionais de Catalogação na Publicação (CIP)

M357q Marques, Sheilla de Oliveira.
Quantum darwinism / Sheilla de Oliveira Marques. – 2020.
141f. : il.

Orientador: Raphael Campos Drumond.
Tese (doutorado) – Universidade Federal de Minas Gerais,
Departamento de Física.
Bibliografia: f. 88-97.

1. Sistemas quânticos. I. Título. II. Drumond, Raphael Campos. III.
Universidade Federal de Minas Gerais, Departamento de Física.

CDU – 530.145 (043)



UNIVERSIDADE FEDERAL DE MINAS GERAIS
Instituto de Ciências Exatas
Programa de Pós-Graduação em Física

ATA DA SESSÃO DE ARGUIÇÃO DA 372ª TESE DO PROGRAMA DE PÓS-GRADUAÇÃO EM FÍSICA, DEFENDIDA POR SHEILLA DE OLIVEIRA MARQUES orientada pelo professor Raphael Campos Drumond, para obtenção do grau de **DOUTORA EM CIÊNCIAS, área de concentração física**. Às 14:00 horas de vinte e sete de agosto de dois mil e vinte reuniu-se, por videoconferência, a Comissão Examinadora, composta pelos professores **Raphael Campos Drumond** (Orientador - Departamento de Matemática/UFMG), **Sebastião José Nascimento de Pádua** (Departamento de Física/UFMG), **Pedro Ernesto Schiavinatti Tavares** (Departamento de Física/UFMG), **Nadja Kolb Bernardes** (Departamento de Física /UFPE) e **Fernando da Rocha Vaz Bandeira de Melo** (Centro Brasileiro de Pesquisas Físicas) para dar cumprimento ao Artigo 37 do Regimento Geral da UFMG, submetendo a Mestra **SHEILLA DE OLIVEIRA MARQUES** à arguição de seu trabalho de Tese de Doutorado, que recebeu o título de "**Quantum Darwinism**". A candidata fez uma exposição oral de seu trabalho durante aproximadamente 50 minutos. Após esta, os membros da comissão prosseguiram com a sua arguição, e apresentaram seus pareceres individuais sobre o trabalho, concluindo pela aprovação da candidata.

Belo Horizonte, 27 de agosto de 2020.

Prof. Raphael Campos Drumond
Orientador da estudante
Departamento de Matemática/UFMG








Sebastião José Nascimento de Pádua
Departamento de Física/UFMG

Prof. Fernando da Rocha Vaz Bandeira de Melo
Centro Brasileiro de Pesquisas Físicas

Prof. Pedro Ernesto Schiavinatti Tavares
Departamento de Física/UFMG

Profa. Nadja Kolb Bernardes
Departamento de Física /UFPE

Candidata

	Documento assinado eletronicamente por Sheilla de Oliveira Marques, Usuário Externo , em 28/08/2020, às 15:43, conforme horário oficial de Brasília, com fundamento no art. 6º, § 1º, do Decreto nº 8.539, de 8 de outubro de 2015 .
	Documento assinado eletronicamente por Raphael Campos Drumond, Professor do Magistério Superior , em 28/08/2020, às 15:48, conforme horário oficial de Brasília, com fundamento no art. 6º, § 1º, do Decreto nº 8.539, de 8 de outubro de 2015 .
	Documento assinado eletronicamente por Pedro Ernesto Schiavinatti Tavares, Professor do Magistério Superior , em 28/08/2020, às 16:03, conforme horário oficial de Brasília, com fundamento no art. 6º, § 1º, do Decreto nº 8.539, de 8 de outubro de 2015 .
	Documento assinado eletronicamente por Fernando da Rocha Vaz Bandeira de Melo, Usuário Externo , em 28/08/2020, às 17:27, conforme horário oficial de Brasília, com fundamento no art. 6º, § 1º, do Decreto nº 8.539, de 8 de outubro de 2015 .
	Documento assinado eletronicamente por Nadja Kolb Bernardes, Usuário Externo , em 29/08/2020, às 12:03, conforme horário oficial de Brasília, com fundamento no art. 6º, § 1º, do Decreto nº 8.539, de 8 de outubro de 2015 .
	Documento assinado eletronicamente por Sebastião José Nascimento de Padua, Membro de comissão , em 29/08/2020, às 15:40, conforme horário oficial de Brasília, com fundamento no art. 6º, § 1º, do Decreto nº 8.539, de 8 de outubro de 2015 .
	A autenticidade deste documento pode ser conferida no site https://sei.ufmg.br/sei/controlador_externo.php?acao=documento_conferir&id_orgao_acesso_externo=0 , informando o código verificador 0234669 e o código CRC 268C4CFE .

Acknowledgements

First of all, I would like to thank my mother, Maria, for all she has done for my education. Even with a meager income, she prioritized my education, dedicating her entire life to it. I owe her all that I conquered. The second person I thank is my husband, that always supported me and never let me down. He does not just respect my choice but also is willing to go along with me anywhere I go. I thank my sister Linda for all her emotional support when I needed it; she is the best. I also thank my nephew Italo, who is like a brother to me, and I thank my aunt Maria Jose for being so kind.

I thank Dr. Ana Lucia, who is responsible for maintaining me sane and helping me on this long journey.

I would like to thank everyone in UFMG with who I had very nice times, including Roberto Baldijão, Arthur Matoso, Renan Cunha, Ana Paula Gomes, Alessandra Chioquetta, João Guilherme Conde, Liliane, Rafael Nunes, Leonardo Calazans, Ana Clara Sampaio, Danielle Cristina, Mateus Leal, Paulo and Wesley Valeriano.

I especially thank my friend and physicist researcher Cristiano Duarte. He always believed in me, even when I didn't. When I started my journey in quantum physics, I wouldn't know if I would be able to get a master's and a Ph.D., but Cris never let me down. He always helped me with my difficulties and formation deficiencies. He, thus, showed me that I could become a scientist and that I just needed to dedicate and fight for this.

I thank some amazing professors for their pleasant conversations and encouraging me, including Pedro Tavares, Carlos Monken, Jose Marcos, Paulo Sergio, Bismarck Costa, and Mario Mazone.

I want to thank my friends at OIST, whom I will never forget. They made me feel at home when I was on the other side of the world, especially Daniel Wong, Ratnesh Gupta, Chris Campbell, Sawako Koki, Friederike Metz, Muhammad Sirajul Hasan, and Jing Li.

I thank my closest friends, Priscila Romagnoli, Marcia Cristina, Natalia Moler, Paula D'Avila, Diego Leonardo, Sahar, and Luiza Daiane. Pri, thank you for all the support you gave me on OIST; you are my friend and loved sister. Marcia, your company is fantastic. I am happy to have you with me for all these years. Nati, we can fight like sisters, but I love you. Paulinha, all cups of tea we drank together improved my afternoons. Dieguinho, thank you for being that friend who always calms me, even in tough moments. Sahar is the most welcoming and kind person that I know; I can say that she also became my sister. Dada is my niece and friend; she is someone I can really rely on.

I thank the two best supervisors in this world, Raphael Drumond and Thomas Busch. Raphael accepted supervising me in a tough moment and has been with me since my master's. He always believed and encouraged me. Raphael is careful and attentive to all his students. He is a supervisor and a friend with whom I want to continue working in collaboration. Thomas Busch accepted me as a research intern student at OIST and supervised me for six months. He makes me feel like a real OIST and team Busch member. He supervised me during my internship at OIST and advised me until the end of my Ph.D. I can not forget Thomas Fogarty, who became a fantastic friend beyond co-supervising me on OIST.

I thank UFMG, CAPES, and CNPq for supporting my Ph.D., and I thank OIST for the opportunity of the research internship in 2019. More importantly, I thank each Brazilian citizen who maintains public universities like UFMG and the CAPES and CNPq institutions.

And, finally, I thank God. I cannot prove His existence, but it is fair to consider this possibility since I cannot even prove which quantum mechanics interpretation is correct (if there is one).

Resumo

Nesta tese, eu apresento meu trabalho de doutorado sobre Darwinismo quântico. É um projeto original que foi revisado por pares e aceito para publicação num jornal internacional respeitado. Nos primeiros capítulos eu introduzo os conceitos essenciais para entender Darwinismo quântico e nos dois últimos eu apresento meus trabalhos. O conceito de Darwinismo quântico foi construído para explicar uma possível transição do quântico para o clássico. Meus principais interesses são encontrar as implicações do Darwinismo quântico na dinâmica dos sistemas e encontrar modelo mais realistas onde ele se aplica. No primeiro trabalho eu estudei Darwinismo quântico em um sistema de muitos corpos composto por osciladores harmônicos quânticos em que os sub-ambientes não interagem e nem se correlacionam entre si. Por meio de cálculos numéricos e analíticos pudemos observar o Darwinismo quântico por meio de duas abordagens diferentes. Nós mostramos o Darwinismo quântico em um modelo pela abordagem BPH pela primeira vez. Além disso, em contraste com um trabalho publicado recentemente, nós mostramos que o Darwinismo quântico pode ser observado mesmo em system com um grau de não-Markovianidade alto e propusemos uma forma mais adequada para quantificá-lo. No segundo trabalho nós investigamos o Darwinismo quântico em um modelo mais realista em que os sub-ambientes podem ficar fortemente correlacionados. O modelo consiste de um átomo de dois níveis inserido em um ambiente fermiônico que foi usado para estudar a catástrofe de ortogonalidade. Como tanto a catástrofe de ortogonalidade quanto o Darwinismo quântico vem com o fenômeno de decoerência, nós estamos investigando se estes dois conceitos estão correlacionados. Além disso, nós escolhemos esse modelo porque ele pode ser mapeado no modelo bosônico de um gás de Tonks Girardeau tornando possível uma implementação experimental por meio de átomos frios. Estamos estudando esse modelo através de cálculos analíticos e numéricos. No penúltimo capítulo eu apresento o primeiro resultado e descrevo o que ainda está faltando nesse estudo.

Palavras-chave: darwinismo quântico; transição do quântico para o clássico; sistemas de muitos corpos; não-markovianidade; catástrofe de ortogonalidade; fundamentos de mecânica quântica; decoerência.

Abstract

In this thesis, I present my work during my Ph.D. in quantum Darwinism. It is a original project, which has been peer-reviewed and accepted for publication in a respected international journal. In the first chapters, I recalled the essential concepts to understand quantum Darwinism, and in the two last, I present my works. The quantum Darwinism concept was constructed to explain a possible quantum-to-classical transition. My main interests are to find the quantum Darwinism implications in the system's dynamics and to find more realistic models where it applies. The first work was finished and published while the second is still in progress. In the first model I studied quantum Darwinism in a many-body system of quantum harmonic oscillators where the subenvironments neither interact nor correlate between themselves. Through analytical and numerical calculations, we observed quantum Darwinism from two different approaches. We show quantum Darwinism through the BPH approach in a model for the first time. In contrast with a recently published work, we also show that quantum Darwinism can be observed even in a system with a high degree of non-Markovianity, and proposed a more suitable way to quantify it. In the second work, we investigate quantum Darwinism in a more realistic model where the subenvironments can become strongly correlated. The model consists of a two-level atom interacting with a fermionic environment and was used to study orthogonality catastrophe. As both orthogonality catastrophe and quantum Darwinism comes with decoherence, we are investigating if these two concepts are correlated. Beyond that, we chose this model because it can be mapped in a bosonic model of the Tonks-Girardeau gas enabling an experimental implementation with cold atoms. We are performing numerical and analytical calculations in this work. In the sixth chapter, I present the first result and describe what is missing.

Keywords: quantum Darwinism; quantum-to-classic transition; many-body systems; non-Markovianity; orthogonality catastrophe; foundations of quantum mechanics; decoherence.

Contents

1	INTRODUCTION	13
2	OPEN QUANTUM SYSTEMS	14
2.1	Closed and Open Systems	14
2.1.1	Closed Quantum Systems	15
2.1.2	Open Quantum Systems	16
2.2	Decoherence	17
2.2.1	Quantum Decoherence Formalism	18
2.2.2	Environment-induced superselection	19
2.3	The Quantum-to-Classic Transition	21
2.3.1	The Measurement Problem	22
2.3.2	Decoherence in the Reduced Density Matrix of the System	23
3	QUANTUM DARWINISM	25
3.1	From Decoherence to Quantum Darwinism	25
3.2	The preferential Observable	26
3.3	Objectivity and Quantum Darwinism	27
3.4	Partial Information Plot Approach	28
3.5	BHP Approach	30
3.6	Exemplifying and comparing BPH and PIP approaches	32
3.7	Quantum Darwinism Examples	35
3.7.1	Quantum Darwinism in Quantum Brownian Motion	35
3.7.2	Quantum Darwinism in a Spin Model	38
4	MARKOVIAN AND NON-MARKOVIAN DYNAMICS	42
4.1	Markovianity in classical processes	42
4.1.1	Formal Definition	42
4.1.2	Divisibility Property	43
4.1.3	Kolmogorov Distance	45
4.2	Quantum Markov processes	46
4.2.1	Divisibility of Quantum Maps	46
4.2.2	Memoryless and Contractive properties in Quantum Markovian Processes	48
4.3	Quantification and detection of non-Markovianity	49
4.3.1	Quantification Via Quantum Maps	50
4.3.2	Detection Via Quantum Witness	52
4.3.3	Witnesses of Local Completely Positive Maps	52

4.4	Trace Distance and Fidelity	53
4.4.1	the BLP Quantifier	53
4.4.2	Fidelity	54
5	QUANTUM DARWINISM AND NON-MARKOVIANITY	56
5.1	Quantifying Quantum Darwinism Through the Non-Monotonicity of f_δ	56
5.2	Quantum Darwinism and non-Markovianity in a Model of Quantum Harmonic Oscillators	60
5.2.1	The Model	61
5.2.2	Model Dynamics	64
5.2.3	The preferential observable	65
5.2.4	Quantum Darwinism from PIP Approach	67
5.2.5	Quantum Darwinism from BPH Approach	71
5.2.6	Non-Markovianity degree in this model	73
5.2.7	Quantum Darwinism and Non-Markovianity	74
6	QUANTUM DARWINISM IN ULTRACOLD GASES	77
6.1	Anderson Orthogonality Catastrophe	78
6.2	Orthogonality Catastrophe in Ultracold Fermi Gases	79
6.2.1	The model	79
6.2.2	Overlaps	80
6.2.3	Orthogonality Catastrophe and Entanglement	82
6.2.4	Tonks-Girardeau Gas	83
6.3	Quantum Darwinism in a Fermi sea	85
6.3.1	Preliminary Results	85
6.4	Quantum Darwinism in Ultracold Atoms	86
7	CONCLUSIONS AND FUTURE PERSPECTIVES	87
7.1	Quantum Darwinism and Non-Markovianity	87
7.2	Quantum Darwinism in Ultracold Gases	87
7.3	Future Perspectives	88
	BIBLIOGRAPHY	89
	APPENDIX	99
	APPENDIX A – THE FOUNDATIONS OF QUANTUM MECHANICS	100
A.1	Linear Algebra and some Quantum Notation	101

A.1.1	Vectors	101
A.1.2	Basis	101
A.1.3	Linear Operators	102
A.1.4	Inner Products, Outer Products, and Tensor Products	102
A.1.5	Eigenvectors and Eigenvalues	103
A.1.6	Eigenspaces	103
A.2	Quantum states and Their Evolution	103
A.3	Measurement of Quantum systems	105
A.3.1	Projective Measurements	106
A.4	Composite Systems	109
A.5	Density Matrix	110
A.5.1	Density Matrix Properties	112
A.5.2	Composite Systems and Reduced Density Matrix	114
APPENDIX B – SOME FUNDAMENTAL CONCEPTS OF QUAN-		
TUM MECHANICS		116
B.1	Uncertainty Principle	116
B.1.1	Average Value and Standard Deviation	116
B.1.2	Heisenberg Uncertainty Principle	117
B.2	Coherent states	119
B.2.1	Quantum Harmonic Oscillators	119
B.2.2	Radiation of a Classical Current	121
B.2.3	Coherent States of Quantum Harmonic Oscillator	122
B.2.4	Properties of Coherent states	124
B.3	Angular Momentum	126
B.3.1	Orbital Angular Momentum	127
B.3.2	Spin Angular Momentum	128
B.3.3	Spin 1/2	128
B.3.4	Addiction of Spin Angular Momentum	129
B.4	Identical Particles	130
B.4.1	Different State Vectors Associated to a Same Physical State	131
B.4.2	Symmetric and Antisymmetric Wave Functions	132
B.4.3	Symmetry of Bosons and Fermions	133
APPENDIX C – DYNAMICS OF A MANY-BODY QUANTUM		
HARMONIC OSCILLATORS IN COHERENT STATES		134
C.1	Constant Coupling	136
C.2	Non-Constant coupling: γ and $\bar{\gamma}$	137

APPENDIX D – MANY-BODY ENVIRONMENT AS A TWO LEVEL SYSTEM	140
---	-----

1 Introduction

The concept of quantum Darwinism was introduced and popularized by W. Zurek to investigate and explain a possible emergence of the classical world from the quantum world by studying the open quantum systems dynamics. Since the beginning of the formulation of quantum mechanics, such emergence has been discussed. Schrödinger [1–3], Heisenberg [4], and Borh [5,6] already opened this discussion (see also [7]).

Conceptually, quantum states are quite different from classical states. Classical states are objective and deterministic, which means that, for example, we can predict with arbitrarily small uncertainty the position and linear momentum of a particle. However, as is well known in quantum mechanics, due to the Heisenberg uncertainty principle, there is a trade-off between the uncertainties associated with position and momentum: if we can predict very well one of them, the other one is necessarily uncertain (see Appendix B). Another peculiarity is the possibility of superposition states; even though some quantum states may have an apparently intuitive meaning, like the state of a particle in a definite position in space, one can have a superposition of such states for different positions (see Appendix A.2). These particularities make quantum phenomena considerably counterintuitive, making it crucial to understand their foundations as much as possible.

In this thesis, we describe quantum Darwinism from the foundations of quantum mechanics and investigate its connection with two other concepts: non-Markovianity and orthogonality catastrophe. In the first work, we study quantum Darwinism in a model where several quantum harmonic oscillators make the system and environment, and the system dynamics can be controlled to be Markovian or not. In contrast with a recent result in literature, we show that the non-Markovianity degree does not hinder the quantum Darwinism in this model. We also introduce a more suitable quantifier of quantum Darwinism in Markovian and non-Markovian systems. The second work is still in progress, and we are studying quantum Darwinism in a more realistic model where the environment is highly correlated. We are also investigating if there is some relation between quantum Darwinism and orthogonality catastrophe.

In Chap. 2, we present the concept of quantum-to-classical transition from decoherence in open quantum systems. This gives us the necessary tools to introduce the concept of quantum Darwinism in Chap. 3. In Chap. 4, we introduce the quantum Markovianity and non-Markovianity from an approach that allows us to trace a classical counterpart. In chapter 5, we present our work of quantum Darwinism in quantum Harmonic oscillators. Finally, in Chap. 6 we introduce the concept of orthogonality catastrophe and present our first results of quantum Darwinism in a model with a strongly correlated environment.

2 Open Quantum systems

Usually, textbooks introduce quantum theory by analyzing closed systems. This is the most intuitive way since the postulates were constructed from closed quantum systems. However, we must consider quantum systems interacting with their surroundings to understand nature. Strictly speaking, the only perfectly closed system in nature is the whole universe; any other system interacts at some level with the environment in which it is inserted. At some level, any (sub)system inside the universe is an *open quantum system*.

From the most fundamental studies of quantum mechanics to technological applications, it is essential to understand the dynamics of open quantum systems. For example, an open quantum system can lose coherence when it interacts with its environment (or other systems); then, this interaction directly affects its evolution. Also, during a measurement process, the system is never closed; it interacts directly with the measurement apparatus [8]. Another example is quantum information processing studies where, for the best conditions, the quantum system must be as closed as possible. In this case, one can consider that the interaction of the system with its environment results in undesirable *noises*. Such noises can frequently be understood and controlled through the open quantum system dynamics [9–11].

In Sec. 2.1, we shall recall the concepts of closed and open physical systems in classical and quantum mechanics. The interaction between an open quantum system and its environment can come with a sharing of information between them. Sec. 2.2 introduces the concept of decoherence that gives an intuition of how the system and environment can exchange information. Finally, in Sec. 2.3, we introduce the old discussion about the quantum-to-classic transition and trace a possible connection with decoherence.

2.1 Closed and Open Systems

If a physical system does not interact with any other system, one can say that it is closed, which means that the system's dynamics depend on itself only, and nothing else can disturb it. For example, consider a classical pendulum under only conservative forces. If it starts moving due to an instantaneous external action, its movement continues until other external force ceases. In this case, the system is closed since no external system interferes with its dynamics. However, if the pendulum interacts with an external damping force, its movement will be affected and can cease, meaning that this system is open.

As in the classical world, the quantum system also can be defined as open or closed. The dynamics of an open quantum system will depend on its interaction with the

environment, and its description is essential to several areas of quantum mechanics. Let us briefly recall the dynamics of closed quantum systems to better understand open quantum systems.

2.1.1 Closed Quantum Systems

A pure quantum state subjected to some Hamiltonian $H(t)$ can be represented by a state vector $|\psi(t)\rangle$ and it evolves in time according to Schrödinger's equation,

$$i\hbar \frac{d}{dt} |\psi(t)\rangle = H(t) |\psi(t)\rangle. \quad (2.1)$$

The solution of Schrödinger's equation can be formulated in terms of a time-evolution unitary operator $U(t, t_0)$ such that

$$|\psi(t)\rangle = U(t, t_0) |\psi(t_0)\rangle.$$

Therefore, defining $\hbar = 1$, Eq.(2.1) can be rewritten as,

$$i\hbar \frac{d}{dt} U(t, t_0) = H(t)U(t, t_0). \quad (2.2)$$

For a time-independent Hamiltonian H with initial condition $U(t_0, t_0) = I$ we get the expression

$$U(t, t_0) = \exp[-iH(t - t_0)], \quad (2.3)$$

see Appendix. A.2.

In some cases, the system's state can not be characterized as a single state vector but as a collection of pure states $|\psi_i(t)\rangle$, where the index i is associated with a probability p_i . Such *mixed states* may be described through the density operator (or density matrix) ρ defined as

$$\rho(t) = \sum_i p_i |\psi_i(t)\rangle \langle \psi_i(t)|, \quad (2.4)$$

see Appendix. A.4. Each state $|\psi_i(t)\rangle$ evolves according to the Schrödinger equation. Then, the time evolution density matrix of closed systems is also described by a unitary operator $U(t, t_0)$,

$$\begin{aligned} \rho(t) &= \sum_i p_i U(t, t_0) |\psi_i(t_0)\rangle \langle \psi_i(t_0)| U^\dagger(t, t_0) \\ &= U(t, t_0) \rho(t_0) U^\dagger(t, t_0). \end{aligned} \quad (2.5)$$

Differentiating Eq. (2.5) and using Eq. (2.2) we get the *Liouville-von Neumann equation*

$$\frac{d}{dt} \rho(t) = -i [H(t), \rho(t)], \quad (2.6)$$

that can be written as

$$\frac{d}{dt} \rho(t) = \mathcal{L} \rho(t), \quad (2.7)$$

where \mathcal{L} is the Liouville operator that is defined as

$$\mathcal{L}\rho(t) = i[H(t), \rho(t)]. \quad (2.8)$$

Then, similarly to the pure state differential equation, $\rho(t)$ is given by

$$\rho(t) = \exp[\mathcal{L}(t - t_0)]\rho(t_0) \quad (2.9)$$

for a time-independent Hamiltonian.

2.1.2 Open Quantum Systems

Here we will focus on cases where an open quantum system interacts with its surroundings. The interaction between the system S and its environment E leads to the emergence of correlations between them. Once these correlations are created, the system's dynamics can no longer be described by a unitary operator. The system description for some time instant can be made by its *reduced state*, which results from the partial trace of the environment over the global system.

The Hilbert space of the system \mathcal{H}_S and the Hilbert space of the environment \mathcal{H}_E compose the Hilbert space of the global system that can be defined as

$$\mathcal{H} = \mathcal{H}_S \otimes \mathcal{H}_E. \quad (2.10)$$

The total Hamiltonian may be described as

$$H(t) = H_S \otimes I_E + I_S \otimes H_E + H_I(t), \quad (2.11)$$

where H_S is the free Hamiltonian of the system, H_E is the free Hamiltonian of the environment, and $H_I(t)$ is the Hamiltonian of the interaction between the system and the environment.

In the case of multipartite quantum systems, observables related to some specific part acts just in the Hilbert space of this part. For example, consider a global system composed of a system S , an environment E , and an observable $A_S \otimes I_E$ that acts only in the system. The operator A_S acts in the Hilbert space of the system, \mathcal{H}_S , while an identity acts in the environment subspace, \mathcal{H}_E . Therefore, the expectation value of the observable A is given by

$$\langle A \rangle = \text{tr}_S \{A (\text{tr}_E \rho)\}, \quad (2.12)$$

where ρ is the density matrix of the global system. The analysis is analogous to an observable that acts just on the environment, and the expectation value of some observable B of the environment is

$$\langle B \rangle = \text{tr}_E \{B (\text{tr}_S \rho)\}. \quad (2.13)$$

Even if the global system $S + E$ is closed and a unitary operator can describe its whole dynamics, the dynamics of the reduced systems do not follow a unitary evolution. The time evolution of any reduced state X that composes a global system $X + Y$ can be obtained from the Liouville-von Neumann equation (2.6)

$$\begin{aligned} \mathrm{tr}_Y \left[\frac{d}{dt} \rho(t) \right] &= \mathrm{tr}_Y [-i [H(t), \rho(t)]] \\ \frac{d}{dt} \rho_X(t) &= -i \mathrm{tr}_Y [H(t), \rho(t)]. \end{aligned} \quad (2.14)$$

There are several relevant differential equations for reduced density matrices that describe approximately open systems, such as the *Markovian master equation* and the *generalized master equation* [8]. However, in the models explored in this thesis (Chaps. 5 and 6), we can afford to describe the complete dynamics of both the system and the environment.

2.2 Decoherence

Some interactions allow the environment to acquire information about the open quantum system. In this case, the environment behaves as a measurement apparatus. This process creates correlations between the system and the environment, enabling the environment to keep information about the system. By observing the evolution of the density matrix, it is noticeable that the superposition of the system's states vanishes, and for some basis, the system loses coherence. This phenomenon is known as *decoherence*. Through decoherence, it is possible to understand why *non-classical states* are so fragile. Decoherence describes how the entanglement between the system and the environment singles out a specific set of quantum states and excludes other fragile states like the Schrödinger cat states [12]. In Sec. 3.4, we specify this information and how to measure it. For a while, we will treat it generically.

In the early '70s, studies of quantum-to-classical transition and *the measurement problem* by Zeh [13] were used as a basis for the theory of quantum decoherence. In the '80s, Refs [14] and [15] show how the environment can select some system states and destroy its superposition states. From this, it was possible to connect decoherence with the quantum-to-classical transition (see Ref [16]). The loss of coherence of an open quantum system induced by its environment has been widely studied for the last fifty years or so, so there is currently extensive literature about it [17–19].

The decoherence theory applies from the fundamental studies of quantum mechanics to the technological applications of quantum information. Superposition states that are at the core of quantum information processing can be strongly affected by decoherence. Thus, designs for quantum computing need to take decoherence into account. Experimental

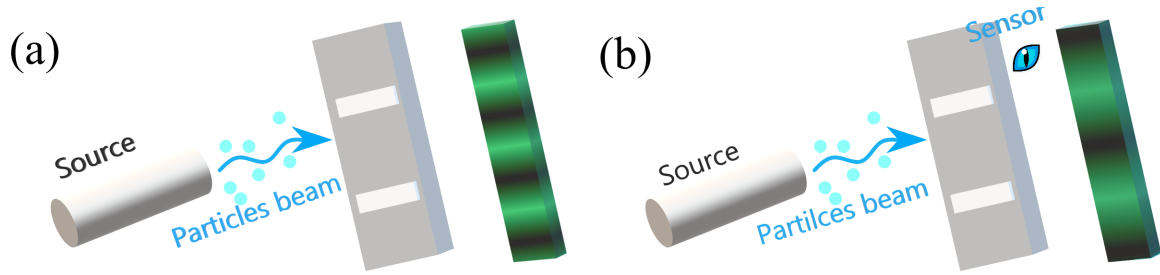


Figure 1 – (a) Interference pattern of a particle beam crossing a double slit with no path recording. (b) When a detector is capable of inferring the particle path, the Interference pattern vanishes.

techniques recently developed are capable of observing and controlling decoherence [20–23]. For example, in cavity quantum electrodynamics (CQED) experiments, it is possible to time resolve the effects of decoherence [24].

2.2.1 Quantum Decoherence Formalism

Quantum decoherence enables us to understand how the environment affects the states of an open quantum system. To introduce the quantum decoherence formalism, let us describe the simple but rich example with the double slits experiment presented in Ref. [18]. Consider a particle beam passing through a wall with two slits and reaching a screen that can record the position of each incident particle. Each particle from the beam is an open quantum system, S , and can cross or the slit 1 or the slit 2. In the first situation, we can not know for what slit the particle passed through, and the pattern of interference is visible (Fig.1(a)). However, if we place a sensor in slit 1 that can record the particle path, the interference pattern vanishes (Fig.1(b)). The which-path information destroys the interference pattern. The more distinguishable the path is of the particle, the less visible the interference pattern. In this idealized example, the sensor is the environment E . The environment's degrees of freedom interact with the particle, creating correlations between these two systems.

Consider that the particle's quantum states related to slits 1 and 2 are $|s_1\rangle$ and $|s_2\rangle$, respectively, and that the initial state of the environment is $|E\rangle$. After the interaction between the system and the environment, the evolution of the global state can be described as

$$|\Psi_0\rangle = (\alpha |s_1\rangle + \beta |s_2\rangle) |E\rangle \longrightarrow |\Psi\rangle = \alpha |s_1\rangle |E_1\rangle + \beta |s_2\rangle |E_2\rangle, \quad (2.15)$$

where $|E_1\rangle$ and $|E_2\rangle$ are the states of the environment if the state of the system is $|s_1\rangle$ and $|s_2\rangle$, respectively.

By tracing out the degrees of freedom of the environment from the global state,

ρ_{SE} , one gets the reduced density matrix of the system,

$$\rho_S = \text{Tr}_E (\rho_{SE}), \quad (2.16)$$

where all information about the system is stored. Namely, for observables that acts only on the system, that is, $O = O_S \otimes I_E$, the expectation value of O depends only on ρ_S . For the double slit example, ρ_S is obtained by tracing out the environment from Eq. (2.15),

$$\rho_S = \text{Tr}_E (\rho_{SE}) \quad (2.17)$$

$$= |\alpha|^2 |s_1\rangle \langle s_1| + |\beta|^2 |s_2\rangle \langle s_2| + \alpha\beta^* |s_1\rangle \langle s_2| \langle E_2|E_1\rangle + \alpha^*\beta |s_2\rangle \langle s_1| \langle E_1|E_2\rangle \quad (2.18)$$

For a given operation that measures the position of the particle in the screen, one can define an operator $O = |x\rangle \langle x| \otimes I_E$. The expected value of O gives the probability density $P(x)$ of detecting the particle in a particular position x . As this observable lies only in the Hilbert space of the system, we get

$$\begin{aligned} P(x) &= \langle O \rangle = \text{Tr}_S (\rho_S O) \\ &= \langle x | (\rho_S) | x \rangle \\ &= |\alpha|^2 |\psi_1(x)|^2 + |\beta|^2 |\psi_2(x)|^2 + 2\text{Re} \{ \alpha\beta^* \psi_1(x)\psi_2^*(x) \langle E_2|E_1 \rangle \}, \end{aligned} \quad (2.19)$$

where $\psi(x_1) = \langle x|s_1\rangle$ and $\psi(x_2) = \langle x|s_2\rangle$. The last term represents the visibility of the interference pattern and can vanish as the states of the environment become orthogonal. The coherence between the states of the system vanishes when the states of the environment are orthogonal. Therefore, we can conclude that the orthogonality between $|E_1\rangle$ and $|E_2\rangle$ indicates how much coherence the system lost.

In the case of complete decoherence, the environment states in Eq. (2.18) become completely distinguishable and all off-diagonal terms of the density matrix vanishes. In large environments, the number of interaction events is also significant, which results in a faster vanishing of the off-diagonal terms.

2.2.2 Environment-induced superselection

Generally, the interactions' correlations entangle the system, and the environment states. These correlations can destroy the superposition but do not affect the system's specific set of pure states. Consider the time evolution of a density matrix $\rho_S(t)$ of the von Neumann example in Eq. (2.18). At $t = 0$, there are no correlations between the system and the environment, and all elements of the matrix ρ_S will be nonzero if all $\gamma_i \neq 0$. As time progresses, the system and the environment become entangled, and the coherence in the superposition states of the system will vanish. The environment can effectively monitor the system through correlations [25]. For several kinds of interactions and on a proper basis, the off-diagonal elements of ρ_S decrease quickly, and just the diagonal states survive the decoherence process.

One can conclude that environment interaction can select and highlight the “strongest” states of the system. This environment-induced superselection is known in the literature as *einselection* [14, 15, 26]. Such robust states are also called *pointer states* or *preferred states*. The basis composed only by pointer states is known as *pointer basis* or *preferred basis*. The decoherence process also highlights a *preferential observable* or a *POVM of preferential observables*; that is, those observables that are diagonal in the preferential basis.

We can understand the highlighting of the pointer states through the total Hamiltonian that drives the system and the environment. Consider a Hamiltonian H composed of three parts, the self-Hamiltonians of the system and environment, H_S and H_E , respectively, and the Hamiltonian describing their interaction, H_I , so

$$H = H_S + H_E + H_I. \quad (2.20)$$

We shall consider three different situations: $H \approx H_I$, $H \approx H_S$, and $H_S \approx H_I$. Cases that H_I dominates are known as the *quantum-measurement limit of decoherence* [14, 17]. In these situations, $H_I \gg H_S + H_E$ and the preferred basis is enclosed in H_I . This case satisfies the primary condition to einselection known as *commutativity criterion*

$$[O, H_I] = 0, \quad (2.21)$$

where O is the preferential observable.

Consider the case where the interaction Hamiltonian is given by

$$H_I = O_S \otimes O_E. \quad (2.22)$$

To determine the pointer states, we need to find the system states that neither entangle with the environment nor change with the interaction when subject to H_I . In particular, these states coincide with the eigenstates $\{|s_i\rangle\}$ with eigenvalues $\{\lambda_i\}$ of the part of H_I that acts on the system’s Hilbert space, O_S . Thus, if H_I is time-independent, for each state $|s_i\rangle$ of the system associated with the environment state $|E(0)\rangle$ at $t = 0$, we get

$$\begin{aligned} e^{-iH_I t/\hbar} |s_i\rangle |E(0)\rangle &= e^{-iO_S t/\hbar} |s_i\rangle e^{-iO_E t/\hbar} |E(0)\rangle \\ &= e^{-i\lambda_i t} |s_i\rangle |E(t)\rangle. \end{aligned} \quad (2.23)$$

Note that any state of $\{|s_i\rangle\}$ remains a product state with the environment at any t and does not decohere. However, superpositions of pointer states can decohere and become entangled with the environment as, for example,

$$e^{-iH_I t/\hbar} \sum_i |s_i\rangle |E(0)\rangle = \sum_i e^{-i\lambda_i t} |s_i\rangle |E_i(t)\rangle. \quad (2.24)$$

Finding the eigenvectors of H_I in the system subspace allows us to identify the pointer states and the system preferred observable, $O = \sum_i |s_i\rangle \langle s_i|$, where the commutativity criterion in

Eq. (2.21) can be accomplished exactly. Therefore, $H_I = O_S \otimes O_E$ can represent a physical observable (the preferential observable) that will be monitored by the environment.

The regime $H_S \gg H_I$ is known as the *quantum limit of decoherence* [27]. Since H_S dominates the dynamics, the environment frequencies are small compared to the frequency of the system. Even if the system and the environment are correlated through the position or momentum, the selected pointer states will be the energy eigenstates.

In the most common models found in nature, neither H_I nor H_S dominates over H ; usually, H_S and H_I have the same weight. The characterization of the pointer states can be performed by the *predictability sieve* method [28–30]. This technique consists of measuring the decoherence during a time evolution for several different initially pure states of the system. The pointer states are that those better survive to decoherence. When a pure state is not robust, it loses coherence while it becomes entangled with the environment's states. The loss of purity leads to an increase in entropy. Pointer states do not entangle with the states of the environment, do not decohere, and the increase of the entropy is minimal.

Decoherence leads to an increase in the reduced system's entropy, which means that the system becomes even less predictable. However, the states that do not lose coherence are capable of keeping some information, and, at least for these classes of states, the predictability can survive.

2.3 The Quantum-to-Classic Transition

Quantum mechanics is a solid theory. Up to now, there is no conflict between experiments and theoretical predictions. However, it is hard to reconcile our perceptions with quantum theory predictions. For example, we can see directly neither superpositions of states nor entanglement. Some interpretations were developed to overcome this situation. In 1928, Bohr proposed that the measurement of quantum systems should be made by classical apparatus [5, 6]. Such interpretation, known as *Copenhagen Interpretation*, makes necessary the existence of a border (that can be mobile) separating quantum and classical. Wheeler emphasized that, from this point of view, “no phenomenon is a phenomenon until it is a recorded phenomenon” [31]. Another alternative is the *Many World Interpretation*. Proposed by Everett in 1957. This approach eliminates the necessity of a line separating the quantum from the classical [32]. It consists of considering all alternatives of the state vectors as existing results. The whole universe evolves according to the Schrödinger equation. When systems interact, the superposition states split into branches, and this process repeats indefinitely, giving rise to infinite worlds.

2.3.1 The Measurement Problem

Even with these interpretations, the key questions remain: “If can exist more than one outcome simultaneously, why do we see just one? What decides the outcome?”

Significant advances were reached with the decoherence theory. We can start our analysis from the *measurement problem* raised by Von Neumann in 1932 [33]. Instead of considering that the measurement apparatus is classical as Bohr did, Von Newmann investigated the situation where it is also a quantum system.

This analysis can be exemplified with a 1/2 spin system S that is measured by a quantum detector D . Consider that in this situation, the Hilbert space \mathcal{H}_S of the system has two dimensions with possible states $\{|\uparrow\rangle, |\downarrow\rangle\}$ and the Hilbert space \mathcal{H}_D of the quantum detector also have two possible states $\{|d_\uparrow\rangle, |d_\downarrow\rangle\}$. If the apparatus, initially in $|d_\downarrow\rangle$, detects a particle in the state $|\uparrow\rangle$ its state flips to $|d_\uparrow\rangle$, that is

$$\begin{aligned} |\downarrow\rangle |d_\downarrow\rangle &\rightarrow |\downarrow\rangle |d_\downarrow\rangle \\ |\uparrow\rangle |d_\downarrow\rangle &\rightarrow |\uparrow\rangle |d_\uparrow\rangle. \end{aligned} \quad (2.25)$$

Assuming that the initial state of the system is

$$|\psi_S\rangle = \alpha |\uparrow\rangle + \beta |\downarrow\rangle, \quad (2.26)$$

with $|\alpha|^2 + |\beta|^2 = 1$ and the initial state of the apparatus is $|\psi_D\rangle = |d_\downarrow\rangle$, we get

$$|\Psi^i\rangle = |\psi_S\rangle \otimes |\psi_D\rangle = (\alpha |\uparrow\rangle + \beta |\downarrow\rangle) \otimes |d_\downarrow\rangle \Rightarrow \alpha |\uparrow\rangle |d_\uparrow\rangle + \beta |\downarrow\rangle |d_\downarrow\rangle = |\Psi^c\rangle. \quad (2.27)$$

The interaction between the system and the detector transforms the initial product state $|\Psi^i\rangle$ in a correlated state $|\Psi^c\rangle$.

Describing a measurement just as described in Eq. (2.27) can be problematic; we can not see the two outcomes $|d_\uparrow\rangle$ and $|d_\downarrow\rangle$ simultaneously in the real world. Aware of this issue, Von Newmann proposed to analyze the density matrix of the state $|\Psi^c\rangle$,

$$\begin{aligned} \rho^c &= |\Psi^c\rangle \langle \Psi^c| \\ &= |\alpha|^2 |\uparrow\rangle \langle \uparrow| |d_\uparrow\rangle \langle d_\uparrow| + |\beta|^2 |\downarrow\rangle \langle \downarrow| |d_\downarrow\rangle \langle d_\downarrow| + \alpha\beta^* |\uparrow\rangle \langle \downarrow| |d_\uparrow\rangle \langle d_\downarrow| + \alpha^*\beta |\downarrow\rangle \langle \uparrow| |d_\downarrow\rangle \langle d_\uparrow|. \end{aligned} \quad (2.28)$$

The quantum correlations in Eq. (2.28) are represented by the off-diagonal terms of the matrix ρ^c . However, a measurement process only detects classical states. Then, Von Neumann postulated a non-unitary reduction of the state vector, eliminating the off-diagonal terms,

$$\rho^r = |\alpha|^2 |\uparrow\rangle \langle \uparrow| |d_\uparrow\rangle \langle d_\uparrow| + |\beta|^2 |\downarrow\rangle \langle \downarrow| |d_\downarrow\rangle \langle d_\downarrow|. \quad (2.29)$$

The evolution

$$\rho^c \Rightarrow \rho^r \quad (2.30)$$

is known as *wave packet collapse*, and it is easier to interpret than looking just at $|\Psi^c\rangle$. However, it is not yet clear how this transition happens.

The reduction $\rho^c \Rightarrow \rho^r$ increases the entropy of the global system by the amount

$$\begin{aligned}\Delta H &= H(\rho^c) - H(\rho^r) \\ &= |\alpha|^2 \ln |\alpha|^2 + |\beta|^2 \ln |\beta|^2,\end{aligned}\quad (2.31)$$

where $H(\rho) = -\text{Tr}\rho \ln \rho$. This means that the system becomes less predictable and loses information when its states become classical.

2.3.2 Decoherence in the Reduced Density Matrix of the System

As pointed out by Zeh [13] and strongly emphasized by Zurek [14, 15, 34], the Schrödinger equation is not only applicable in single systems but also in composite systems. Most of the systems in nature interact with their neighborhood. The destiny of the lost information can be explained by the decoherence theory (see Sec. 2.2) which treats the system's environment as an active element.

When an environment interacts with the set system+apparatus, their states can become correlated. In the case of large environments, information can be dispersed on several degrees of freedom. To exemplify this analysis, let us include the environment in the example in Eq. 2.27. Now, the global system is composed of the system S , the detector D , and the environment E initially in the state $|\mathcal{E}_0\rangle$. The evolution of the global system is given by

$$|\Psi^c\rangle |\mathcal{E}_0\rangle = (\alpha |\uparrow\rangle |d_\uparrow\rangle + \beta |\downarrow\rangle |d_\downarrow\rangle) |\mathcal{E}_0\rangle \Rightarrow \alpha |\uparrow\rangle |d_\uparrow\rangle |\mathcal{E}_\uparrow\rangle + \beta |\downarrow\rangle |d_\downarrow\rangle |\mathcal{E}_\downarrow\rangle = |\Phi\rangle. \quad (2.32)$$

The state of system+apparatus is found by tracing out the degrees of liberty of the environment

$$\begin{aligned}\rho_{SD} &= \text{Tr}_E |\Phi\rangle \langle \Phi| \\ &= |\alpha|^2 |\uparrow\rangle \langle \uparrow| |d_\uparrow\rangle \langle d_\uparrow| + |\beta|^2 |\downarrow\rangle \langle \downarrow| |d_\downarrow\rangle \langle d_\downarrow| \\ &\quad + \alpha\beta^* |\uparrow\rangle \langle \downarrow| |d_\uparrow\rangle \langle d_\downarrow| \langle \mathcal{E}_\downarrow| \mathcal{E}_\uparrow\rangle + \alpha^*\beta |\downarrow\rangle \langle \uparrow| |d_\downarrow\rangle \langle d_\uparrow| \langle \mathcal{E}_\uparrow| \mathcal{E}_\downarrow\rangle.\end{aligned}\quad (2.33)$$

In particular, when the environment states $\{|\mathcal{E}_\downarrow\rangle, |\mathcal{E}_\uparrow\rangle\}$ are orthogonal, $\langle \mathcal{E}_i | \mathcal{E}_{i'} \rangle = \delta_{i,i'}$, we recover the completely mixed state predicted by Von Neumann in Eq. (2.29).

$$\rho_{SD} = \rho^r = |\alpha|^2 |\uparrow\rangle \langle \uparrow| |d_\uparrow\rangle \langle d_\uparrow| + |\beta|^2 |\downarrow\rangle \langle \downarrow| |d_\downarrow\rangle \langle d_\downarrow|. \quad (2.34)$$

As presented in Sec. 2.2, when the system interacts with its environment, its states become correlated, destroying the superposition of the system's states. Just the

strongest states can survive; these are the pointer states. As the pointer states are robust and fittest, they change minimally during decoherence, and only their superpositions are destroyed. The pointer states form the pointer basis with the classic outcome options of the preferential observable (or POVM). In this process of einselection (see in detail in Sec. 2.2.2), the interaction between system and environment results in highlighting the classical states of the system, that in the example of Eq. (2.34) are the diagonal states of ρ_{SD} .

When decoherence and einselection occur, obtaining information about the system is possible by measuring small fractions of the environment. This is attainable when information about the system is spread redundantly in the environment, and it is known as *Quantum Darwinism*.

3 Quantum Darwinism

As we could see in the previous chapter, the interaction between the system and the environment can highlight a set of pure states that form the pointer basis. Such states do not entangle with the environment's states and, therefore, do not lose coherence.

In some cases, information about the system can be found redundantly spread in the environment, so that a small fragment of the environment can contain almost all information that the whole environment has about the system. Such *redundant* information is about a specific observable, the preferred observable [15]. The pointer states, beyond being able to survive the environmental decoherence, are capable of *multiplying* and encoding information about them in the environment states. Then we can say that the *fittest* states survive to decoherence and multiply information about themselves in the environment.

The survival of some system states from decoherence and their redundant proliferation in the environment is known as *quantum Darwinism*. Wojciech Zurek popularized this concept in Ref. [35] and made an analogy with Charles Darwin's work. Zurek has been investigating the consequences of decoherence since the early '80s, inspired by Zeh's work (see Sec. 2.2).

The redundancy of information can be quantified through mutual information and is also a measure of *classicality* of the system. The works published in 1983 [34] and 1998 [30] bring the first mentions to *redundancy of information* in the context of open quantum systems, and the way to quantify it was introduced in 2000 in Ref. [36]. In 2003 Quantum Darwinism was first introduced in Ref. [37], where the author connected decoherence, einselection, and redundancy and was widely disclosed through Ref. [35] in 2009.

3.1 From Decoherence to Quantum Darwinism

Depending on the kind of interaction, the environment can effectively measure the open quantum system. The states of the environment correlate with the states of the system. This “measurement kind” process destroys the superposition states of the system, and just a set of resilient pure states can resist the pointer states. Then, we can say that this system suffered decoherence. The remaining pure states are einselected, that is, selected by the environment through the decoherence process (Sec. 2.2).

The entanglement produced by the decoherence process makes it possible to obtain information about the system by measuring the environment. In some cases, it is necessary

to measure nearly the entire environment to obtain almost all information about the system. However, there are cases where just a small fragment of the environment carries enough information to infer the state of the system.

Redundancy in the *information theory* context is defined as the difference between the minimal number of bits required to decode the message with no ambiguity and the size of the complete encoded message [38]. It follows similarly in quantum information. For some kinds of interaction, information can be “decoded” from a small environment fraction. In general, the Hilbert space of the environment \mathcal{H}_E is much larger than the Hilbert space of the system \mathcal{H}_S , and information about the system can be spread redundantly over the environment. During the interaction, the environment measures, records, and encodes the states of the system. The states related to the preferential observables are recorded redundantly in the environment (see Sec. 2.2.2).

In a case where there is no redundancy, it is required to measure the whole environment to obtain such information. Once the quantity of redundancy is relevant, the measurement of a small fragment of the environment is enough to detect the state of the system related to the preferential observable; this is the case of quantum Darwinism.

Observe that the set of system states related to a specific observable is selected (or einselected) by the environment through the decoherence process. Furthermore, the information about these states not just survives, it also proliferates in the environment’s states. Therefore, it is noticeable that “Darwinism” is related to the Charles Darwin theory, which claims that in nature, only the strongest and fittest can survive in the environment and reproduce themselves.

3.2 The preferential Observable

In a redundant scenario, the information about the preferred observable is encoded in the environment states, and by measuring a small fraction of the environment, one can infer the system state. In contrast, non-preferential observables cannot be measured by small environment fractions.

Consider a two-level atom with the possible states $|e\rangle$ and $|g\rangle$ coupled to an environment such that each individual subenvironment has two possible spin states, $|\uparrow\rangle$ and $|\downarrow\rangle$. Suppose that the state $|\Psi_{SE}\rangle$ of the composite system is given by

$$\Psi_{SE} = \frac{1}{\sqrt{2}} (|e\rangle |\uparrow\uparrow \cdots \uparrow\rangle + |g\rangle |\downarrow\downarrow \cdots \downarrow\rangle) \quad (3.1)$$

$$= \frac{1}{\sqrt{2}} (|e\rangle |\mathcal{E}_\uparrow\rangle + |g\rangle |\mathcal{E}_\downarrow\rangle). \quad (3.2)$$

By measuring the entire environment, it is possible to infer the atom’s state, as we can see in Eq (3.2). However, in this case, it is not necessary to measure all the environment, the

result of the measurement of just one subenvironment tells us precisely the state of the system, Eq. (3.1).

Notwithstanding, it is not guaranteed the redundancy of information about other observables of the system. By rewriting the states of the system on the basis

$$\begin{aligned} |1\rangle &= \frac{1}{\sqrt{2}} (|e\rangle + |g\rangle) \\ |0\rangle &= \frac{1}{\sqrt{2}} (|e\rangle - |g\rangle) \end{aligned} \quad (3.3)$$

the global state becomes

$$|\Psi_{SE}\rangle = \frac{1}{2} |1\rangle (|\uparrow\uparrow \cdots \uparrow\rangle + |\downarrow\downarrow \cdots \downarrow\rangle) + \frac{1}{2} |0\rangle (|\uparrow\uparrow \cdots \uparrow\rangle - |\downarrow\downarrow \cdots \downarrow\rangle) \quad (3.4)$$

$$= \frac{1}{\sqrt{2}} (|1\rangle |\mathcal{E}_1\rangle + |0\rangle |\mathcal{E}_0\rangle). \quad (3.5)$$

To obtain information about the system on the basis $\{|1\rangle, |0\rangle\}$ it is necessary to measure the whole environment, indicating that this is not the preferential basis and that there is no redundancy on it. In this example, the preferential basis is $\{|e\rangle, |g\rangle\}$, and it is capable of encoding information of the preferential observable redundantly in the environment.

In the next sections, we present two ways to determine if quantum Darwinism can be observed in a quantum system.

3.3 Objectivity and Quantum Darwinism

Different observers on Earth can see the moon by accessing different tiny fractions of all photons scattered from it, agreeing with what they observed. This is an example of *classical objectivity*. In the context of the quantum-to-classical transition, quantum Darwinism is presented to elucidate the arising of the objective reality from the quantum world.

To pinpoint the features of classical objectivity, consider a system S interacting with \mathcal{E} , which is composed of several subenvironments. Objectivity is reached when:

- There exists an observable (or POVM) that can be measured by multiple observers and it is capable of inferring information about the system by probing the environment. This is the preferential observable (Sec. 3.2) that can be described by the pointer states selected by einselection;
- a large number of observers should have access to information of the pointer observable through different subenvironments of \mathcal{E} simultaneously;
- and all observers must agree with the result obtained.

The information about a system observable becomes objective when these conditions are fulfilled. Such information is selected with the preferred states by the einselection and is proliferated redundantly in the environment states. Therefore, objectivity indicates the emergence of classical reality.

3.4 Partial Information Plot Approach

When Zurek introduced the quantum Darwinism concept, he proposed quantifying it by calculating the redundancy of information [35] that can be seen as a consequence of einselection (See Ref. [34]).

As *information* is a term that can have multiple meanings, it is important to define which “information” we are talking about. Since elements of information theory can be adapted to quantum information, Zurek proposed to use the *quantum mutual information* to characterize quantum Darwinism [35]. The mutual information between a system S and its environment \mathcal{E} is defined as

$$I(S : \mathcal{E}) := H(S) + H(\mathcal{E}) - H(S, \mathcal{E}), \quad (3.6)$$

where $H(S)$ is the von Neumann entropy of the system, $H(\mathcal{E})$ is the entropy of the environment, and $H(S, \mathcal{E})$ is the joint entropy of system and environment. The von Neumann entropy of a certain system X , $H(X)$, is given by $H(X) = -\text{Tr} [\rho(X) \ln \rho(X)]$. Mutual information $I(S : \mathcal{E})$ defines the quantity of information that the whole environment has about the system. If the system and environment are in a product state, $\rho = \rho(S) \otimes \rho(\mathcal{E})$, the mutual information is zero. If the system and the environment are in a maximally entangled state, as for example in

$$|\Psi\rangle = \frac{1}{\sqrt{2}} (|\uparrow_S\rangle |\uparrow_E\rangle + |\downarrow_S\rangle |\downarrow_E\rangle), \quad (3.7)$$

the mutual information is maximal. In this case, one can know precisely the state of the system by measuring the environment. Therefore, mutual information is an excellent metric to quantify how much information the environment has about the system. In this approach, quantum mutual information is crucial to measure the quantity of redundant information contained in the environment.

To calculate the redundancy, we need to consider fragments \mathcal{F} of the environment, composed of m subenvironments \mathcal{E}_k . Each \mathcal{E}_k is the smallest portion possible of the environment. Consider also that \mathcal{E} is divisible in N subenvironments. To understand how the information is spread, we can look at fragments of the environment that contains m subenvironments. The number of subenvironments, m , contained in \mathcal{F}_m is given by $m = fN$, where f is the fraction of the environment contained in \mathcal{F}_m , that is, $f = m/N$.

The mutual information

$$I(S, \mathcal{E}_k) = H(S) + H(\mathcal{E}_k) - H(S, \mathcal{E}_k) \quad (3.8)$$

gives the amount of information that a single subenvironment has about the system. In the example of Eq. (3.1), where a single environment \mathcal{E}_k gives all information about the preferential observable, the mutual information between the system and \mathcal{E}_k is $I(S, \mathcal{E}_k) = H(S)$. As the mutual information is antisymmetric around $H(S)$ and $f = 1/2$ for pure states [39], $I(S, \mathcal{E}_k) \geq H(S)$ indicates that the subenvironment \mathcal{E}_m has all available information about the preferred observable; If this is valid to any k , the redundancy is maximal, and quantum Darwinism can be observed. In contrast, if to reach $I \geq H(S)$, it is required to get the whole environment, that is, $I = I(S, E)$, the redundancy is minimal, and there is no quantum Darwinism.

Typically, redundancy is not maximal, but it can be large enough to characterize quantum Darwinism. It is possible to obtain almost all information about the system by taking more than one subenvironment. First, it is necessary to define what amount of information about the system is acceptable to guarantee a good approximation to the ideal condition. We shall define an arbitrary parameter $0 < \delta < 1$ so that $(1 - \delta)H(S)$ is the desired good approximation.

The second step is to compute the average mutual information for a fraction f . Each fraction contains fragments \mathcal{F}_m of the environment composed by m subenvironments. The mutual information of each \mathcal{F}_m is given by

$$I(S, \mathcal{F}_m) = H(S) + H(\mathcal{F}_m) - H(S, \mathcal{F}_m). \quad (3.9)$$

For $1 < m < N$, there are $C = \binom{N}{m}$ different possible combinations of subsystems. Then, the average mutual information of a fraction f of the environment is given by the average value of $I(S, \mathcal{F}_m)$ for all combinations:

$$\bar{I}(f) = \langle I(S, \mathcal{F}_m) \rangle \quad \text{to all } C \text{ combinations } m. \quad (3.10)$$

In the third step, one can finally calculate the redundancy. The quantity f_δ is the smallest fraction required to obtain all information of the system's preferential observable but a percentage δ ; that is, $I(S, f_\delta) = (1 - \delta)H(S)$. It is clear that the smaller is f_δ , the larger is redundancy. Then, one can define the redundancy related to δ , R_δ , as the inverse of f_δ ,

$$R_\delta = \frac{1}{f_\delta}. \quad (3.11)$$

Therefore, to find the redundancy of information in this approach, it is necessary to find the fraction f_δ necessary to obtain almost all information about the system spread in the environment. Fig. 2 presents three examples. In the solid line, quantum Darwinism can be observed. Although it does not represent the perfect case, f_δ that provides almost all information about the system is relatively small, which means that R_δ is high. In contrast, in the long-dashed line, $f_\delta \sim 0.5$ and in the short-dashed line $f_\delta = 0.5$, implying in small values of R_δ .

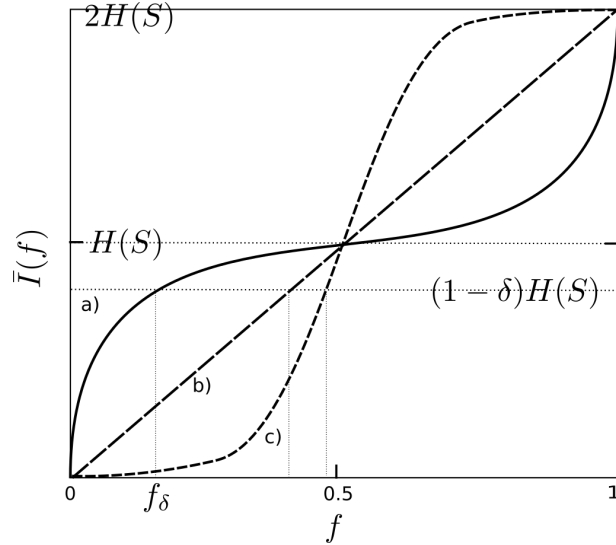


Figure 2 – figure

Three qualitatively distinct possibilities for a partial information plot (*PIP*) [40]. The solid line *a)* corresponds to a case where a small fraction of the environment already has average mutual information close to $H(S)$, being the signature of quantum Darwinism. The linear profile *b)* can be seen (approximately) in our model for small interaction times (see Sec. 5.2.4). In profile *c)*, f_δ is close to 0.5, so the redundancy is very small. This kind of profile can be obtained from random pure states drawn according to the Haar measure [39].

3.5 BHP Approach

In the quest to understand the conditions required to observe quantum Darwinism, F. Brandão, M. Piani, and P. Horodecki proposed looking at how the system's initial states are mapped into states of the environment [41]. We call this method *the BPH approach* for short.

The authors observed that the general conditions for quantum Darwinism were still not clear. One needs to look at the system's dynamics individually to see if quantum Darwinism is applicable or not; it is not possible to infer this from the Hamiltonian, for example. This investigation produced a significant result. It showed that some of the requirements for quantum Darwinism were naturally and generically satisfied.

They formulated the concepts of emergent objectivity of the observables and outcomes and showed under which circumstances one can validate quantum Darwinism. In Sec. 3.3, it was defined under which conditions objectivity emerges. We can separate these conditions into two groups. The first group defines the *objectivity of observables*: there exists an observable accessible to different observers by probing parts of the environment. The second is the *objectivity of the outcomes*: all observers shall be able to measure the system through the environment and find the same result.

The objectivity of the outcomes was found as a consequence of the quantum

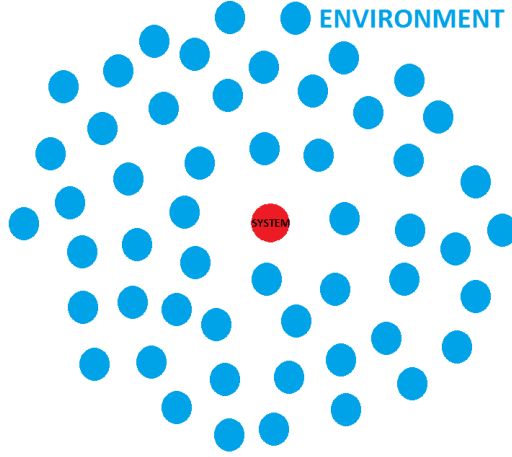


Figure 3 – (Color) Open quantum system (red particle) and its environment (blue particles). As the system is identical to the environment particles, any subenvironment could be the system.

mechanics postulates. To understand the idea, let us consider a set with $N + 1$ initially uncorrelated systems. Any system can be considered the main system S ; the only restriction is that it shall have finite dimension d_S . The remaining systems, E_1, \dots, E_N , compose the environment E with no restrictions to dimension (See Fig.3). Once S and E interact, E acquires information about S . This operation can be described by a completely positive trace-preserving (CPTP) map $\Lambda : \mathcal{D}(S) \rightarrow \mathcal{D}(E_1 \otimes \dots \otimes E_n)$, where $\mathcal{D}(X)$ represents the set of all possible density matrices of the system X Hilbert space.

One can define the difference between two quantum operations Λ_1 and Λ_2 as the diamond norm of their difference, that is

$$\|\Lambda_1 - \Lambda_2\|_{\diamond} = \frac{\sup_X \|(\Lambda_1 - \Lambda_2) \otimes \text{id}_X\|_1}{\|X\|_1} \quad (3.12)$$

where $\|X\|_1 = \text{tr} \left((X^\dagger X)^{1/2} \right)$. Let ϵ be the maximal tolerable error, such that $\|\Lambda_1 - \Lambda_2\|_{\diamond} \leq \epsilon$ allow us to consider λ_1 and λ_2 approximately equal.

From the map $\Lambda : \mathcal{D}(S) \rightarrow \mathcal{D}(E_1 \otimes \dots \otimes E_N)$, define a quantum operation that takes the state of S on the states of the subenvironment E_j as $\Lambda_j := \text{tr}_{\setminus E_j} \circ \Lambda$, where $\text{tr}_{\setminus E_j}$ is the partial trace over all subenvironment except for E_j ; that is, $\Lambda_j : \mathcal{D}(S) \rightarrow \mathcal{D}(E_j)$. Also consider a fixed δ , such that $0 < \delta < 1$. In the first theorem of Ref. [41], BPH proved that there exists a measurement described by a POVM $\{M_k\}_k$, an operation \mathcal{E}_j , and an environment subset $F \subseteq \{1, \dots, N\}$ with $|F| \geq (1 - \delta)N$, such that for all subenvironments j and all possible F 's,

$$\|\Lambda_j - \mathcal{E}_j\|_{\diamond} = \left(\frac{27 \ln(2) d_S^6 \log(d_S)}{N \delta^3} \right)^{\frac{1}{3}}, \quad (3.13)$$

with

$$\mathcal{E}_j = \sum_k \text{tr}(M_k X) \sigma_{j,k}, \quad (3.14)$$

where $\sigma_{j,k} \in \mathcal{D}(E_j)$ are k -th subenvironment states. Note that δ establishes how close can be the maps Λ_j and \mathcal{E}_j . For example, if S and E are perfectly correlated we can learn about the state of S by measuring all environment in any situation. Then, the quantity δ means that we want to find an operation that describes a measurement equivalent to measure all subenvironments but a percentage δ of N .

The smaller $\|\Lambda_j - \mathcal{E}_j\|_\diamond$ is, the more suitable is the POVM $\{M_k\}_k$ to measure the system. For a fixed δ , N , and d_S , the right side of Eq. (3.13) defines how close \mathcal{E}_j and Λ_j are. The large the environment is and the smaller d_S , the smaller is the distinguishability between Λ_j and \mathcal{E}_j .

The operation in Eq. (3.14) gives some details about the dynamics $\Lambda_j : \mathcal{D}(S) \rightarrow \mathcal{D}(E_j)$. The operation \mathcal{E}_j describes the subenvironment E_j “measuring” the system states through the POVM $\{M_k\}_k$ during the interaction. Then, the states of E_j , $\sigma_{j,k}$ are prepared according to the result of this measurement. The operation \mathcal{E}_j is properly named as *measure and prepare map*.

This POVM can be interpreted as the preferential observable, meaning that the observable’s objectivity is a general characteristic of quantum systems in a Hilbert space of finite dimension. Extending this theorem, it is also possible to prove that if different observers with access to different parts of the environment have almost all information about the pointer observable, they will agree on the outcomes obtained, validating objectivity of outcomes [41].

It is important to stress that this theorem does not guarantee the objectivity of the outcomes. The outcomes become objective only if the states of the POVM are distinguishable. For example, Ref. [39] used Page’s formula for the Haar-average entropy to compute the averaged mutual information \bar{I} over the Hilbert space of pure states $\mathcal{H} = S \otimes E$. It was shown that for a fixed fraction f , $\lim_{N \rightarrow \infty} \langle \bar{I}(f) \rangle = 0$ for $f < 1/2$. It is necessary to take at least half of the environment to infer the system state, and therefore, there is no redundancy or objectivity of the observable. One can conclude that the objectivity of the outcomes is not a general consequence of quantum mechanics postulates and depends on the details of the dynamics.

3.6 Exemplifying and comparing BPH and PIP approaches

To clarify the idea and difference between these approaches, we show two examples and discuss their particularities. First, we analyze the dynamics of a particular model to give a qualitative idea of the preferential observable and redundancy. We will then apply

both approaches, BPH and PIP, to give a quantitative notion of quantum Darwinism. Finally, we will compare the two methods.

Example 1: Consider a qubit system S inserted in an environment \mathcal{E} composed of N qubit subenvironments, with $\mathcal{E} = \{\mathcal{E}_1, \dots, \mathcal{E}_N\}$, where the possible states of S and each \mathcal{E}_i are respectively $\{|0\rangle, |1\rangle\}$ and $\{|0\rangle_{\mathcal{E}_i}, |1\rangle_{\mathcal{E}_i}\}$. Assume the initial state of \mathcal{E} as $|0\rangle_{\mathcal{E}} = |0\rangle_{\mathcal{E}_1} \otimes \dots \otimes |0\rangle_{\mathcal{E}_N}$ and the interaction dynamics for a specific time interval $\Delta t = t_f - t_i$ as

$$\begin{aligned} |0\rangle |0\rangle_{\mathcal{E}} &\rightarrow |0\rangle |0\rangle_{\mathcal{E}} \\ |1\rangle |0\rangle_{\mathcal{E}} &\rightarrow |1\rangle |1\rangle_{\mathcal{E}}. \end{aligned} \quad (3.15)$$

If the system is initially in a superposition state

$$\frac{1}{\sqrt{2}}(|0\rangle + |1\rangle), \quad (3.16)$$

then at $t = t_f$ the dynamics of Eq. (3.15) evolves the global system to

$$|\Psi(t_f)_{S\mathcal{E}}\rangle = \frac{1}{\sqrt{2}}(|0\rangle |0_{\mathcal{E}}\rangle + |1\rangle |1_{\mathcal{E}}\rangle), \quad (3.17)$$

whose density matrix is $\rho_{S\mathcal{E}} = |\Psi(t_f)_{S\mathcal{E}}\rangle \langle \Psi(t_f)_{S\mathcal{E}}|$. For any fragment $F \subset \mathcal{E}$ of the environment composed by one or more subenvironments, the reduced density matrix is

$$\begin{aligned} \rho_{SF} &= \text{tr}_{\setminus F} \rho_{S\mathcal{E}} \\ &= \frac{1}{2} |0\rangle \langle 0| |0_F\rangle \langle 0_F| + \frac{1}{2} |1\rangle \langle 1| |1_F\rangle \langle 1_F|, \end{aligned} \quad (3.18)$$

where $|0_F\rangle = \otimes_{k \in F} |0\rangle_k$ and analogously for $|1_F\rangle$. Therefore, by measuring the environment fraction F on the basis $\{|0_F\rangle, |1_F\rangle\}$, one can infer the state of S on the basis $\{|0\rangle, |1\rangle\}$, at a time t_f .

However, is it possible to infer the state of S by measuring F on another basis? What can we learn about other observables through F ? To answer this question, we can rewrite Eq. (3.17) in the basis $\{|+\rangle, |-\rangle\}$, where $|\pm\rangle = \frac{1}{\sqrt{2}}(|0\rangle \pm |1\rangle)$, for the system, and in the basis $\{|GHZ_+\rangle, |GHZ_-\rangle\}$, with $|GHZ_{\pm}\rangle = \frac{1}{\sqrt{2}}(|0_E\rangle \pm |1_E\rangle)$, for the environment. The global system will become

$$\rho_{SF} = \frac{1}{\sqrt{2}}(|+\rangle |GHZ_+\rangle + |-\rangle |GHZ_-\rangle). \quad (3.19)$$

Now, differently from Eq. (3.17), only by measuring the whole environment one can learn the system's state. Note that, moreover, the same is true for any system observable, defined by an arbitrary orthonormal basis. In this example, the preferential observable is described by the basis $\{|0\rangle, |1\rangle\}$, and the information about it is spread redundantly over the environment; one can infer the value of this observable even when F contains only one subenvironment.

It is easy to check that the partial information plot for state (3.17) is an exact plateau: $\bar{\mathcal{I}}(0) = 0$ by definition, $\bar{\mathcal{I}}(f) = H(S) = \ln 2$ for every $0 < f < 1$ and $\bar{\mathcal{I}}(f) = 2H(S) = 2 \ln 2$ for $f = 1$. This reflects the fact that any proper subset of the environment only has information about the preferred observable.

To understand this example in terms of the BPH approach, we need to find the map Λ_F of this dynamic. Since the environment is composed of many subsystems, one can define, via composition with partial tracing, corresponding maps $\Lambda_F : D_S \rightarrow D_F$ to each fragment $F \subset E$ of the environment, namely

$$\begin{aligned}\Lambda_F &= \text{Tr}_{\mathcal{E}-F} \circ \Lambda_{\mathcal{E}} \\ \Lambda_F(\rho) &= \text{Tr}(|0\rangle\langle 0| \rho) |0_F\rangle\langle 0_F| + \text{Tr}(|1\rangle\langle 1| \rho) |1_F\rangle\langle 1_F|. \end{aligned} \quad (3.20)$$

Note that Λ_F is exactly a measure and prepare map, as defined in Eq. (3.14), and the POVM $\{|0\rangle\langle 0|, |1\rangle\langle 1|\}$ is the preferential observable. These facts characterize the objectivity of observables. The map Λ_F shows that the states $\{|0\rangle_F, |1\rangle_F\}$ of F are perfectly correlated to the pointer basis states of S $\{|0\rangle, |1\rangle\}$. The objectivity of the outcomes is conditioned on the distinguishability between the states of the fragments. In this case, the two possible states of the fragment, $\{|0_F\rangle, |1_F\rangle\}$, are orthogonal. Then, we can conclude that by measuring just one fraction, one can know precisely the state of the system. Furthermore, the smallest possible fraction gives all information about S , which means that redundancy is maximal.

Note that in the *PIP* approach, since one considers only the specific global state (3.17), a strong claim can be made: if someone observes a particular outcome upon the $\{|0_F\rangle, |1_F\rangle\}$ measurement in an environment fragment F , we can be sure that a $\{|0\rangle, |1\rangle\}$ measurement in the system itself if performed, will show the same outcome. There is no analog claim in the *BPH* approach. It is not correct to say in general that, upon seeing the outcome 0 in an environment F , the system *was* in state $|0\rangle$ at $T = 0$, since the system could have been, say, in the initial state $\frac{1}{\sqrt{2}}(|0\rangle + |1\rangle)$. In this case, there would be a positive probability of observing the outcome 1 in the environment fractions.

Example 2: Now, consider a slight modification in the dynamics:

$$|0\rangle |0_{\mathcal{E}}\rangle \mapsto |0\rangle |0_{\mathcal{E}}\rangle, \quad (3.21)$$

$$|1\rangle |0_{\mathcal{E}}\rangle \mapsto |0\rangle |1_{\mathcal{E}}\rangle. \quad (3.22)$$

No matter what initial state we choose for system S , it will never correlate with the environment, so the *PIP* is always trivial. From this perspective then, it appears that this is a bad instance of quantum Darwinism.

From the *BPH* perspective, however, they are necessarily the same. Indeed, the maps Λ_F defined by such new dynamics are exactly the same as in Eq. (3.20) for every *proper* subset $F \subset E$. Nevertheless, as a side note, it is interesting to see that they do differ

for $F = E$. In this case, having access to the whole environment does have a consequence. Indeed, the dynamics essentially transfer any initial state of the system to the environment:

$$(\alpha |0\rangle + \beta |1\rangle) |0_{\mathcal{E}}\rangle \mapsto |0\rangle (\alpha |0_{\mathcal{E}}\rangle + \beta |1_{\mathcal{E}}\rangle). \quad (3.23)$$

Therefore, one can choose to obtain information about an arbitrary system observable, in the sense that there exists some (in general, global) measurement that can be done in the whole environment with the same statistics of the corresponding system observable in the initial system state. Of course, these measurements being global makes meaningless the notion of objectivity, since it would not be possible to compare the outcomes of different observers.

As we could see, albeit these approaches are different they are complementary; one can be more suitable than the other depending on the situation.

3.7 Quantum Darwinism Examples

There are quite interesting theoretical models in the literature that can help us clarify the concept of quantum Darwinism. This section shows two works [42, 43] where the objectivity of the system emerges from einselection.

3.7.1 Quantum Darwinism in Quantum Brownian Motion

Quantum Brownian motion is a well-studied model for open systems [26, 42, 44–46]. Its similarity with systems often found in nature makes it suitable in open quantum experimental systems investigations [47, 48].

In this model, the system S and the environment \mathcal{E} are a collection of $N + 1$ quantum harmonic oscillators. The system and the environment can interact and are coupled in position. Therefore, the environment is a set of quantum harmonic oscillators $\mathcal{E} = \{\mathcal{E}_1, \dots, \mathcal{E}_N\}$ where each \mathcal{E}_i is a subenvironment (see Fig. 4).

In this model, the Hamiltonian is given by

$$H = H_S + H_{\mathcal{E}} + H_I, \quad (3.24)$$

with

$$H_S = \frac{p_S^2}{2M} + \frac{M\Omega^2 x^2}{2}, \quad (3.25)$$

$$H_{\mathcal{E}} = \frac{1}{2} \sum_{i=1}^N \left(\frac{q_i^2}{m_i} + m_i \omega_i^2 y_i^2 \right), \quad (3.26)$$

and

$$H_I = x \sum_{i=1}^N C_i y_i, \quad (3.27)$$

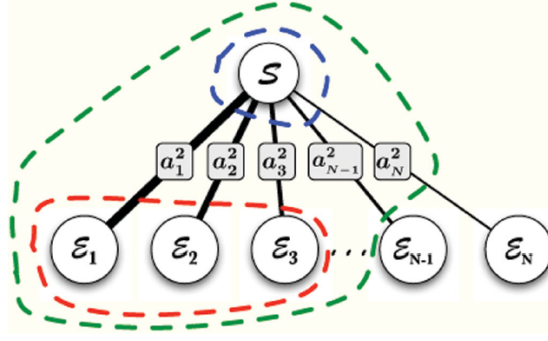


Figure 4 – System S interacting with individual subenvironments \mathcal{E}_i that compose the whole environment \mathcal{E} . In a quantum Brownian motion model each \mathcal{E}_i is a quantum harmonic oscillator coupled to S , which is also a quantum harmonic oscillator. Figure extracted from Ref. [42].

where C_i are constants of the spectral density:

$$J(\omega) = \sum_i^N \frac{C_i^2}{2m_i\omega_i} \delta(\omega - \omega_i). \quad (3.28)$$

As the interaction between S and \mathcal{E}_i depends linearly on the position, one expects the emergence of position as the preferential observable. Furthermore, the harmonic potential produces Gaussian pointer states that are well localized in x and p . The dynamic of this system can be described by master equations associated to the Hamiltonian in Eq. (3.24) [26], and the exact solution of the reduced state of the system ρ_S was calculated in Ref. [44].

In Ref [26], the authors used this model to investigate quantum Darwinism. They considered an Ohmic bath [49] with a cutoff frequency Λ , at zero temperature. The system is initially in a squeezed Gaussian state with squeezing parameters $s_x = \frac{1}{s_p}$, where $s_x = s_p$ for coherent ground states. For $s_{x(p)} \gg 1$, this state is a kind of Schrödinger cat state where the superposition is in position (or momentum).

At $t = 0$, the superposition state of the system $\rho_S(0)$ forms a product with the environment state $\rho_{\mathcal{E}}(0)$, $\rho_{S,\mathcal{E}}(0) = \rho_S(0) \otimes \rho_{\mathcal{E}}(0)$. For $t > 0$, the interaction between S and \mathcal{E} destroys the superposition of the system, and ρ_S becomes a mixed state. This increases system entropy and its correlation with the environment.

They analyzed the redundancy of information from the PIP approach (Sec. 3.4). The subset

$$\mathcal{F} = \{\mathcal{E}_i\} \subset \{\mathcal{E}_1, \dots, \mathcal{E}_N\} = \mathcal{E}$$

is a fragment of the environment that contains a fraction f of \mathcal{E} (see Fig. 4). Then, the mutual information between \mathcal{F} and S is given by Eq. (3.9), and the averaged mutual information of all possible combinations of \mathcal{F} that contains the same fraction f of \mathcal{E} , is given by Eq. (3.10).

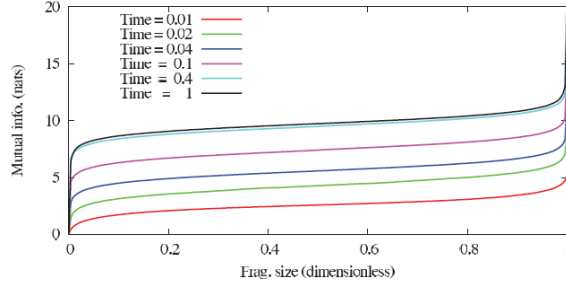


Figure 5 – (Color). Partial information plots (PIPs), $I(S, \mathcal{F})$ for a random fragment $\mathcal{F} \subset \mathcal{E}$, at different time instants. This figure was taken from the Ref. [42].

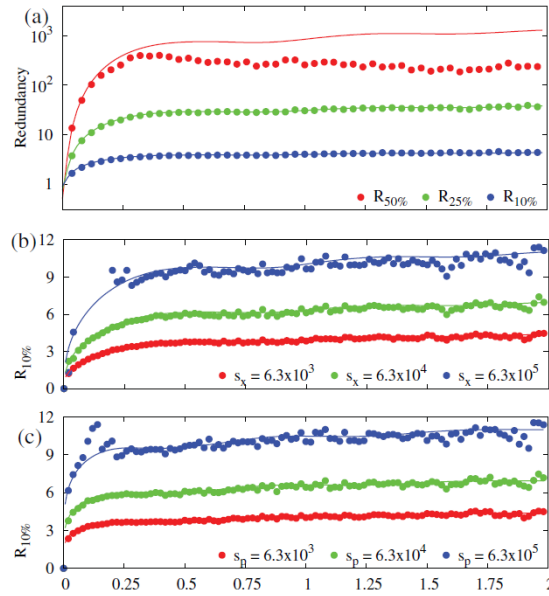


Figure 6 – (Color). (a) Redundancy R_δ varying with t for S is initially squeezed in position with $s_x = 6.3 \times 10^3$ for different values of δ . (b) Redundancy varying with t with fixed $\delta = 0.1$ for different squeezing factors in position s_x (C) and in momentum p_x . This figure was taken from the Ref. [42].

To calculate the reduced states of the system and the fragments, they performed exact numerical calculations of an environment with 1024 oscillators with S initially in an x -squeezed state. The PIP (see Fig. 5) has a plateau form even for small values of t , indicating that the system decoheres very quickly; this behavior is expected, since $s_{x(p)} \gg 1$. The plateau form qualitatively shows that the fraction required to obtain almost all information about the system is quite small, which means that the redundancy is high.

The fraction f_δ is the fraction size that gives almost all information about the system, but a percentage δ , that is, the fraction such that

$$I(S, f) \geq (1 - \delta) H(S). \quad (3.29)$$

Redundancy R_δ , as defined in Sec. 3.4, is the inverse of f_δ , $R_\delta = \frac{1}{f_\delta}$ and reaches larger

values as δ increases (see Fig. 6(a)). Redundancy also grows faster and reaches larger values as the squeezing parameters grow up (see Figs. 6(b) and (c)). The larger s_x or s_p , the more distinguishable the states in the superposition of ρ_S and, therefore, the faster the system decoheres. As shown in Sec. 3.1, quantum Darwinism arises from the decoherence of the system states induced by the interaction with the environment. Therefore, it is expected that redundancy grows with decoherence.

In this example of quantum Brownian motion, the dynamic is Markovian, and we can see quantum Darwinism in it. However, there is a work claiming that when the dynamics is non-Markovian, in this same model, quantum Darwinism is “hindered” [50]. We shall discuss this work in Chap. 5 and present a model where non-Markovianity does not eliminate quantum Darwinism.

3.7.2 Quantum Darwinism in a Spin Model

Another example of quantum Darwinism in the literature was published by Zwolak, Quan, and Zurek in 2009 [43]. They used an exactly solvable model where the system and all subenvironments are single spin particles. In this model, the entropy of any environment fraction can be computed, making possible the investigation of large environments. We can see more clearly the connection between quantum Darwinism and decoherence through this work.

Consider a system S that interacts with its environment \mathcal{E} composed by N subenvironments \mathcal{E}_i under a total Hamiltonian $H_{S,\mathcal{E}}$ such that $H_I \approx H_{S,\mathcal{E}}$, where H_I is the interaction Hamiltonian. In Sec. 2.2.2 we show that when the interaction is the dominant part of the total Hamiltonian, $H_{S,\mathcal{E}}$ commutes with the preferential observable O . In this case, known as the quantum-measurement limit of decoherence [17], the preferential observable can be identified directly from H_I ; and high redundancy of information can arise in fragments $\mathcal{F} \subset \{\mathcal{E}_i\}$ in the global system with a pure initial state.

The evolution of quantum systems under this kind of Hamiltonian has an important particularity. The states of the system ρ_S and the system plus a fraction $\rho_{S,\mathcal{F}}$ can become maximally mixed and completely decohered. The off-diagonal terms of ρ_S decreases to zero,

$$\rho_S(0) = \begin{pmatrix} S_{00} & S_{01} \\ S_{10} & S_{11} \end{pmatrix} \rightarrow \rho_S(t) \approx \begin{pmatrix} S_{00} & 0 \\ 0 & S_{11} \end{pmatrix} \quad (3.30)$$

This is an explicit example where the decoherence process highlights the pointer states. Further, $\rho_{S,\mathcal{F}}$ presents the same behavior,

$$\rho_{S,\mathcal{F}}(t) \rightarrow \rho_{S,\mathcal{F}} \approx \begin{pmatrix} S_{00}U_0\rho_{\mathcal{F}}U_0 & 0 \\ 0 & S_{11}U_1\rho_{\mathcal{F}}U_1 \end{pmatrix}, \quad (3.31)$$

where U_0 and U_1 are the unitary operators projected onto the pointer states S_{00} and S_{11} , respectively.

Since the eigenstates of $\rho_S(t)$ are the pointer states and the entropy of $\rho_{S,\mathcal{F}}(t)$ is identical to the entropy of $\rho_S(t) \otimes \rho_{\mathcal{F}}(0)$, the mutual information between S and \mathcal{F} at any t becomes

$$I(S : \mathcal{F}) = H(S) + H(\mathcal{F}) - H(S, \mathcal{F}) \quad (3.32)$$

$$\begin{aligned} &= H(\rho_S(t)) + H(\rho_{\mathcal{F}}(t)) - H(\rho_S(t) \otimes \rho_{\mathcal{F}}(0)) \\ &= H(\rho_S(t)) + H(\rho_{\mathcal{F}}(t)) - H(\rho_S(t)) - H(\rho_{\mathcal{F}}(0)) \\ &= H_{\mathcal{F}}(t) - H_{\mathcal{F}}(0) = \Delta H_{\mathcal{F}}. \end{aligned} \quad (3.33)$$

To quantify the information gain of the fragments, one just has to compute its variation. When \mathcal{E} is in a pure state, Eq. (3.33) reduces to $I(S : \mathcal{F}) = H(\mathcal{F})$ and when $\rho_{\mathcal{F}}(t)$ is completely mixed, one gets $I(S : \mathcal{F}) = 0$ for any t .

To be more explicit, consider a model where the system is a single-spin system coupled to an environment composed of N spins, whose Hamiltonian is given by

$$H_{S,\mathcal{E}} = \frac{1}{2} \sum_{k=1}^N \sigma_S^z \sigma_k^z, \quad (3.34)$$

where σ_S^z and σ_k^z are the z -direction system spin and k -th subenvironment spin, respectively.

The system and each subenvironment \mathcal{E}_i are qubits in the σ^z basis, forming initially a product state

$$\rho_{S,\mathcal{E}} = \rho_S \otimes \prod_{k=1}^N \rho_{\mathcal{E}^{[k]}} \quad (3.35)$$

where

$$\rho_{\mathcal{E}^{[k]}} = \begin{pmatrix} e_{00} & e_{01} \\ e_{10} & e_{11} \end{pmatrix}. \quad (3.36)$$

The entropy h for each qubit is given by

$$h = -\text{Tr}(\rho_{\mathcal{E}^{[k]}} \log_2 \rho_{\mathcal{E}^{[k]}}). \quad (3.37)$$

When the qubit is in a completely mixed state, it reaches the maximal value, $h = 1$.

The reduced density matrices ρ_S and $\rho_{S,\mathcal{F}}$ at any instant t are given, respectively, by

$$\rho_S = \begin{pmatrix} S_{00} & S_{01} \Lambda_{\mathcal{E}}(t) \\ S_{10} \Lambda_{\mathcal{E}}^*(t) & S_{11} \end{pmatrix} \quad (3.38)$$

and

$$\rho_{S,\mathcal{F}} = \begin{pmatrix} S\mathcal{F}_{00} & S\mathcal{F}_{01} \Lambda_{\mathcal{E}/\mathcal{F}}(t) \\ S\mathcal{F}_{10} \Lambda_{\mathcal{E}/\mathcal{F}}^*(t) & S\mathcal{F}_{11} \end{pmatrix} \quad (3.39)$$

with

$$\Lambda_i(t) = \prod_{k \in i} \Lambda_k t \quad (3.40)$$

and

$$\Lambda_k = \cos(t) + (e_{11} - e_{00}) \sin(t), \quad (3.41)$$

where $i = \# \mathcal{E}$ for all environment and $i = \# \mathcal{E} / \# \mathcal{F}$ for all environment but the fraction \mathcal{F} . The quantity $\Lambda_i(t)$ is the decoherence factor of the reduced density matrices $\rho_S(t)$ and $\rho_{S\mathcal{F}}(t)$. The off-diagonal terms of these matrices in the pointer basis S go to zero for $N \gg \# \mathcal{F}$ and small $\Lambda_k(k)$, highlighting the pointer states.

By diagonalizing exactly $\rho_S(t)$ and $\rho_{S\mathcal{F}}(t)$, the mutual information for general conditions is given by

$$I(S : \mathcal{F}) = \Delta H_{\mathcal{F}}(t) + \left[H(\kappa_{\mathcal{E}}(t)) - H(\kappa_{\mathcal{E}/\mathcal{F}}(t)) \right], \quad (3.42)$$

with $H(x) = -x \log_2 x - (1-x) \log_2 (1-x)$ and

$$\kappa_i(t) = \frac{1}{2} \left(1 + \sqrt{(s_{11} - s_{00})^2 + 4 |s_{01}| |\Lambda_i(t)|^2} \right). \quad (3.43)$$

Except for a completely mixed \mathcal{E} and $\mathcal{F} = \mathcal{E}$, both $\rho_S(t)$ and $\rho_{S\mathcal{F}}(t)$ always decoheres. For example, for $e_{00} = 1/2$, $\Lambda_i(t) = 0$ at $t = \pi/2$.

Fig. 7 shows the evolution of the mutual information varying with t and $\# \mathcal{F}$ for $N = 100$, $\rho_S(0) = |+\rangle \langle +|$, $r_{00} = 1/2$ where $|+\rangle = \frac{1}{\sqrt{2}}(|0\rangle + |1\rangle)$. At the initial time instants to get nearly almost all information about the system $I(S : \mathcal{F}) \approx H(S) = H(s_{00})$, it is necessary to take a fragment $\# \mathcal{F} \approx (1/2)\# \mathcal{E}$. As the system and environment interact, they become correlated and S decoheres transferring its information to the environment. The initial state of \mathcal{E} is pure in Fig. 7(a), and mixed with $h \approx 0.8$ in Fig. 7(b). Note that in both cases, the $I(S : \mathcal{F})$ curve gets a plateau form, showing that a small fragment is enough to obtain almost all information about the system. It is also worth mentioning that although the plateau form is reached in both cases, pure and mixed states, it is slower for mixed states. Further, for totally mixed states ($h = 1$), we always get $I(S : \mathcal{F}) = 0$.

In particular, we get

$$R_{\delta} = \frac{N}{\# \mathcal{F}} = \frac{1}{f_{\delta}} \quad (3.44)$$

where f_{δ} is the fraction of the environment that gives $I(S : \mathcal{F} = f_{\delta}) \sim H(S)$. From Eqs. (3.41) and (3.42), we can observe that for $t = \pi/2$, any single spin of \mathcal{E} contains almost all information about S .

Another important result of this work is the link between redundancy and decoherence. As mentioned previously, h measures the purity of the subenvironments, with \mathcal{E}_i maximally mixed for $h = 1$. We also know that the larger h , the smaller the decoherence.

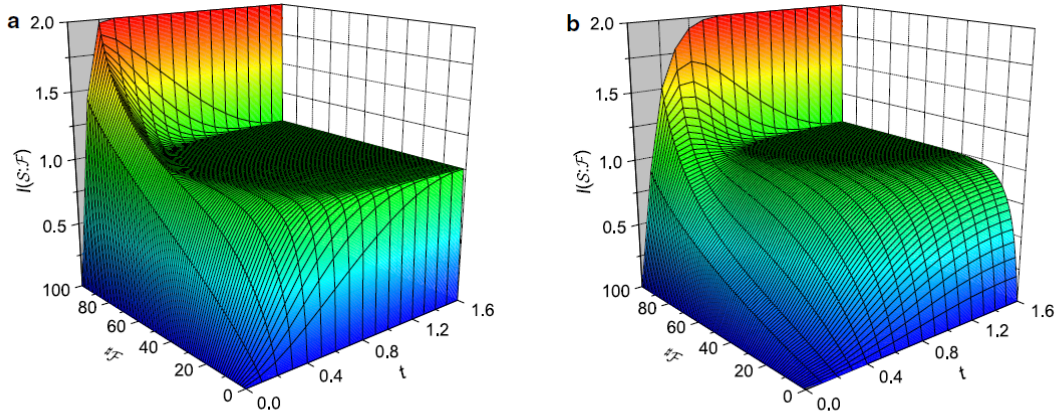


Figure 7 – Mutual information $I(S : \mathcal{F})$ between S and \mathcal{F} varying with t and the number ($\#$) of spins in a fragment \mathcal{F} for (a) \mathcal{E} initially pure, where $h = 0$ and (b) a \mathcal{E} mixed with $h \approx 0.8$. This figure was taken from the Ref. [43].

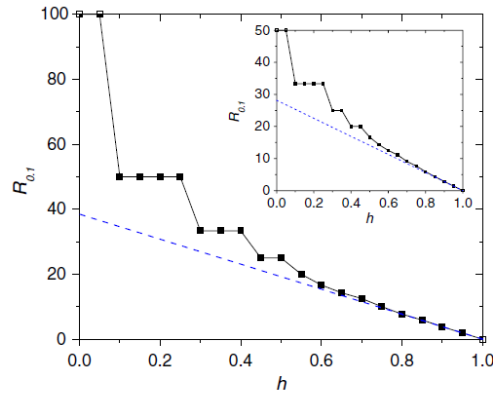


Figure 8 – Redundancy R_δ for $\delta = 0.1$ varying with the purity of $\rho_\mathcal{E}$, where $h = 0$ for pure states and $h = 1$ for maximally mixed states. The time was fixed at $t = \pi/2$ in the larger plot and at $t = \pi/3$ in the inset. This figure was taken from the Ref. [43].

The plot in Fig. 8 shows R_δ as a function of h for $\delta = 0.1$ at $t = \pi/2$ and $t = \pi/3$. For both time instants, R_δ decreases with h . This shows that the redundancy of information depends directly on decoherence and scales as $R_\delta \propto 1 - h$.

4 Markovian and non-Markovian Dynamics

The definition of Markovianity and non-Markovianity is well established for classical stochastic processes. Its definition can be constructed in terms of the Kolmogorov hierarchy of the n -point joint probability, favoring a connection with some definitions of quantum Markovianity.

In this section, we show two definitions of Markovianity in quantum systems and their counterpart with the classical cases. To give some intuition, we first revisit the classical definition of Markovian processes and its divisibility property. This allows a connection with two definitions of quantum Markovian processes: one based on divisibility of quantum maps and the other on the behavior of the distance between two quantum states.

4.1 Markovianity in classical processes

The concept of classical Markovianity is constructed for stochastic processes. A *stochastic process* is defined as a set of random variables $X = \{x_0, x_1, \dots, x_n\}$ in the same probability space (Ω, Σ, P) where Ω is the sample space, Σ the possible events, and P the probability measure. In simple words, it is a set of random variables X that depends on the parameter t . For simplicity, we shall restrict our analysis to discrete random variables $x_i \in \chi$, where χ is a finite set with all possible outcomes and consider cases where t represents time.

4.1.1 Formal Definition

A stochastic process is *Markovian* if the probability of the random variable X takes the value x_n at any arbitrary $t_n \in I$, depends only on the value x_{n-1} at t_{n-1} , being insensitive to any value taken by X at times previous to t_{n-1} . One can write this definition of Markov process can be defined in terms of conditional probabilities,

$$P(x_n, t_n | x_{n-1}, t_{n-1}; \dots; x_0, t_0) = P(x_n, t_n | x_{n-1}, t_{n-1}), \quad \text{for all } \{t_n \geq t_{n-1} \geq t_0\}. \quad (4.1)$$

From Eq.(4.1), it is possible to visualize the famous statement that “a Markov process does not have memory”.

Consider now the interval $t_3 \geq t_2 \geq t_1$. In a Markov process, one can split the conditional probability $P(x_3, t_3 | x_1, t_1)$ in a product of the two probabilities $P(x_3, t_3 | x_2, t_2)$ and $P(x_2, t_2 | x_1, t_1)$. This result can be deduced from the discrete description of the *Chapman-Kolmogorov equation*. Consider the joint probability density function $P(x_1, t_1; \dots; x_n, t_n)$.

Then, the discrete Chapman-Kolmogorov equation is

$$P(x_1, t_1; \cdots; x_{n-1}, t_{n-1}) = \sum_{x_n \in \mathcal{X}} P(x_1, t_1; \cdots; x_n, t_n) \quad (4.2)$$

By definition, the joint probability of three consecutive times, $t_3 \geq t_2 \geq t_1$, in terms of the joint probability is

$$\begin{aligned} P(x_3, t_3; x_2, t_2; x_1, t_1) &= P(x_3, t_3 | x_2, t_2; x_1, t_1) P(x_2, t_2; x_1, t_1) \\ &= P(x_3, t_3 | x_2, t_2; x_1, t_1) P(x_2, t_2 | x_1, t_1) P(x_1, t_1). \end{aligned} \quad (4.3)$$

For a Markovian process $P(x_3, t_3 | x_2, t_2; x_1, t_1) = P(x_3, t_3 | x_2, t_2)$ Eq. 4.3 becomes

$$P(x_3, t_3; x_2, t_2; x_1, t_1) = P(x_3, t_3 | x_2, t_2) P(x_2, t_2 | x_1, t_1) P(x_1, t_1). \quad (4.4)$$

By dividing both sides by $P(x_1, t_1)$ and taking the sum over x_2 we can apply the Chapman-Kolmogorov equation (Eq. 4.2) in the left side. Then, we get

$$P(x_3, t_3 | x_1, t_1) = \sum_{x_2 \in \mathcal{X}} P(x_3, t_3 | x_2, t_2) P(x_2, t_2 | x_1, t_1). \quad (4.5)$$

Therefore, one can conclude that a family of conditional probabilities $P(x_n, t_n | x_{n-1}, t_{n-1})$ with $t_n \leq t_{n-1}$ represents a Markovian process if it satisfies Eq. (4.5).

4.1.2 Divisibility Property

Some definitions of quantum Markovianity are based on the divisibility of quantum maps, and it is possible to construct a characterization of classical Markovianity similarly. Then, the *dynamic maps divisibility* property of classical Markovian processes helps to connect the classical and quantum Markovianity concepts.

Consider a time-dependent one-point probability $P(x, t)$ of a random variable X that describes a stochastic process. Let T be a dynamical map of the evolution of $P(x, t)$. Then, $P(x_1, t_1)$ for given an initial state $P(x_0, t_0)$, with $t_1 \geq t_0$, is given by

$$P(x_1, t_1) = \sum_{x_0 \in \mathcal{X}} T(x_1, t_1 | x_0, t_0) P(x_0, t_0). \quad (4.6)$$

Since $\sum_{x_1 \in \mathcal{X}} P(x_1, t_1) = 1$, $\sum_{x_0 \in \mathcal{X}} P(x_0, t_0) = 1$ and $P(x_1, t_1) \geq 0$ for all $P(x_0, t_0)$, T follows the properties

$$\sum_{x_1 \in \mathcal{X}} T(x_1, t_1 | x_0, t_0) = 1 \quad (4.7)$$

and

$$T(x_1, t_1 | x_0, t_0) \geq 0 \quad \text{with } x_1, x_0 \in \mathcal{X}. \quad (4.8)$$

Therefore, $T(x_1, t_1 | x_0, t_0)$ is a matrix that takes the probability $P(x_0, t_0)$ in $P(x_1, t_1)$ and, since it describes the evolution of stochastic processes, it is known as *the stochastic matrix*.

Stochastic matrices can be related to conditional probabilities. For an initial time $t = t_0$ of a stochastic process, the joint probability in terms of the conditional probability for t_2 and t_0 is

$$P(x_2, t_2; x_0, t_0) = P(x_2, t_2 | x_0, t_0) P(x_0, t_0). \quad (4.9)$$

By applying the Chapman-Kolmogorov equation we get

$$P(x_2, t_2) = \sum_{x_0 \in \mathcal{X}} P(x_2, t_2 | x_0, t_0) P(x_0, t_0), \quad (4.10)$$

Since $P(x_2, t_2 | x_0, t_0)$ obeys the properties Eq. (4.7) and Eq. (4.8), $T(x_2, t_2 | x_0, t_0) = P(x_2, t_2 | x_0, t_0)$ for all t_2 . Therefore, given an initial x_0 at t_0 , the stochastic matrix gives the one-point probability at any t_2 . Note, this does not ensure a Markovian process. As shown previously, in a Markovian dynamics, $P(x_2, t_2 | x_0, t_0)$ shall satisfy Eq. (4.5). For $t_2 \geq t_1 \geq t_0$, it can occur $T(x_2, t_2 | x_1, t_1) \neq P(x_2, t_2 | x_1, t_1)$.

In a Markovian process we can write $P(x_2, t_2; x_1, t_1) = P(x_2, t_2 | x_1, t_1) P(x_1, t_1)$ and, therefore

$$P(x_2, t_2) = \sum_{x_1 \in \mathcal{X}} P(x_2, t_2 | x_1, t_1) P(x_1, t_1), \quad (4.11)$$

what makes $T(x_2, t_2 | x_1, t_1) = P(x_2, t_2 | x_1, t_1)$. Consider now the times $t_3 \geq t_2 \geq t_1 \geq t_0$ in a Markov process. Similarly to Eqs. (4.7) and (4.8), we get the properties

$$\sum_{x_2 \in \mathcal{X}} T(x_2, t_2 | x_1, t_1) = 1 \quad (4.12)$$

$$T(x_2, t_2 | x_1, t_1) \geq 0, \quad \text{and} \quad (4.13)$$

$$T(x_3, t_3 | x_1, t_1) = \sum_{x_2 \in \mathcal{X}} T(x_3, t_3 | x_2, t_2) T(x_2, t_2 | x_1, t_1). \quad (4.14)$$

The process described by $T(x_3, t_3 | x_1, t_1)$ is known as a *divisible process*, and all Markovian processes are divisible. However, there are also divisible non-Markovian processes (see examples in Refs. [51, 52]). A divisible process is always Markovian when the transitional matrix describes the dynamics of one-point probabilities.

Therefore, the process is Markovian if the transition matrix of the one-point probability is such that,

$$P(x_2, t_2) = T(x_3, t_3 | x_1, t_1) P(x_1, t_1), \quad (4.15)$$

can split as

$$P(x_3, t_3) = \sum_{x_2 \in \mathcal{X}} T(x_3, t_3 | x_2, t_2) T(x_2, t_2 | x_1, t_1) P(x_1, t_1) \quad (4.16)$$

for all t_2 .

4.1.3 Kolmogorov Distance

The L_1 – norm of a vector $v(x)$ is defined as

$$\|v(x)\|_1 := \sum_x |v(x)|. \quad (4.17)$$

Consider a random variable X whose probability distribution is given either by $p_1(x)$ or $p_2(x)$. By defining $w(x) := p_1(x) - p_2(x)$, the distance between $p_1(x)$ and $p_2(x)$ is given by the L_1 – norm of $w(x)$,

$$D_k(p_1, p_2) = \|w(x)\|_1 = \frac{1}{2} \|p_1(x) - p_2(x)\|_1. \quad (4.18)$$

This distance is known as *Kolmogorov distance* and can identify the divisibility of a stochastic process [53–55].

Consider two different probability distributions $p^{[1]}(t)$ and $p^{[2]}(t)$ whose evolution can be described by the transformation matrix $T(x_2, t_2|x_1, t_1)$. Then, this process is divisible if the Kolmogorov distance $D_k(p^{[1]}(t), p^{[2]}(t))$ does not increase when $T(x_2, t_2|x_1, t_1)$ is applied to $(p^{[1]}(t) - p^{[2]}(t))$. We can check this by recovering the definition of Eq. (4.17), the positivity of $T(x_2, t_2|x_1, t_1)$ and the fact that each of its rows sums up to one. Then, for $t_2 \geq t_1$ and from the properties (4.12) and (4.13), we get

$$\begin{aligned} D_k(p^{[1]}(t_2), p^{[2]}(t_2)) &= \frac{1}{2} \left\| T(x_2, t_2|x_1, t_1) (p^{[1]}(t_1) - p^{[2]}(t_1)) \right\|_1 \\ &= \frac{1}{2} \sum_{x_2 \in \mathcal{X}} \left| \sum_{x_1 \in \mathcal{X}} T(x_2, t_2|x_1, t_1) (p^{[1]}(t_1) - p^{[2]}(t_1)) \right| \end{aligned} \quad (4.19)$$

$$\begin{aligned} &\leq \frac{1}{2} \sum_{x_2 \in \mathcal{X}} \sum_{x_1 \in \mathcal{X}} T(x_2, t_2|x_1, t_1) |p^{[1]}(t_1) - p^{[2]}(t_1)| \\ &= \frac{1}{2} \sum_{x_1 \in \mathcal{X}} |p^{[1]}(t_1) - p^{[2]}(t_1)| = D_k(p^{[1]}(t_1), p^{[2]}(t_1)). \end{aligned} \quad (4.20)$$

In a Markovian process, the distance between two one-point probability distributions described by a transition matrix shall decrease monotonically. The best chance to distinguish them is at the initial times. As time goes, these probabilities distributions become even more indistinguishable. This shows that a Markovian process can not be traced back to the one-point probabilities. However, this distance can increase in non-Markovian processes, which indicates an underlying memory in the process since the system retains some information about the probabilities distributions at t_0 .

Therefore, it is possible to characterize the Markovianity of a stochastic process by means of its divisibility and by looking at one-point probability distributions distance. These properties are the basis of some definitions of quantum Markov processes.

4.2 Quantum Markov processes

It is possible to define Markovianity in quantum systems, and there are several different definitions [56–58]. Here, we shall focus on a definition that has a close analogy with the classical counterpart. However, even using this analogy, this link does not come directly.

The main problem of a straightforward definition of quantum Markovianity from the classical one is the non-commutative algebra of quantum mechanics. Although quantum mechanics can be interpreted statistically, the measurement process can directly affect the state of a system. The sampling of quantum systems is made by measurement processes, and measurement disturbs the system states. The description of $P(x_n, t_n | x_{n-1}, t_{n-1}; \dots; x_0, t_0)$ can be impracticable since each pair (x_i, t_i) , with $t \geq i \geq 0$, depends on the measurement process. Then, in the quantum realm, we do not describe a Markovian process with $P(x_n, t_n | x_{n-1}, t_{n-1}; \dots; x_0, t_0) = P(x_n, t_n | x_{n-1}, t_{n-1})$. A solution for this issue is to define the Markovianity of quantum processes with properties that do not depend on measurements.

4.2.1 Divisibility of Quantum Maps

As shown in Sec.4.1.2, the classical Markov process in one-point probability distributions can be defined in terms of divisibility of the map represented by the transition matrix. Divisibility can also be defined in the quantum case in terms of maps. The advantage of this definition is that quantum maps can be described without any knowledge of measures. As in the classical case, divisibility and quantum Markovianity are equivalent to one-point probabilities.

The density matrix ρ (Sec. A.5) of quantum systems can be interpreted as a probability distribution. In the spectral decomposition

$$\rho = \sum_x p(x) |\psi(x)\rangle \langle \psi(x)|, \quad (4.21)$$

where the eigenvalues $p(x)$ are equivalent to the classical probability to finding the system in the corresponding eigenstate $|\psi(x)\rangle$, one can define

$$P(|\psi(x)\rangle) := p(x). \quad (4.22)$$

Consider a quantum system S that has a set of possible quantum states \mathcal{S} with the same eigenvalues. If the spectral decomposition of an initial state $\rho(t_0)$ is preserved,

$$\rho(t_0) = \sum_x p(x, t_0) |\psi(x)\rangle \langle \psi(x)| \longrightarrow \sum_x p(x, t) |\psi(x)\rangle \langle \psi(x)| \rho(t) \in \mathcal{S}, \quad (4.23)$$

this process can be interpreted as stochastic on the variable x . Its divisibility can be defined similarly to classical processes (Sec. 4.1.2). Then, in a Markov process, there is a

matrix $T(x_1, t_1|x_0, t_0)$ that maps $p(x_0, t_0)$ into $p(x_1, t_1)$,

$$p(x_1, t_1) = \sum_{x_0 \in \mathcal{X}} T(x_1, t_1|x_0, t_0)p(x_0, t_0), \quad (4.24)$$

with $t_1 \geq t_0$, satisfying Eqs. (4.12), (4.13), and (4.14).

A dynamical process from the initial state $\rho(t_0)$ to $\rho(t_1)$,

$$\rho(t_0) = \sum_{x_0 \in \mathcal{X}} p(x_0, t_0) |\psi(x_0)\rangle \langle \psi(x_0)| \longrightarrow \sum_{x_1 \in \mathcal{X}} p(x_1, t_1) |\psi(x_1)\rangle \langle \psi(x_1)| = \rho(t), \quad (4.25)$$

can be described by a dynamical map \mathcal{E}_{t_1, t_0} that preserves the spectral decomposition,

$$\rho(t_1) = \mathcal{E}_{t_1, t_0} [\rho(t_0)]. \quad (4.26)$$

By applying Eq. (4.24) to the right side of Eq. (4.26) we obtain

$$\mathcal{E}_{t_1, t_0} [\rho(t_0)] = \sum_{x_0 \in \mathcal{X}} p(x_0, t_0) \mathcal{E}_{t_1, t_0} |\psi(x_0)\rangle \langle \psi(x_0)| \quad (4.27)$$

$$= \sum_{x_0, x_1 \in \mathcal{X}} T(x_1, t_1|x_0, t_0) p(x_0, t_0) |\psi(x_1)\rangle \langle \psi(x_1)| \quad (4.28)$$

$$= \sum_{x_1 \in \mathcal{X}} p(x_1, t_1) |\psi(x_1)\rangle \langle \psi(x_1)|. \quad (4.29)$$

Since \mathcal{E}_{t_1, t_0} obeys the properties of Eqs. (4.12), (4.13), and (4.14), when applied to any state of \mathcal{S} , the trace and positivity are preserved. Then, \mathcal{E}_{t_1, t_0} transforms a physical quantum state in another physical quantum state. Furthermore, these properties guarantee the composition law

$$\mathcal{E}_{t_3, t_1} = \mathcal{E}_{t_3, t_2} \mathcal{E}_{t_2, t_1}, \quad t_3 \geq t_2 \geq t_1. \quad (4.30)$$

We define a trace-preserving linear map \mathcal{E}_{t_2, t_1} as a *positive-divisible map* for all $t_2 \geq t_1 \geq t_0$ if it obeys Eq. (4.30). When the evolution of a quantum system can be described by positive divisible maps that fulfill Eq. (4.30), one defines this dynamics as a *quantum Markovian process*.

The sensibility of quantum systems to measurements makes it difficult to define *quantum Markovianity* in terms of Eq. (4.1). Thus, to come at a definition of quantum Markovianity analog to the classical, we shall focus on one-point probabilities.

An important mathematical result that worth mentioning is the *Gorini-Kossakowski-Sudarshan-Lindblad (GKSL) equation* or *Lindblad equation* [59–61]. It is a master equation in Lindblad form that describes in a general form the Markovian evolution of an open quantum system. The GKSL theorem states that an operator \mathcal{L}_t is a generator of a Markovian process if and only if it can be written as

$$\frac{d\rho(t)}{dt} = \mathcal{L}_t [\rho(t)] = -i [H(t), \rho(t)] + \sum_k \gamma_k(t) \left[V_k(t) \rho(t) v_k^\dagger(t) - \frac{1}{2} \{ V_k^\dagger(t) V_k(t), \rho(t) \} \right], \quad (4.31)$$

where $V(t)$ is a time-dependent operator, $H(t)$ the time-dependent Hamiltonian, and with $\lambda_k(t) \geq 0$ for all values of k and t . The complete proof of this theorem can be found in Refs. [59, 62].

4.2.2 Memoryless and Contractive properties in Quantum Markovian Processes

It is not straightforward from the divisibility property the lack of memory in quantum Markovian systems. Therefore, we may look at the contractive properties of the completely positive (CP) maps to see this memoryless more intuitively.

Hypothesis testing problems are quite useful to understand the contractivity of CP maps. Consider a quantum system S associated with a Hilbert space \mathcal{H} in two possible states: ρ_1 with probability q and ρ_2 with probability $(1 - q)$. To find the density matrix that represents the state of S correctly, we can measure it with a POVM T . Then, the best choice of T that minimizes the probability to choosing the wrong ρ , is such that

$$P_{\min}(\text{Fail}) = \min_{0 \leq T \leq \mathbb{I}} \{(1 - q) \text{Tr} [\rho_2 T] + q \text{Tr} [\rho_1 (\mathbb{I} - T)]\} \quad (4.32)$$

$$= \frac{1 - \|\Delta\|_1}{2} \quad (4.33)$$

with $\|\Delta\|_1 = \text{Tr} \sqrt{\Delta^\dagger \Delta}$ and where $\Delta = q\rho_1 - (1 - q)\rho_2$ is a Hermitian operator also known as *Helstrom matrix* [63]; this is a theorem whose proof can be found in Ref. [53]. Since \mathcal{E} is linear, applying it to Δ is equivalent to

$$\mathcal{E}(\Delta) = q\mathcal{E}(\rho_1) - (1 - q)\mathcal{E}(\rho_2). \quad (4.34)$$

Therefore, when \mathcal{E} acts on ρ_1 and ρ_2 , at some time $t > 0$, the states will become $\rho_1(t)$ and $\rho_2(t)$ respectively.

Note, therefore, that the trace norm of Δ gives the distinguishability between states ρ_1 and ρ_2 through a POVM T . It is also possible to connect trace-preserving and positive maps with the trace norm. In Refs. [64, 65], A. Kossakowski proved that “a trace-preserving” linear map \mathcal{E} is positive if and only if for any Hermitian operator Δ acting on \mathcal{H} ,

$$\|\mathcal{E}(\Delta)\|_1 \leq \|\Delta\|_1, \quad (4.35)$$

This theorem shows that an operator Δ subject to a CPTP map \mathcal{E} decreases the distinguishability between the states $\rho_1(t)$ and $\rho_2(t)$ for any $t > 0$.

As shown in Eqs. (4.27) to (4.30), a quantum Markov process \mathcal{E}_{t_2, t_1} is CPTP for all $t_2 \geq t_1 \geq t_0$. Thus, we can connect the divisibility with the last theorem and conclude that a process is Markovian when

$$\|[\mathcal{E}_{t_2, t_1} \otimes \mathbb{I}](\tilde{\Delta})\|_1 \leq \|\tilde{\Delta}\|_1. \quad (4.36)$$

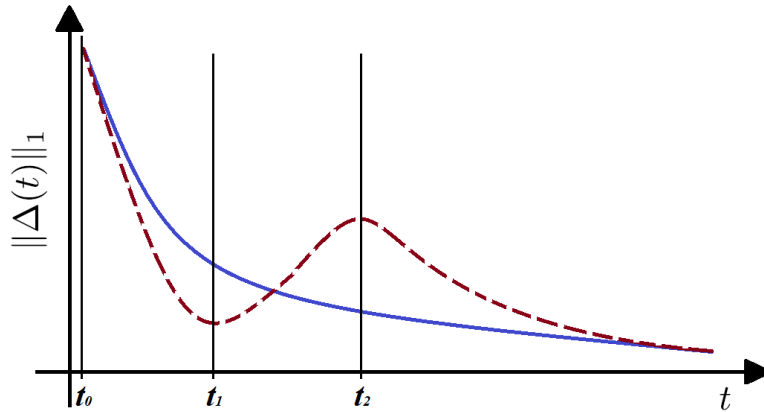


Figure 9 – For $\mathcal{E}(\Delta(t_0)) = \Delta(t)$, $\|\Delta(t)\|_1$ is the distinguishability between two possible states $\rho_1(t)$ and $\rho_2(t)$ of system at some time $t > 0$. The blue (solid) line represents a system under a Markovian process. The red (dashed) line represents a non-Markovian process of a system. It is possible to observe that distinguishability decreases monotonically when the system is subject to a Markovian process. However for non-Markovian cases one can find $\|\Delta(t_2)\|_1 > \|\Delta(t_1)\|_1$, signaling an underlying memory in the dynamics.

where $\tilde{\Delta}$ is any Hermitian operator acting on $\mathcal{H} \otimes \mathcal{H}$. We are considering $\tilde{\Delta}$ instead of Δ because Markovianity just makes sense in open quantum systems since closed systems are trivially Markovian.

Similar to classical evolutions, states of quantum systems become less distinguishable when a CPTP-divisible map can describe its evolution, that is, when \mathcal{E}_{t_2, t_1} is Markovian. The distinguishability of Markovian dynamics decreases monotonically with time. This means that the best chance to distinguish between ρ_1 and ρ_2 is at t_1 , since they become even more indistinguishable with time. However, when \mathcal{E}_{t_2, t_1} represents a non-Markovian dynamics, $P_{\min}(\text{Fail})$ can increase, and the states become more distinguishable at a later time t_2 (Fig. 9). It is also important to highlight that in non-Markovian cases, the distinguishability at t_2 can not be larger than the distinguishability at t_0 , see Fig. 9.

The increase of distinguishability with time can be understood as the presence of memory in the dynamics. As opposed to Markovian dynamics, systems under non-Markovian processes can store information about its initial state that can be recovered at posterior times.

4.3 Quantification and detection of non-Markovianity

Once defined quantum Markovianity, we can define how to quantify and detect it in quantum systems. From the definition of quantum Markovianity presented here and the postulates of quantum mechanics, it is easy to see that closed quantum systems are

trivially Markovian. The dynamics of closed quantum systems are always unitary, and unitary matrices $U(t_1, t_0)$ are CPTP and divisible, that is,

$$U(t_2, t_0) = U(t_2, t_1)U(t_1, t_0). \quad (4.37)$$

Therefore, by definition, $U(t_1, t_0)$ fulfills all requirements of a Markovian process. On the other hand, it was found that the evolution of open quantum systems is, strictly speaking, non-Markovian [8, 66]. We can quantify non-Markovianity in open quantum systems by exploring the concepts of divisibility and distance of maps and channels, and detect it via witness. In this section, we present some methods to quantify and detect non-Markovianity and present a method frequently used to detect and quantify it jointly.

4.3.1 Quantification Via Quantum Maps

The *degree of non-Markovianity* is broadly used to quantify non-Markovianity. It is a normalized quantity between zero and one, where zero is obtained when the process is Markovian and one when its non-Markovianity is maximal. This quantity can be obtained by exploring the concepts of divisibility and distance of maps and channels. As there are available in literature diverse ways to quantify non-Markovianity [67–71], we focus on two of them, the geometric measures and by optimization of the Helstrom matrix norm.

Initially proposed to measure the non-Markovianity of quantum channels, the geometric measure of non-Markovianity is an important approach [67]. To understand this method, consider a system S whose dynamics is described by the map \mathcal{E}_{t,t_0} and a set of Markovian processes $\mathcal{M} = \{\mathcal{E}_{t,t_0}^1, \dots, \mathcal{E}_{t,t_0}^M\}$. The quantity of non-Markovianity of this process can be based on the distance between \mathcal{E}_{t,t_0} and each Markovian dynamics \mathcal{E}_{t,t_0}^i , $\mathcal{D}(\mathcal{E}_{t,t_0}, \mathcal{E}_{t,t_0}^i)$, see Fig. 10. Therefore, the *geometric measure of non-Markovianity* at a time t is defined as

$$\mathcal{N}_{GM}^t(\mathcal{E}_{t,t_0}) := \min_{\mathcal{E}_{t,t_0}^i \in \mathcal{M}} \mathcal{D}(\mathcal{E}_{t,t_0}, \mathcal{E}_{t,t_0}^i). \quad (4.38)$$

Observe that $\mathcal{N}_{GM}^t(\mathcal{E}_{t,t_0})$ is zero only when \mathcal{E}_{t,t_0}^i represent a Markovian process.

A measure of non-Markovianity degree $\mathfrak{D}_{NM}^{\mathcal{I}}$ can be defined as the maximization of $\mathcal{N}_{GM}^t(\mathcal{E}_{t,t_0})$ for a given time interval \mathcal{I} , that is,

$$\mathfrak{D}_{NM}^{\mathcal{I}} := \max_{t \in \mathcal{I}} \mathcal{N}_{GM}^t(\mathcal{E}_{t,t_0}), \quad (4.39)$$

ranging between 0 and 1. The process is Markovian only when $\mathfrak{D}_{NM}^{\mathcal{I}} = 0$ and non-Markovian for values larger than zero.

Although this method is quite precise, it is quite hard to compute. The calculation becomes impracticable in systems with large dimensions.

Another interesting method to quantify non-Markovianity is by optimization of the Helstrom matrix norm. As shown in Sec. 4.2.2, the norm of the Helstrom matrix

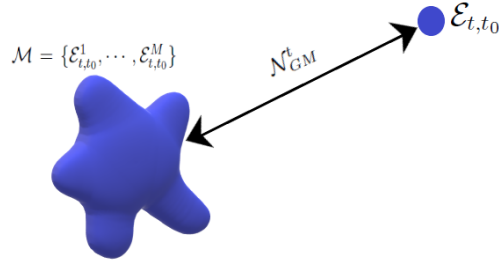


Figure 10 – Geometric measure of non-Markovianity: It is the distance between the map \mathcal{E}_{t,t_0} and the non-convex set of Markovian maps. The degree of non-Markovianity \mathfrak{D} is the maximal value of $\mathcal{N}_{GM}^t(\mathcal{E}_{t,t_0})$ at a time t

$\Delta = q\rho_1 - (1 - q)\rho_2$ gives the distance between two possible states of the system ρ_1 and ρ_2 when these last are subject to a POVM. We could see that when the distance between these states increases with time, that is, $\|\Delta(t)\|_1 < \|\Delta(t + \epsilon)\|_1$ at any $t > 0$, the states ρ_1 and ρ_2 become more distinguishable at $t + \epsilon$. This indicates that the system has a memory where its initial state is stored.

In Markovian systems, one expects the information flows from the system to the environment. The increase in distinguishability can be interpreted as a back-flow of information from the environment to the system [58]. However, the information way is not enough to characterize non-Markovianity because it is possible to find non-Markovian dynamics with no back-flow [72].

As proposed in Ref. [68], it is possible to quantify the non-Markovianity by exploring the concept of distance in a Helstrom matrix. As non-Markovianity is a feature of open quantum systems, we shall consider an environment E in this analysis, and for simplicity, we can consider $\dim\mathcal{H}_E = \dim\mathcal{H}_S$. The Helstrom matrix for the composite system SE is $\tilde{\Delta} = q\rho_1^{SE} - (1 - q)\rho_2^{SE}$ with $\Delta = \text{Tr}_E\tilde{\Delta}$ and $\|\tilde{\Delta}(t)\|_1 = \|[\mathcal{E}_{t,t_0} \otimes \mathbb{I}](\tilde{\Delta}(t_0))\|_1$. For $t > 0$, any increase in the norm of the Helstrom matrix at $t + \epsilon$ in comparison with t indicates that the state's distinguishability increased and the dynamics are non-Markovianity. Then, the maximal distinguishability for a given time t is given by

$$\begin{aligned} \sigma(\tilde{\Delta}, t) &:= \lim_{\epsilon \rightarrow 0^+} \frac{\|\tilde{\Delta}(t + \epsilon)\|_1 - \|\tilde{\Delta}(t)\|_1}{\epsilon} \\ &:= \frac{d\|\tilde{\Delta}(t)\|_1}{dt}. \end{aligned} \quad (4.40)$$

The quantity of non-Markovianity in a time interval I can be obtained by integrating $\sigma(\tilde{\Delta}, t)$ and maximizing over all possible $\tilde{\Delta}$

$$\mathcal{N}_H^I = \max_{\tilde{\Delta}} \int_{t \in I, \tilde{\Delta} > 0} \sigma(\tilde{\Delta}, t) dt. \quad (4.41)$$

The process is Markovian only when $\mathcal{N}_H^I > 0$; otherwise, it is not non-Markovian. The larger \mathcal{N}_H^I , the larger the non-Markovianity. Similar to geometric measures, the quantification of non-Markovianity with this method is quite complex and becomes impracticable for large dimensions.

4.3.2 Detection Via Quantum Witness

Although the characterization and quantization of quantum non-Markovianity can be quite tricky, the violation of any Markovianity criterion is a strong indicator of non-Markovianity. One can establish a criterion for detecting the non-Markovianity and define a quantity linked to it that vanishes when the system dynamics is Markovian. This quantity is known as a *witness of non-Markovianity*, and, albeit it can also vanish in the non-Markovian process, it surely indicates non-Markovianity if larger than zero [53, 59].

From the definition of quantum Markov processes presented in Sec. 4.2, it is possible to define witnesses of monotonicity in dynamics described by *local* completely positive maps and witnesses of monotonicity in dynamics described by *general* completely positive maps. As the main work of this thesis was based on a witness of monotonicity under local completely positive maps, we shall focus on it. However, we may briefly introduce witnesses of monotonicity under completely positive maps.

4.3.3 Witnesses of Local Completely Positive Maps

This witness can be defined in systems whose dynamics are described by a local map. For a system S interacting with its environment E , the dynamic is given by a map acting directly only in the system, $\mathcal{E} = \mathcal{E}_S \otimes \mathbb{I}_E$. In this case, entanglement, mutual information, for example, can be suitable witnesses.

As proposed in Ref. [69], entanglement can be a non-Markovianity witness. By defining the entanglement quantifier E as in Ref [73], a dynamic is non-Markovian in an interval (t_0, t_1) when the quantity

$$\mathcal{Q}^{(E)} := \Delta E + \int_{t_0}^{t_1} \left| \frac{dE(\rho_{SE}(t))}{dt} \right| dt, \quad (4.42)$$

with $\Delta E = E(\rho_{SE}(t_1)) - E(\rho_{SE}(t_0))$, is larger than zero.

Quantum mutual information (Sec. 3.4) can also be a witness of non-Markovianity [74]. We can rewrite the equation that defines quantum mutual information, Eq. (3.6), as

$$I(S, E) = H(\rho_{SE} || \rho_S \otimes \rho_E) \quad (4.43)$$

and apply a local operation $\mathcal{E} = \mathcal{E}_S \otimes \mathbb{I}_E$. Then, for a composed system SE we get

$$I(\mathcal{E}(\rho_{SE})) = H(\mathcal{E}(\rho_{SE}) || \text{Tr}_S[\mathcal{E}(\rho_{SE})] \otimes \text{Tr}_S[\mathcal{E}(\rho_{SE})]) \quad (4.44)$$

$$= H(\mathcal{E}(\rho_{SE}) || \mathcal{E}(\rho_{SE} \otimes \rho_{SE})) \leq H(\rho_{SE} || \rho_S \otimes \rho_E) = I(\rho_{SE}). \quad (4.45)$$

This indicates that the mutual information of SE behaves monotonically when the dynamics are described by a CPTP map, that for definition, represents a Markov process (see Sec. 4.2.1). If mutual information is not monotonic, the process is non-Markovian.

We can also look at states under (not necessarily local) completely positive maps as *quantum relative entropies* [75,76], *Quantum Fisher information* [77], *capacity measures* [78], and *Bloch volume measure* [79]. In the next section, we shall focus on two witnesses of completely positive maps: trace distance and fidelity.

4.4 Trace Distance and Fidelity

It is worth drawing attention to trace distance and fidelity as witnesses of non-Markovianity. These two concepts provide tools that not only identify non-Markovianity but also quantify it. Fidelity and trace distance as witnesses of non-Markovianity come intuitively from the definition of quantum Markov processes given in Sec. 4.2 and can be applied in several numerical computations.

4.4.1 the BLP Quantifier

In Refs. [58, 80], *Breuer, Laine, and Piilo* define a witness of non-Markovianity based on trace distance known as *the BLP quantifier*. To understand it, we may consider an unbiased Helstrom matrix (Sec. 4.2.2), that is, with $q = 1/2$. In this case, we find $\Delta = 1/2(\rho_1 - \rho_2)$ where the probability of finding ρ_1 and ρ_2 is the same. Since the *trace distance* between ρ_1 and ρ_2 is defined as

$$D(\rho_1, \rho_2) := \frac{1}{2} \|\rho_1 - \rho_2\|_1, \quad (4.46)$$

where the L_1 -norm of Δ becomes the trace distance between these two states. For some time instant t and a posterior time $t + \epsilon$ one can define a quantity $\sigma(\rho_1, \rho_2, t)$ as

$$\sigma(\rho_1, \rho_2, t) := \frac{d}{dt} D(\rho_1, \rho_2) := \lim_{\epsilon \rightarrow 0^+} \frac{D(\rho_1(t + \epsilon), \rho_2(t + \epsilon)) - D(\rho_1(t), \rho_2(t))}{\epsilon}. \quad (4.47)$$

Therefore, for any time interval (t_1, t_2) , the dynamic is non-Markovian when the quantity

$$\int_{t \in (t_1, t_2), \sigma > 0} \sigma(\rho_1, \rho_2, t) dt \quad (4.48)$$

is nonzero for two states ρ_1 and ρ_2 . The above integral is taken only when $\sigma > 0$ and the trace distance increases for a time interval t and $t + \epsilon$ with $\epsilon \rightarrow 0^+$, indicating an increase in the distinguishability between ρ_1 and ρ_2 increases. This quantity can also be used to quantify non-Markovianity by taking its maximal value in a time interval $(0, \infty)$,

$$\mathcal{N}_{\text{BLP}} = \rho_1, \rho_2 \max_{t \in (t_1, t_2), \sigma > 0} \int \sigma(\rho_1, \rho_2, t) dt. \quad (4.49)$$

The larger \mathcal{N}_{BLP} , the larger the non-Markovianity of the system.

4.4.2 Fidelity

Fidelity is a concept quite applied in information theory and was adapted to quantum information theory. In general terms, *fidelity* is a quantifier that indicates the accuracy of the signal received in comparison with the signal originally sent.

Consider a classical signal traveling in a communication channel. This signal can suffer some interference and noise during the transmission. The maximal rate that we can send signals by the channel with a vanishingly low probability of error is named *capacity* C . Shannon proved in 1948 that in a discrete and memoryless channel, for all transmission rates $R < C$, a sequence of N signals with a maximal probability of error $\epsilon^{[n]} \rightarrow 0$ exists [38]. Roughly speaking, this theorem shows that it is possible to send in a rate R less than C where the error can be significantly minimized if we adjust the sequence N . In this case, fidelity is a quantifier that indicates the accuracy of the signal received in comparison with the signal originally sent.

In 1994, Jozsa and Schumacher Ref. [81] adapted the channel coding theorem to quantum signals of pure states. The definition of Fidelity for any two pure quantum states $|\psi_1\rangle$ and $|\psi_2\rangle$ is the transition probability between them, that is,

$$\mathcal{F}(|\psi_1\rangle\langle\psi_2|, |\psi_1\rangle\langle\psi_2|) := |\langle\psi_2|\psi_1\rangle|^2. \quad (4.50)$$

Soon later, Jozsa [82] extended fidelity of quantum system for mixed states ρ_1 and ρ_2 and defined

$$\mathcal{F}(\rho_1, \rho_2) := \|\sqrt{\rho_2}\sqrt{\rho_1}\|_1^2 \quad (4.51)$$

$$= \left(\text{Tr} \left[\left(\sqrt{\rho_1\rho_2\rho_1} \right)^{\frac{1}{2}} \right] \right)^2. \quad (4.52)$$

One of the properties of Fidelity is monotonicity under complete positive maps \mathcal{E} , that is

$$\mathcal{F}(\rho_1, \rho_2) \geq \mathcal{F}(\mathcal{E}(\rho_1), \mathcal{E}(\rho_2)). \quad (4.53)$$

Fidelity is constant only when \mathcal{E} is a unitary operator [83] and, therefore, Markovian. Any increase of \mathcal{F} implies a decrease in distinguishability, indicating non-Markovianity in the process. Thus, fidelity can be a Markovianity witness.

As for trace distance, one can also use fidelity to quantify non-Markovianity [84]. Optimizing all pairs of states (ρ_1, ρ_2) in a time interval Δt , one can define the non-Markovianity degree as

$$\mathcal{N}_{\mathcal{F}}(\rho_1, \rho_2) = \max_{\rho_1, \rho_2} \int_{d\mathcal{F}/dt > 0} \frac{d\mathcal{F}(\rho_1, \rho_2)}{dt} dt. \quad (4.54)$$

The maximization is taken by all possible pair (ρ_1, ρ_2) , and $d\mathcal{F}/dt$ is integrated only when its value is positive, that is, only when the fidelity is increasing. Therefore, for all

pairs (ρ_1, ρ_2) and a given Δt , the maximal value of the accumulated increase of \mathcal{F} is a non-Markovianity degree.

This quantifier was used to calculate the non-Markovianity of continuous-variable Gaussian dynamical maps [84], and to relate quantum Darwinism and non-Markovianity [40, 50]. These two last references are detailed in Chap. 5.

5 Quantum Darwinism and Non-Markovianity

In this chapter, we present our main result. We investigated the effect of non-Markovianity on the observation of quantum Darwinism. The primary reference to this investigation is a work claiming that non-Markovianity hinders quantum Darwinism [50]. They used an open quantum system within an environment of quantum harmonic oscillators in quantum Brownian motion.

In our work, we used a similar model. The main system and the environment are composed of quantum harmonic oscillators, all in coherent states. Using both approaches to quantum Darwinism, we showed that the averaged redundancy in a given time interval ΔT is not affected by non-Markovianity. We propose a new point of view to quantify the quantum Darwinism in a given system and show that, in the model studied, the observation of quantum Darwinism is not affected by non-Markovianity.

In Sec. 5.1 we detail the model used in *Galve et al.* and then we briefly describe the approaches used to connect quantum Darwinism and non-Markovianity concepts. Section 5.2 introduces the model and techniques used in our work and presents our results.

5.1 Quantifying Quantum Darwinism Through the Non-Monotonicity of f_δ

A relation between quantum Darwinism and non-Markovianity was first proposed in Ref. [50], where the authors concluded that non-Markovianity hinders quantum Darwinism. They used the same model of quantum harmonic oscillators in quantum Brownian presented in Ref. [42] (Sec. 3.7.1) and computed the non-Markovianity degree using the BPL and fidelity quantifiers (Sec. 4.4).

In this model, the system S is a quantum harmonic oscillator of frequency ω_S inserted in an environment $\mathcal{E} = \otimes_{k=1}^N \mathcal{E}_k$ composed of N other quantum harmonic oscillators with frequency $\omega_k = \omega_0 + k\Delta$, with $\Delta = (\omega_R - \omega_0)/N$. The interaction between S and \mathcal{E} is given by

$$H_I = \kappa x_S \sum_{k=1}^N c_k x_k, \quad (5.1)$$

where x_S and x_k are the position operators of the system and the environment, respectively.

The spectral density is given by

$$J(\omega) = \sum_{k=1}^N \frac{c_k^2}{\omega_k} \delta(\omega - \omega_k). \quad (5.2)$$

When $N \rightarrow \infty$, we can take the continuum limit and the sum in Eq. 5.2 can be substituted by an integral in $d\omega$. Usually, it is used the approximation $J(\omega) \sim \omega^s f(\omega/\omega_R)$, where $f(\omega/\omega_R)$ is the function cut-off. In the case of Ohmic environments, $s = 1$ and $f(\omega/\omega_R)$ decays quickly for $\omega > \omega_R$.

As this work aims to investigate the effects of non-Markovianity in quantum Darwinism, it is important to vary and control the non-Markovianity of the system. In Rubin's model [49, 85], the system is a heavy particle of mass M and the coordinate x and interacts bilinearly with a half-infinite chain of harmonic oscillators of mass m_i , coupling strength g and spring constants $f = m\omega_R^2/4$, where ω_R is the highest frequency of the reservoir modes. The spectral density is given by

$$J(\omega) = \kappa \sqrt{\omega^2 - \omega_0^2} \sqrt{\omega_R^2 - \omega^2}, \quad (5.3)$$

where $\omega_R = \sqrt{\omega_0^2 + 4g}$. For $\omega_0 = 0$, the model achieves ohmic damping, and the non-Markovianity can be controlled by detuning the system in relation to the bath. The system is Markovian only when $\omega_S = \omega_0$ and the non-Markovianity grows with $|\omega_0 - \omega_S|$.

As in the work presented in Sec. 3.7.1, it was considered the initial state of the system squeezed in momentum by a parameter s_p

$$|\psi(0)\rangle_S \propto \int dx e^{\frac{-x^2}{2\sigma^2}} |x\rangle, \quad (5.4)$$

with $2\sigma^2 = e^{2s_p}$, and the environment initially in the vacuum state. As the system and environment interact, the global state evolves to

$$|\psi(0)\rangle_{SE} \propto \int dx e^{\frac{-x^2}{2\sigma^2}} |x\rangle \bigotimes_i |\psi_i(x)\rangle, \quad (5.5)$$

where $|\psi_i(x)\rangle$ is the state of the i -th subenvironment state in relation to the position x .

The perfect condition for the observation of quantum Darwinism in this model happens when the distinguishability between any two subenvironments states is high, that is

$$\langle \psi_i(x) | \psi_i(x') \rangle \sim \delta_{x,x'}. \quad (5.6)$$

In the state $|\psi_i(x)\rangle$, each x is related to a pointer state of the system. When it is possible to differentiate with certainty states with distinct values of x , one can infer the state of the system by measuring a single subenvironment. In more realistic scenarios, it is required more than one subenvironment to obtain an acceptable quantity of information about the system. In this case, one can measure fractions of the environment, and the smaller the fractions required, the larger the quantity of redundant information in the environment.

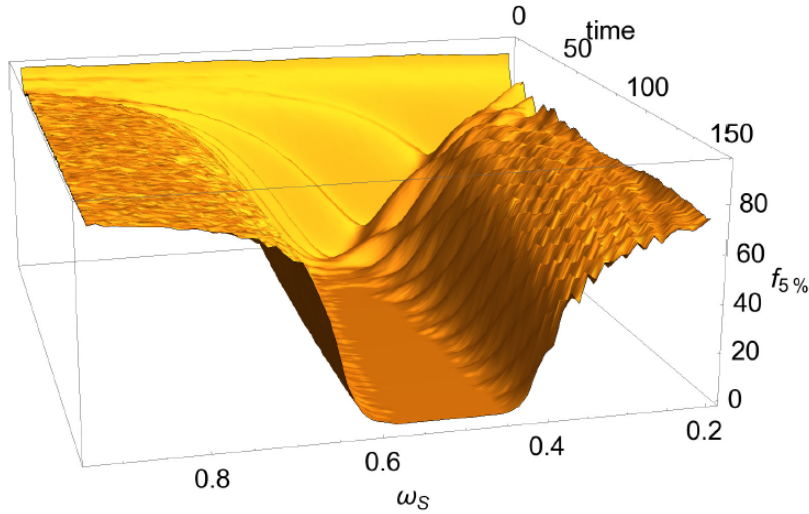


Figure 11 – (Color) For $N = 300$, an initial $s_p = 10$, $\delta = 0.05$, $\omega_0 = 0.3$ and $\omega_R = 0.7$, this 3D plot shows f_δ in function of ω_S and t . This image was taken from Ref. [50].

As fidelity increases monotonically when a completely positive map can represent the system's dynamics, it can be used to quantify non-Markovianity. (Sec. 4.4) [84]. Then, for two different possible states of the system ρ_1 and ρ_2 , the non-Markovianity degree was computed according to

$$\mathcal{N}(\rho_1, \rho_2) = \max_{\rho_1, \rho_2} \int_{d\mathcal{F}/dt > 0} \frac{d\mathcal{F}(\rho_1, \rho_2)}{dt} dt. \quad (5.7)$$

Basically, this equation computes the accumulated value of the fidelity increasing and takes the maximal value between all possible combinations of the states ρ_1 and ρ_2 .

As in Ref. [42], the authors used the PIP approach (Sec. 3.4) where the correlations between the system and the environment are given by the mutual information

$$I(S : f) = H_S + H_f - H_{S,F}, \quad (5.8)$$

where H_S , H_f , and $H_{S,f}$ are the von Neumann entropies of the system S , the fraction of the environment f , and the system and environment jointly, respectively.

They first calculated f_δ as defined in Sec. 3.4. For a system initially in a pure state, they randomly choose the subenvironments of the fractions. For $\delta = 0.05$ and $\omega_0 = 0.3$, the plot in Fig. 11 shows the behavior of $f_{5\%}$ varying on time and with ω_S . Observe that when $\omega_S = \omega_0$, $f_{5\%}$ is minimal, meaning that the fraction necessary to obtain 95% of information about the system available in the whole environment is quite small. Therefore, in this situation, the redundancy is high, indicating that quantum Darwinism is held. However, $f_{5\%}$ grows quickly with the difference $|\omega_S - \omega_0|$; that is, $f_{5\%}$ increases with the system's non-Markovianity. The larger $f_{5\%}$, the smaller the redundancy, decreasing quantum Darwinism observation.

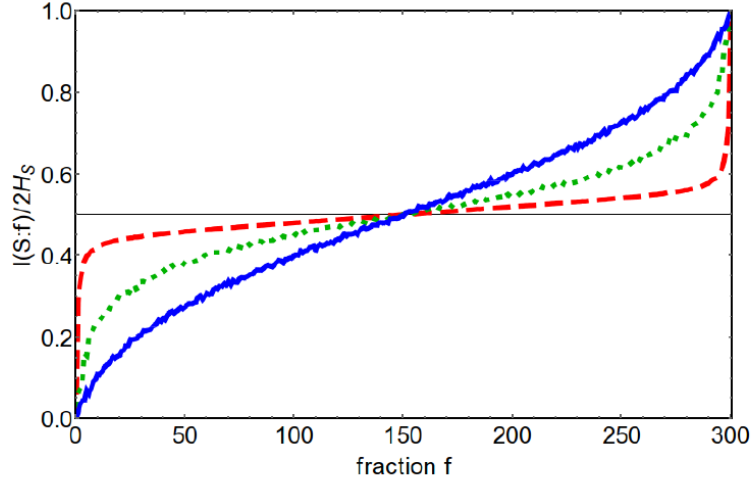


Figure 12 – (Color). PIP for $t = 40(\text{a.u.})$, an initial $s_p = 3$, $\omega_R = 0.7$, $\omega_0 = 0.3$, $\omega_S = 0.3$ (red-dashed line), $\omega_S = 0.7$ (green-dotted line), and $\omega_S = 1$ (blue-solid line). This image was taken from Ref. [50].

This behavior is also clear in PIP. When $\omega_S = \omega_0$ (red-dashed line) in Fig. 12, the plateau shape is evident, and as the difference $|\omega_S - \omega_0|$ increases (green-dotted and blue-solid lines), the plot becomes even more linear. To better visualize the relation between non-Markovianity and quantum Darwinism, we can look at Fig. 13, where $f_{5\%}$, the spectral distribution, and the non-Markovianity degree \mathcal{N} are all plotted together. The fraction $f_{5\%}$ plot (blue-solid line) grows with $|\omega_S - \omega_0|$, and \mathcal{N} (red-dotted line) has a similar behavior up to the edges of spectrum $J(\omega)$ (shaded-gray area). This was interpreted as a connection between the quantum Darwinism observation and the Non-Markovianity degree.

It was proposed the following quantifier of the f_δ non-monotonic behavior:

$$\mathcal{N}_f = \int_{df_\delta/dt > 0} \frac{df_\delta}{dt} dt. \quad (5.9)$$

\mathcal{N}_f infer how many “non-Darwinistic” is the system’s behavior; and it is similar to the definition of non-Markovianity degree \mathcal{N} . The quantity \mathcal{N}_f is the accumulated value of the f_δ increasing; the integral over $\frac{df_\delta}{dt}$ is only taken when f_δ is increasing on time. The plot in Fig. 13 shows that \mathcal{N}_f (green-dashed line) behaves similarly to \mathcal{N} even when the system frequency exceeds the edges frequencies of $J(\omega)$. Therefore the authors used this fact to conclude that non-Markovianity hinders quantum Darwinism.

This model shows a strong connection between quantum Darwinism and non-Markovianity just by analyzing the PIP. However, the quantifier \mathcal{N}_f can sometimes be inappropriate. In some dynamics, the fluctuations of f_δ with time can have larger amplitudes. In such cases, f_δ ranges between very small and very large values. At times where f_δ is small quantum Darwinism can securely be observed and, at times where f_δ is large, it can not. To be more precise, it is better to look at the average of f_δ in a given time

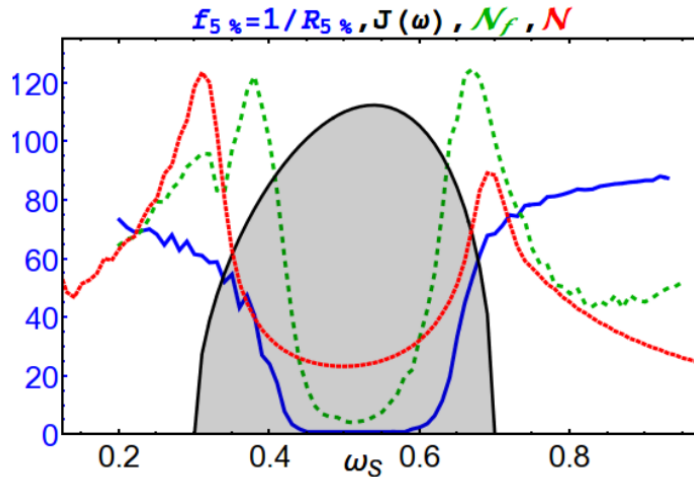


Figure 13 – (Color) For $s_p = 10$, $\delta = 0.05$, $\omega_0 = 0.3$, $\omega_R=0.7$, and $t = 150$, this graphic shows spectral density $J(\omega)$ (shaded-gray line), non-Markovianity degree \mathcal{N} (red-dotted line), fraction f_δ (blue-solid line) and non-monotonicity of $f_\delta \mathcal{N}_f$ (green-dashed line). This image was taken from Ref. [50].

interval when comparing quantum Darwinism in Markovian and non-Markovian systems.

The next section presents the work where we compared quantum Darwinism and non-Markovianity in a model where fluctuations amplitude of f_δ are considerable and present a new method to quantify quantum Darwinism in these situations.

5.2 Quantum Darwinism and non-Markovianity in a Model of Quantum Harmonic Oscillators

To better understand quantum Darwinism (QD), we investigated how information about an open quantum system is spread redundantly in the environment. In this model, the system is a single quantum harmonic oscillator and the environment is an ensemble of several other quantum harmonic oscillators. The degree of non-Markovianity is controllable through the coupling between the system and the environment.

Sec. 5.2.1 and Sec. 5.2.2 describe the model and its dynamics. Sec. 5.2.3 deduces the preferential observable. Sec. 5.2.4 and 5.2.5 analyze QD through the two approaches presented in Sec. 3 and compare the obtained results. The BPH approach was shown to be more robust than the PIP approach; though, both can identify the QD in the model.

As a simple parameter can alter the non-Markovianity in this model, we also explored this concept. However, a metric is required to quantify the non-markovianity. In Sec. 5.2.6, we defined the non-markovianity degree based on the distance between states [58] as in Ref. [50], and studied in our model.

With the methods to characterize the QD and non-Markovianity well-defined, Sec. 5.2.7 examines the possible connections between these two concepts. The results indicate that the time-varying curve of the redundancy in the environment is different from distinct non-Markovianity degrees. However, the averaged redundancy in a specific time interval does not change with the non-Markovianity degree, indicating that the observation of the QD in this model does not depend on non-Markovianity.

5.2.1 The Model

The model consists of a single quantum harmonic oscillator, which is designated as the “system”, and a set of quantum harmonic oscillators designated as the “environment”. The system interacts individually with each oscillator of the environment and the environment oscillators do not interact with each other, see Fig. 3. The Hamiltonian that drives this system is given by

$$H = \hbar\omega_0 a^\dagger a + \hbar \sum_{k=1}^N \omega_k b_k^\dagger b_k + \hbar \sum_{k=1}^N \gamma_k (a^\dagger b_k + a b_k^\dagger), \quad (5.10)$$

where ω_0 is the main oscillator frequency, ω_k is the k -th environment oscillator frequency, a , a^\dagger , b_k , and b_k^\dagger are the creation and annihilation operators of the main system and the k -th environment oscillator respectively, and γ_k are coupling constants for the interaction between the k -th environment oscillator and the main oscillator. We shall set from now on $\hbar = 1$. This model has been used, to study dissipation in optical cavities [86], the dynamical properties of multipartite entanglement [87], and principles of quantum thermodynamics [88].

By using the ansatz presented in [86], if the system is initially in a coherent state with a parameter $\alpha_0 \in \mathbb{C}$ and the environment is in a vacuum,

$$|\alpha_0\rangle \otimes \prod_{k=1}^N |0_k\rangle, \quad (5.11)$$

then, the evolved state is given by

$$|\alpha(t)\rangle \otimes \prod_{k=1}^N |\lambda_k(t)\rangle, \quad (5.12)$$

where $|\alpha(t)\rangle$ and $|\lambda_k(t)\rangle$ denote coherent states of the main oscillator and the k -th environment oscillator, respectively. Applying Schrödinger’s equation to the Hamiltonian in Eq. (5.10), the parameters $\alpha(t)$ and $\lambda_k(t)$ satisfy the relation (Appendix C)

$$i\dot{\alpha}(t) = \omega_0\alpha(t) + \sum_k \gamma_k \lambda_k(t), \quad (5.13)$$

$$i\dot{\lambda}_k = \omega_k \lambda_k + \gamma_k \alpha(t). \quad (5.14)$$

As the global system is closed, neither dissipation nor external forces exist, conserving the total amount of excitations. Moreover, Ref. [89] shows that in the absence of external forces, a coherent state remains coherent during time evolution. For all times t , the system excitations $|\alpha(t)|^2$, the bath excitations $\sum_{k \in E} |\lambda_k(t)|^2$, and the total excitations $|\alpha_0|^2$ follow the relation

$$|\alpha(t)|^2 + \sum_{k \in E} |\lambda_k(t)|^2 = |\alpha_0|^2. \quad (5.15)$$

Consider two kinds of coupling γ_k to each oscillator k , constant and non-constant. In the constant case, each oscillator of the environment is coupled to the system with the same magnitude,

$$\gamma_k = \gamma, \text{ for all } k. \quad (5.16)$$

For the non-constant coupling case, all oscillators of the environment are coupled with the main oscillator with the same magnitude, except for one,

$$\gamma_k = \begin{cases} \gamma, & \text{if } \omega_k \neq \omega_0 \\ \bar{\gamma}, & \text{if } \omega_k = \omega_0 \end{cases} \text{ for some constants } \gamma, \bar{\gamma}. \quad (5.17)$$

Consider a large number of oscillators in the environment. Taking the limit of a continuum of oscillators for both couplings, the solution of Eqs. (5.13) and (5.14) can be calculated analytically. One can make the following substitutions:

$$\begin{aligned} \sum_k &\rightarrow \int \rho(\omega) d\omega \\ \gamma_k &\rightarrow \gamma(\omega) \\ \lambda_k(t) &\rightarrow \lambda(\omega, t), \end{aligned} \quad (5.18)$$

where $\rho(\omega)$ is the density of oscillators with frequency ω . Thus, $\rho(\omega)d\omega$ is the number of oscillators in the environment with frequencies in the interval $(\omega, \omega + d\omega)$ and $|\lambda(\omega, t)|^2 \rho(\omega)$ represents the density of excitations in oscillators with frequency ω at time t .

By assuming $\gamma^2(\omega)\rho(\omega)$ is constant, that is,

$$\gamma^2(\omega)\rho(\omega) = \gamma^2 \rho = \text{const} = C, \quad (5.19)$$

and that the distribution of modes is localized around ω_0 , the values of α and γ_k can be obtained (Appendix C).

Constant Coupling

: By integrating Eq. (5.14) and substituting in Eq. (5.13), we get

$$\alpha(t) = \alpha_0 e^{-\Gamma t/2}, \quad (5.20)$$

$$\lambda(\omega, t) = i\alpha_0 \gamma \frac{e^{(-\Gamma/2 + i\Delta\omega)t}}{\Gamma/2 + i\Delta\omega}, \quad (5.21)$$

where $\Delta\omega = \omega_0 - \omega$ and $\Gamma = 4\pi\gamma^2\rho$ (recall Eq. (5.19)).

Note the quantity (5.19) gives the rate at which the excitations of the main system $|\alpha(t)|^2$ decays exponentially, $\Gamma = 4\pi C$.

For an asymptotic limit of time, the main system reaches the vacuum state and the environment excitations follow a Lorentzian centered around ω_0

$$|\lambda(\omega, t \rightarrow \infty)|^2\rho = \frac{|\alpha_0|^2}{\pi} \frac{\Gamma}{(\Gamma/2)^2 + (\omega - \omega_0)^2}. \quad (5.22)$$

Non-Constant Coupling:

In this case, we made the same approximations as in the constant case and applied the distribution of couplings defined in Eq. (5.17). Therefore, the result obtained is:

$$\alpha(t) = \frac{\alpha_0}{2\Omega} e^{-\Gamma t/4} \left[\Gamma/4 (e^{-\Omega t} - e^{\Omega t}) + \Omega (e^{-\Omega t} + e^{\Omega t}) \right], \quad (5.23)$$

$$\lambda(\omega_0, t) = \frac{i\alpha_0\bar{\gamma}}{2\Omega} e^{-\Gamma t/4} (e^{-\Omega t} - e^{\Omega t}), \quad (5.24)$$

$$\lambda(\omega, t) = \frac{-i\alpha_0\bar{\gamma}}{2\Omega} \left[\frac{(\Gamma/4 + \Omega) (1 - e^{-(\Gamma/4 + i\Delta\omega + \Omega)t})}{\Gamma/4 + i\Delta\omega + \Omega} + \frac{(\Gamma/4 - \Omega) (1 - e^{-(\Gamma/4 + i\Delta\omega - \Omega)t})}{-\Gamma/4 - i\Delta\omega + \Omega} \right], \quad (5.25)$$

with $\Omega = \sqrt{(\Gamma/4)^2 - \bar{\gamma}^2}$.

Taking the asymptotic limit of t with $\bar{\gamma} \gg \Gamma$, the environment excitations distribute approximately as a sum of two Lorentzian curves (instead of one) centered at $\omega_0 + \bar{\gamma}$ and $\omega_0 - \bar{\gamma}$:

$$|\lambda(\omega, t \rightarrow \infty)|^2\rho \approx \frac{|\alpha_0|^2}{4\pi} \left[\frac{\Gamma}{(\Gamma/4)^2 + (\omega - (\omega_0 + \bar{\gamma}))^2} + \frac{\Gamma}{(\Gamma/4)^2 + (\omega - (\omega_0 - \bar{\gamma}))^2} \right]. \quad (5.26)$$

Note Eq. (5.23) to (5.25) present two important exponentials, one describing the decay of excitations in the system,

$$e^{-\Gamma t/4},$$

and the other describing oscillations in the transfer of excitations,

$$e^{-\Omega t} - e^{\Omega t}.$$

The exchange of excitations oscillates with amortization in the amplitude given by Γt . As the total number of excitations remains constant, one can conclude that the system and

environment excitations will oscillate with the same frequency Ω . Furthermore, as the difference between γ and $\bar{\gamma}$ becomes more significant, the frequency of the oscillations in the transfer of the excitations becomes larger.

5.2.2 Model Dynamics

For the state in Eq. (5.12), the system and environment never correlate and the composed system remains as a product state during time evolution. This correlation is crucial for selecting the preferred states of the system by the environment (Sec. 2.2). We set the system initially in a superposition of coherent states and the environment in the vacuum

$$|\Psi(0)\rangle = G \left[(a|\alpha_0\rangle + b|-\alpha_0\rangle) \otimes \prod_{k=1}^N |0_k\rangle \right], \quad (5.27)$$

where $|\pm\alpha_0\rangle$ are coherent states with parameters $\pm\alpha_0$, a , and b are complex coefficients, and G is the normalization factor given by $G = (|a|^2 + |b|^2 + ab^* \langle -\alpha_0 | \alpha_0 \rangle + \text{c.c.})^{-1/2}$.

From the linearity of Schrödinger's equation, the same ansatz from Eqs. (5.13) and (5.14) can determine the evolved state of the global system at time t ,

$$|\Psi(t)\rangle = G (a|\alpha(t)\rangle \otimes |\Lambda(t)\rangle + b|-\alpha(t)\rangle \otimes |-\Lambda(t)\rangle), \quad (5.28)$$

where $|\pm\Lambda(t)\rangle = \pm \otimes \prod_{k=1}^N |\lambda_k(t)\rangle$, and $\alpha(t)$ and $\lambda_k(t)$ are the solutions of Eqs. (5.13) and (5.14) subjected to the initial conditions $\alpha(0) = \alpha_0$ and $\lambda_k(0) = 0$ for all k .

For both, constant and non-constant couplings, we assume the system is initially in the ‘‘cat state’’ described by Eq. (5.27) with $a = 1$, $b = 1$, and $\alpha_0 = 3$. The global system is given by

$$|\Psi(0)\rangle = G \left[(|\alpha_0\rangle + |-\alpha_0\rangle) \otimes \prod_{k=1}^N |0_k\rangle \right] \quad (5.29)$$

with

$$G = \frac{1}{[2(1 + e^{-2|\alpha_0|^2})]^{1/2}}. \quad (5.30)$$

In both cases of coupling distributions, we have used $N = 900$ and $\omega_0 = 1$, with the environment frequencies linearly distributed between 0.1 and 1.9. From the analytical solution, we can estimate the decay rate as $\Gamma = 4\pi\gamma^2 \frac{N}{\Delta\omega}$, where $\Delta\omega = 1.8$ is the window of frequencies of environment oscillators for a frequency interval between 0.1 and 1.9. Therefore, $N/\Delta\omega$ is the (uniform) density of oscillators.

For the excitations dynamic with constant coupling, we took $\gamma_k = 0.1/30$ for all k . As the excitations of the system decay exponentially, the environment excitations increase such that the total amount of excitations is conserved. Note the excitations migrate from the system to the bath monotonically (Fig.14(a)). Fig.14(b) shows the normalized distribution (with a maximum of 1) of excitations in the environment. As expected from

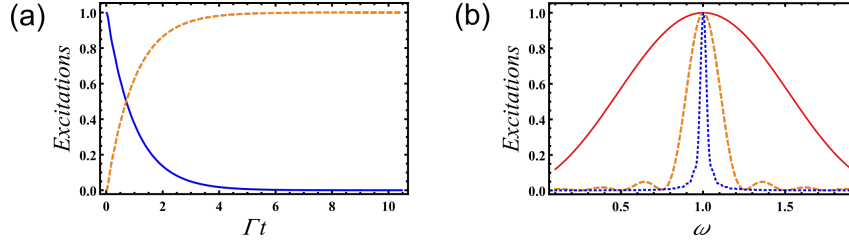


Figure 14 – Constant coupling: (a) Main oscillator excitations, $|\alpha(t)|^2$ (blue line) and environment excitations $\sum |\gamma_k(t)|^2$ (orange dashed line) as a function of Γt . (b) Distribution of the environment excitations for $\Gamma t = 0.35$ (red line), $\Gamma t = 1.75$ (orange dashed line), and $\Gamma t = 10$ (blue dotted line).

Eq.(5.22), with $\Gamma t \sim 1$, most of the excitations are concentrated within the oscillators with frequencies close to the frequency of the main oscillator for large t .

Since for a large enough time, all excitations of the system are transferred to the environment, the system reaches a vacuum state, $|0\rangle$, decoupling from the environment. Therefore, the global system turns back into a product state, and the correlations vanish

$$|\Psi(t \rightarrow \infty)\rangle \sim G \left[(|0\rangle) \otimes \prod_{k=1}^N (|\lambda_k\rangle + |-\lambda_k\rangle) \right] \quad (5.31)$$

where $\sum_{k=1}^N |\lambda_k|^2 = |\alpha_0|^2$.

We set the non-constant coupling distribution as in Eq. (5.17), with $\gamma = 0.1/30$ and $\bar{\gamma}$ ranging from 10γ to 100γ . In Fig. 15a, while the excitations of the system also decay exponentially with the rate of Γ , the curve is no longer monotonic, and the exchange of excitations oscillates. The exponential terms inside the squared brackets in Eq. (5.23) can be rewritten as two sinusoidal terms highlighting the oscillations in the exchange of excitations; the same analogy is valid for Eq.(5.24) and (5.25). Note that these oscillation frequencies are proportional to the difference between γ and $\bar{\gamma}$; the oscillation frequencies increase with larger $\bar{\gamma}$. As time progress, the single peak around $\omega_k = \omega_0$ in the distribution of the environment excitations splits into two peaks, as predicted in Eq. (5.26) (Fig. 15(b)).

The monotonic behavior for the transfer of excitations with constant coupling can mean that information about the system moves in just one direction: from system to environment. However, in the non-constant case, the oscillations can be interpreted as a “backflow” of information from the bath to the system, indicating that the system can be non-Markovian in this regime. To elucidate the Markovianity in this model, sections 5.2.6 and 5.2.7 compute the non-Markovianity degree and discuss its effects on the system.

5.2.3 The preferential observable

QD observations are possible when information about the preferential observable of the system is recorded redundantly in different portions of the environment. In this model,

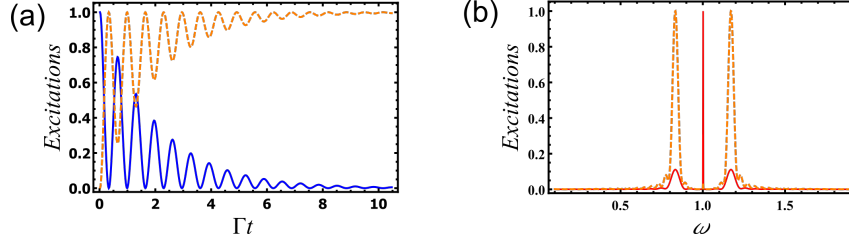


Figure 15 – Non-constant coupling: (a) Main oscillator excitations $|\alpha(t)|^2$ (blue line) and environment excitations $\sum |\gamma_k(t)|^2$ (orange dashed line) as a function of Γt . (b) Distribution of environment excitations for $\Gamma t = 7$ (red line) and $\Gamma t = 10$ (orange dashed line).

we identify the preferential observable and the preferential basis from the dynamics of the excitations exchange. The measurement of the entire environment on a preferential basis allows observers to infer the state of the system for $t > 0$. Therefore, this basis describes the preferential observable (or POVM of observables) of the system. By describing the states of the system on the proper basis, the reduced states of the environment will be orthogonal. (Sec. 2.2.2 gives a very intuitive illustration of the preferential basis concept.)

It is easy to check that

$$|\langle \alpha(t) | - \alpha(t) \rangle|^2 = e^{-2|\alpha(t)|^2} \quad (5.32)$$

$$\begin{aligned} |\langle \Lambda(t) | - \Lambda(t) \rangle|^2 &= \prod_{k \in E} |\langle \lambda_k(t) | - \lambda_k(t) \rangle|^2 \\ &= e^{-2(|\alpha_0|^2 - |\alpha(t)|^2)}. \end{aligned} \quad (5.33)$$

For simplicity, let us analyze the constant coupling case. From Eq. (5.20), if $|\alpha_0| \gg 1$ and $\Gamma t \sim 1$, $\langle \alpha(t) | - \alpha(t) \rangle \approx \langle \Lambda(t) | - \Lambda(t) \rangle$ is approximately $e^{-c|\alpha_0|}$, for some constant $c \sim 1$. Note besides this approximation is valid for any $|\alpha_0|^2$, the states of the system and environment are approximately orthogonal for values of Γt around 1.

The analysis for the non-constant case follows similarly. However, one must consider the oscillations of the amplitude of the excitations as shown in Eq. (5.23). Thus, except at times when all excitations are in the environment, the system states and environment states are also orthogonal. This indicates that the environment monitors the system, and with the initial state of the system defined in Eq. (5.29), one can also identify the preferential observable. Following Eq. (2.15) and the discussion presented in Sec. 2.2.1, we see that our evolution closely matches the evolution of the von Neumann measurement scheme.

Therefore, we can conclude that the preferential observable lies in any quadrature of the plane whose axes are momentum and position where the observable to be monitored will depend on the value of α_0 . For example, if α_0 is a real number, with the states of the system in a superposition of positions, the environment monitors it in the position space, if α_0 is a pure imaginary number, the preferential observable is in the momentum

space, but if both, the imaginary and the real part of α_0 are nonzero values, then the environment monitors the system in a combination between momentum and position.

5.2.4 Quantum Darwinism from PIP Approach

The concept of QD relies on the “quantity” of redundant information about the system spread in the environment named as *redundancy*. As shown in Sec.3.4, to determine the redundancy, the PIP approach analyzes the curve shape of the mutual information between the system and fragments of the environment as a function of fraction size f . From PIP, we can infer the minimal environment fraction, f_δ , necessary to obtain almost all information available about the system but a small percentage δ of $H(s)$.

To investigate QD using the PIP approach, the average of the partial mutual information over all possible environment fragments F is taken for each possible size f . However, this process becomes impracticable for a large number of oscillators. Thus, as many fragments as possible were sorted before computing the partial information plot and tanking the average. Therefore, the solutions obtained are very close to those of the continuum limit.

Consider the same parameter configuration presented in Sec. 5.2.2 for the following computations. To calculate the averaged mutual information between each fragment F with a size f , (1) randomly select a set of individual oscillators F_i with a size f , (2) compute the total excitation of this set of oscillators, (3) calculate the reduced density matrices ρ_S , ρ_{F_i} , and ρ_{S,F_i} , and their eigenvalues, Von Neumann entropies $H(S)$, $H(F_i)$, and $H(S, F_i)$, and, mutual information $I(S : F_i)$ for this system and subenvironment, (4) repeat steps (1) to (3) M times and calculate the averaged value of the mutual information for a fragment with size f

$$\bar{I}(S : f) \approx \frac{1}{M} \sum_{i=1}^M I(S : F_i). \quad (5.34)$$

These steps were followed for each fraction, with f ranging from 0 to 1, where f is 1 when accounting for all environment oscillators. In this work, we set $M = 100$.

Constant Coupling

Taking $\gamma_k = 0.1/30$ for all k , we computed the PIP from the excitations of the environment oscillators calculated previously. In this model, the mutual information $I(S, F)$ can be calculated for each fragment F at each time t of the evolution. Following the algorithm described in Eq. (5.34), we computed $I(S, F)$ for Γt varying from 0 to approximately 10 and f ranging from 0 to 1 (0 to 900 oscillators). After a large enough time, the information about the system will be spread in the environment very redundantly (Fig. 16a). However, for $\Gamma t \sim 6.0$, the averaged mutual information decreases quickly,

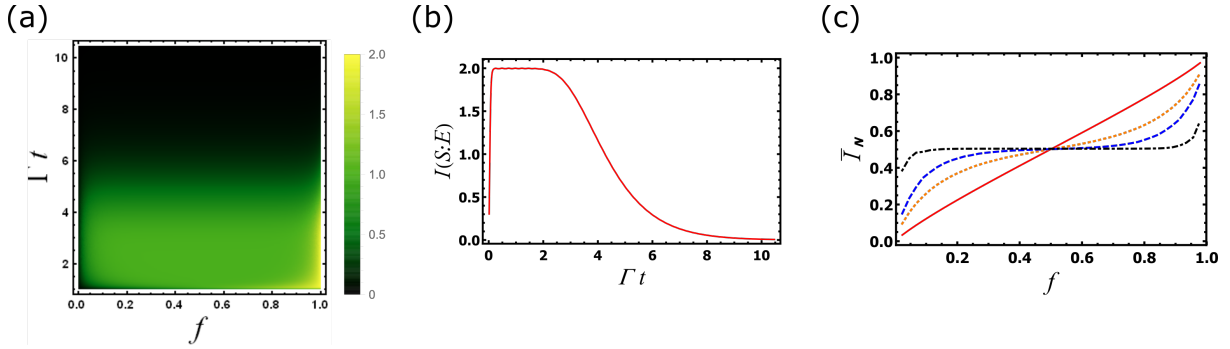


Figure 16 – (a) Average mutual information $\bar{I}(f)$ map for a constant coupling with Γt going from 0 to 10 and the environment fractions f from $1/900$ to 1. (b) Mutual information between the system and the whole environment, $I(S : E)$, as a function of Γt . (c) Normalized mutual information $\bar{I}_N(f)$ for the constant coupling case. The red (solid), orange (dotted), blue (dashed), and black (dot-dashed) lines represent the PIP for $\Gamma t = 0.03$, $\Gamma t = 0.17$, $\Gamma t = 0.35$, and $\Gamma t = 6$, respectively.

which agrees with the exact calculations of the dynamics of the excitations. For $\Gamma t \sim 0.6$, nearly all excitations of the global system are concentrated in the bath. Therefore, the average mutual information between the system and any fraction of the environment is expected to be minimal. Thus, the time $\Gamma t = 6.0$ is taken as the limit for the following analysis given the magnitude of the averaged mutual information is negligible beyond this time.

In the most common scenario of QD one can observe $I(S : f)$ raising quickly with f up to $H(S)(1 - \delta)$ for $f = f_\delta$, raising slowly up to f close to 1, and once again raising quickly until $f = 1$. If the information is spread redundantly, the PIP has a plateau shape indicating that the quantity of information contained in a fraction grows fast with the fraction size (see Fig. 16).

Fig. 16(a) shows that $I(S : f = 1, t)$ increases quickly with t as the system and environment interact. As the PIP approach analyzes f_δ and the PIP shape we calculated the normalized mutual information $\bar{I}_N(f)$ as a function of f from 0 to 1 for each time. Fig. 16c compares the PIP to different instants of time, from $\Gamma t = 0.03$ to $\Gamma t = 6$. For $\Gamma t = 0.03$ (red line), the PIP is practically linear; to obtain almost all information about the system, one needs to include nearly half of the environment. This may be expected for short times given the system and environment do not interact sufficiently to produce sufficient correlations. With increasing time, the PIP changes form from the red solid curve to the orange dotted curve, to the blue dashed curve, before reaching the closest form of a plateau in the dot-dashed black line with $\Gamma t = 6$.

The PIP curve provides a qualitative way to identify QD. However, this characterization can also be performed quantitatively by computing redundancy. As shown in Sec. 3.4,

redundancy requires defining how close we want to get to complete information about the system $H(S)$. Thus, we define a percentage δ of H_S to find almost all information about the system in the environment, $H_S(1 - \delta)$. The quantity f_δ is the minimal fraction required to obtain a quantity of $H_S(1 - \delta)$ of information about the system in the environment. Thus, the redundancy is given by:

$$R_\delta = \frac{1}{f_\delta}. \quad (5.35)$$

For constant coupling, we computed f_δ and R_δ for different values of δ . Given that the system and the environment share information as they interact (Fig. 17a-b), R_δ grows with t , while f_δ decreases with t , for all values of δ . One can expect that the longer the system and environment interact with each other, the larger R_δ becomes. The quantity R_δ also depends on the value of δ . Observe also that for a given time interval, the closer to complete information about system $H(S)$ we want to reach, the smaller the maximum value of R_δ becomes. However, even for a small δ , the redundancy increases and we assert that QD can be observed in this model.

Since the PIP approach defines QD from the concept of mutual information, it does not make sense to classify QD at times instants at which the maximal mutual information is insignificant. To quantify redundancy accurately, we need to consider the mutual information between the system and the whole environment at each time instant. Therefore, we define the relative redundancy $R_r(t)$ as

$$R_r(t) = R_\delta(t)I(S : E)(t), \quad (5.36)$$

where $I(S : E)(t)$ is the total mutual information between the system and the whole environment at a time t .

In this dynamic, the global system is initially a product state between the system and the environment states. After interacting for some time, the system and environment correlate and increase the redundancy. However, for a long enough time nearly all excitations will be concentrated in the environment (Fig. 16 (b)). In this case, even with high redundancy, the number of correlations between the system and the environment becomes negligible; and the global system will become increasingly close to a product state. Therefore, relative redundancy is more appropriate to quantify the QD. Compared to the monotonic growth of redundancy Fig. 17(b), the relative redundancy R_r grows with Γt to a maximal value before decreasing to zero. Nevertheless, we can affirm that in this model, QD can be observed in the interval between $\Gamma t \sim 1.0$ and $\Gamma t \sim 5.0$ with a maximum at $\Gamma t \sim 2.5$.

Non-Constant Coupling

Using the same parameters as the constant coupling case and the same initial cat state, we assume the distribution of couplings between each oscillator of the environment and the system follows Eq. 5.17 while varying the value of $\bar{\gamma}$.

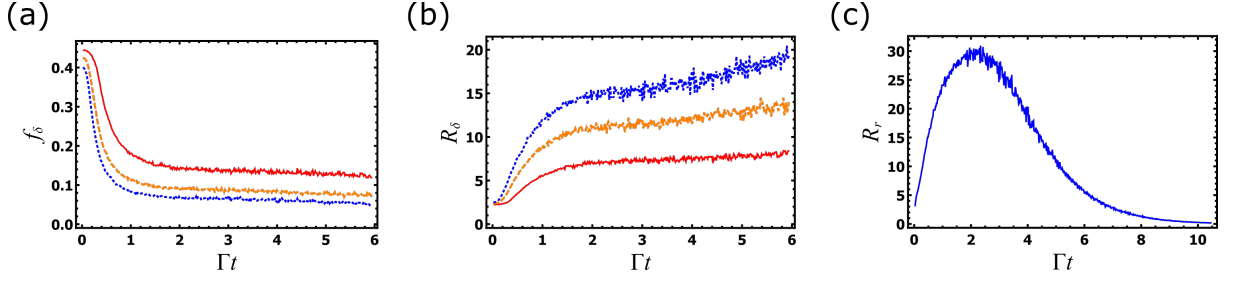


Figure 17 – For $\delta = 0.01$ in the red (solid line), $\delta = 0.05$ in the orange (dashed line), and $\delta = 0.1$ in the blue (dotted line) in (a) is plotted the fraction f_δ and in (b) the Redundancy R_δ in function of time. For $\delta = 0.05$, in (c) is plotted the relative redundancy varying with time.

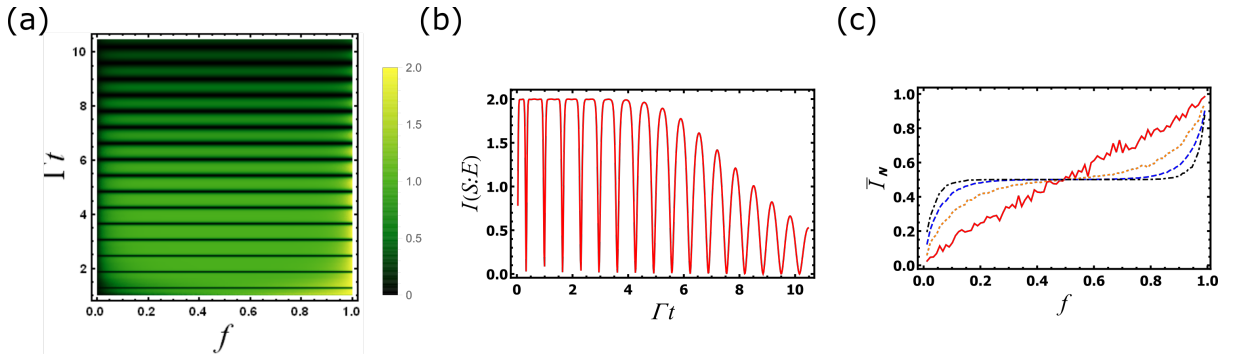


Figure 18 – For non-constant coupling with $\bar{\gamma} = 50\gamma$: (a) Average mutual information $\bar{I}(f)$ map with Γt going from 0 to 10 and the environment fractions f from $1/900$ to 1. (b) Mutual information between the system and the whole environment, $I(S : E)$, as a function of Γt . (c) Normalized mutual information $\bar{I}_N(f)$ versus f for $\Gamma t = 0.07$ (red line), $\Gamma t = 0.52$ (orange and dotted line), $\Gamma t = 1.04$ (blue and dashed line) and $\Gamma t = 6.0$ (black and dot-dashed line).

As shown in Sec. 5.2.1, for $\bar{\gamma} > \gamma$, the transfer of excitations from system to environment oscillates. These oscillations are also present in the mutual information. For $\bar{\gamma} = 50\gamma$, PIPs were plotted for different lengths of time, with f between 0 and 1 (Fig. 18a). Observe in Fig. 18b that the mutual information oscillates several times with the same frequency as the oscillations during the exchange of excitations. These oscillations in PIPs can indicate a backflow of information from the system to the environment that relates to the non-Markovianity of the system.

In Fig. 18(c), as in the constant case, for time length $\Gamma t = 0.07$ (red solid line), the mutual information depends almost linearly on the fragment size f , since the number of correlations created between the system and the environment is still relatively minimal. As time increases from $\Gamma t = 0.52$ (orange dotted line) and to $\Gamma t = 1.04$ (blue dashed line), the correlation between the system and environment increases and the plateau becomes more evident. At $\Gamma t = 6.00$ (black dot-dashed line), the plateau becomes even more defined.

This behavior repeats with each cycle. However, the PIP never returns to its

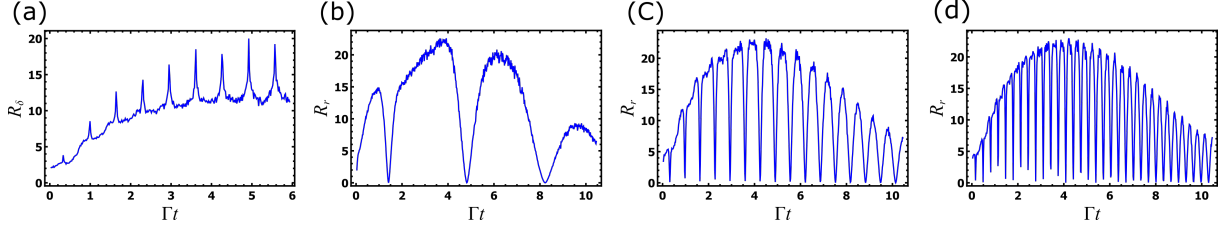


Figure 19 – (a) Redundancy R_δ with $\delta = 0.05$ and $\bar{\gamma} = 50\gamma$ varying with time. Relative redundancy R_r with $\delta = 0.05$ and varying with time for: (b) $\bar{\gamma} = 10\gamma$, (c) $\bar{\gamma} = 50\gamma$, and (d) $\bar{\gamma} = 10\gamma$.

linear form, and the redundancy R_δ never returns to zero. Note that, where $\bar{\gamma} = 50\gamma$, the redundancy again oscillates with the same frequency as the exchange of excitations and the minimum value of each oscillation never decreases. However, as with the constant coupling case, it is not correct to assume QD can be observed after any time instant. To demonstrate, we calculated the relative redundancy R_r for non-constant coupling from $\bar{\gamma} = 10\gamma$ to $\bar{\gamma} = 100\gamma$. The frequency of the oscillations in R_r increases with $\bar{\gamma}$ (Fig. 19a).

5.2.5 Quantum Darwinism from BPH Approach

This approach relies upon the fact that, from the quantum mechanics formulation, there always exists a preferential observable or POVM for any quantum system. Also, in cases of QD, there exists a map $\Lambda_F : D_S \rightarrow D_F$ that describes the preferential observable (or POVM) by connecting the states of the system D_S to the states of the environment fraction D_F (see Sec. 3.5). We can, then, assume that the environment effectively prepares its states accordingly with the result of the “measurement” that it performed on the system. With this *measure and prepare map*, we can describe the preferential observable as a POVM $\{M_i\}$ and distinguish it by the condition

$$\Lambda_F(\rho) \approx \sum_i \text{Tr}(M_i \rho) \sigma_{i,F},$$

for every system operator ρ and some states $\sigma_{i,F}$ for environment fraction F .

The map that describes the measurement of the initial state of the system $\rho_S = G^2(a|\alpha_0\rangle + b|-\alpha_0\rangle)(a^*\langle\alpha_0| + b^*\langle-\alpha_0|)$ and preparation of the environment states for every t can be computed from the evaluated global state in Eq. (5.27):

$$\Lambda_F^t(\rho_S) = \text{Tr}_{S,E-F}(|\Psi(t)\rangle\langle\Psi(t)|) \quad (5.37)$$

$$= G^2|a|^2 \prod_{j \in F} |\lambda_j(t)\rangle\langle\lambda_j(t)| \quad (5.38)$$

$$+ G^2|b|^2 \prod_{j \in F} |-\lambda_j(t)\rangle\langle-\lambda_j(t)| \quad (5.39)$$

$$+ D(t) \prod_{j \in F} |\lambda_j(t)\rangle\langle-\lambda_j(t)| + \text{H.c.}, \quad (5.40)$$

where

$$D(t) = G^2 ab^* \langle \alpha(t) | -\alpha(t) \rangle \prod_{j \in E-F} \langle \lambda_j(t) | -\lambda_j(t) \rangle.$$

As we are assuming that $|\alpha_0| \gg 1$, note that $\langle \alpha_0 | -\alpha_0 \rangle = e^{-2|\alpha_0|^2} \approx 0$ and, therefore, $G \approx 1$. From these approximations, we can assume that $D \approx 0$ and, then,

$$\Lambda_F^t(\rho) \approx \text{Tr}(|\alpha_0\rangle \langle \alpha_0| \rho) \prod_{j \in F} |\lambda_j(t)\rangle \langle \lambda_j(t)| \quad (5.41)$$

$$+ \text{Tr}(|-\alpha_0\rangle \langle -\alpha_0| \rho) \prod_{j \in F} |-\lambda_j(t)\rangle \langle -\lambda_j(t)|. \quad (5.42)$$

Observe that, indeed, the maps described by Eq. (5.42) are approximately a measure and prepare map in the subspace generated by $|\pm\alpha_0\rangle$ with the (approximate) POVM $\{|\pm\alpha_0\rangle \langle \pm\alpha_0|\}$, and environment states $\sigma_{F,\pm}^t = \prod_{j \in F} |\pm\lambda_j(t)\rangle \langle \pm\lambda_j(t)|$.

Let us check now two relevant regimes, $\Gamma t \sim 1$ and $\Gamma t \gg 1$. At $\Gamma t \sim 1$ and the constant coupling case, $D(t)$ is small since $\langle \alpha(t) | -\alpha(t) \rangle = e^{-c|\alpha(t)|^2} \approx 0$ where $c \sim 1$. For the non-constant case coupling case, we have $|\langle \alpha(t) | -\alpha(t) \rangle|^2 = \langle \alpha_0 | -\alpha_0 \rangle^{2\Xi(t)}$, where $\Xi(t)$ is the proportional system excitations ranging from 0, none excitations, to 1, total excitations in the closed system (see appendix C). Therefore, in the non-constant coupling, we have $D \sim 0$ for $\Gamma t \sim 1$ and $\Xi(t) \sim t$, that is, in instants of time where the excitations go back to the main oscillator (see Fig. 15).

For $\Gamma t \gg 1$, we can assume that almost all excitations are in the environment. Then, any environment fragment with size F will have $|\alpha_0|^2 f$ excitations, where $f = F/N$ is the fraction of the environment. Therefore, the complementary part to this fraction $(1-f)$ will have $|\alpha_0|^2(1-f)$ excitations. Then, for f not too close to 1, $\prod_{j \in E-F} \langle \lambda_j(t) | -\lambda_j(t) \rangle \approx e^{-2|\alpha_0|^2(1-f)} \approx 0$ leading to $D(t) \approx 0$.

Also for $\Gamma t \gg 1$, for constant and non-constant coupling cases, we can infer the quantum Darwinism by the distinguishability given by $1 - \prod_{j \in F} |\langle \lambda_j(t) | -\lambda_j(t) \rangle|$. Approximating the distinguishability by $1 - e^{-2|\alpha_0|^2 f}$, note that it quickly converges to 1 with the environment fraction f .

In Sec. 3.6, we present two examples comparing the two approaches, PIP and BPH, where in the first example, we can identify the quantum Darwinism through both approaches but, in the second, just the second approach can characterize it. In this model, for $\Gamma t \sim 1$, the dynamic of the distribution of information about the system in the environment approximately

$$\begin{aligned} |\alpha_0\rangle |0\rangle &\mapsto |\alpha(t)\rangle \prod_{j \in F} |\lambda_j(t)\rangle, \\ |-\alpha_0\rangle |0\rangle &\mapsto |-\alpha(t)\rangle \prod_{j \in F} |-\lambda_j(t)\rangle, \end{aligned} \quad (5.43)$$

that is very similar to the first example. However, for $\Gamma t \gg 1$ and taking to account the whole dynamic, we have

$$\begin{aligned} |\alpha_0\rangle |0\rangle &\mapsto |0\rangle \prod_{j \in F} |\lambda(t)\rangle, \\ |-\alpha_0\rangle |0\rangle &\mapsto |0\rangle \prod_{j \in F} |-\lambda(t)\rangle, \end{aligned} \quad (5.44)$$

which resembles the second example. In the second case, it does not make sense of talking about quantum Darwinism from the PIP perspective since the number of correlations is negligible. However, from the BPH perspective, we can infer the preferential observable, since the environment recorded redundantly this information in its states. Then, in this regime, even when there is no more a significant quantity of correlations, it is still meaningful to address Darwinism from the BPH perspective.

5.2.6 Non-Markovianity degree in this model

As there are many ways to calculate the non-Markovianity degree, we need to set up which method to use. Here, we used the same method as in [50], where the authors compute the non-Markovianity degree by the distance between two states. As shown in the Sec4.4, when a system is Markovian, the fidelity between two states, ρ_1 and ρ_2 , increases monotonically under the action of the completely positive and trace-preserving map. When it is non-Markovian, besides the fidelity still increases for a long enough time, it decreases temporarily for some time intervals. Therefore, it is possible to quantify the non-Markovianity degree from Eq.(5.7) by optimizing all pairs of states. However, there exists an infinite number of possible states in this system and, to make possible this quantization, we approximated the fidelity by sorting 1000 values for α_0 to determine the initial states. In this way, we can rewrite Eq.(5.7) as,

$$\mathcal{N} = \max_{1K\text{Rand.}\rho_1, \rho_2} \left[- \int_{\dot{\mathcal{F}} < 0} \dot{\mathcal{F}}(\rho_1, \rho_2) dt \right], \quad (5.45)$$

where $1K\text{Rand}$ means that the maximization will be made under 1000 initial states $\rho_1(0)$ and $\rho_2(0)$ chosen randomly.

When we set the coupling between the system and each environment oscillator with the same magnitude, we observed that the fidelity increasing is monotonic (see Fig. 20(b)), and, therefore, the quantity \mathcal{N} is zero for any time interval; this is the case where the dynamic is Markovian. The information about the system flows just in one direction, from system to environment.

By defining the distribution as in Eq. (5.17), the scenario changes. In Figs. 20(b) to (d) is shown that the fidelity behavior is no longer monotonic for non-constant coupling. For a considerable time interval, the fidelity still increases; however, in shorter periods, it

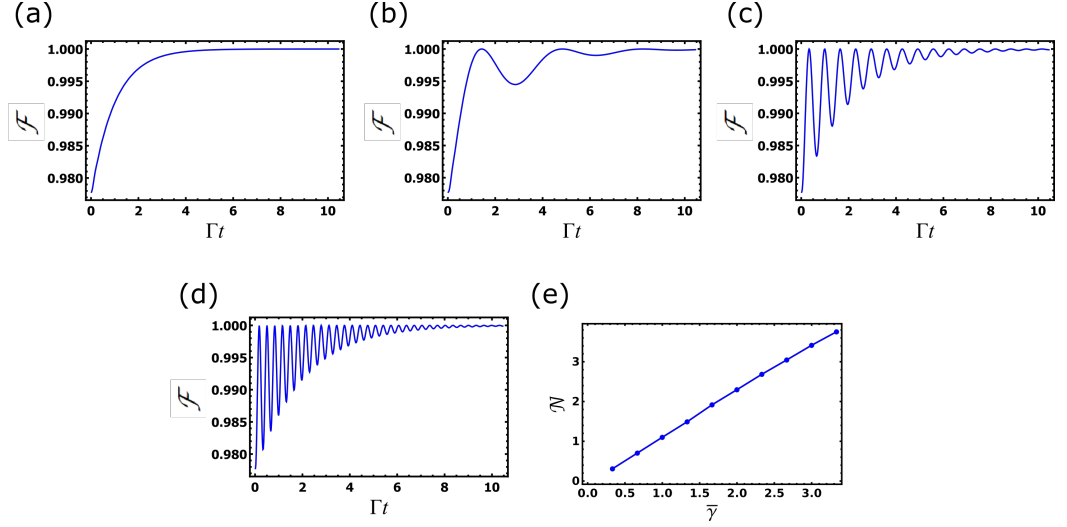


Figure 20 – Fidelity \mathcal{F} as a function of time for (a) Constant coupling, (b) $\bar{\gamma} = 10\gamma$, (c) $\bar{\gamma} = 50\gamma$, and (d) $\bar{\gamma} = 10\gamma$. (e) Non-markovianity degree as a function of $\bar{\gamma}$. In (e), we sort 1000 initial states coherent states and \mathcal{N} was calculated for all combinations of pairs.

decreases and increases again. By comparing the fidelity variation with Fig. 15(a), one can note that the frequency of this oscillation is the same as the oscillation in the excitations. Moreover, as in the excitations curve, the frequency of the oscillations in the fidelity curve is proportional to $|\bar{\gamma} - \gamma|$.

From Eq. 5.45 we can see that, to quantify the non-Markovianity in the system, the fidelity is integrated just in time intervals where its values are decreasing. Then it is expected that the quantity \mathcal{N} is proportional to oscillations frequency in \mathcal{F} . Then, we can connect qualitatively the type of coupling with the non-Markovianity degree. This relation can be observed in Fig. 20(e), where it is plotted the \mathcal{N} as a function of $\bar{\gamma}$.

In this model, we understand the Markovianity dynamic, and the QD quantitative and qualitatively. Therefore, now we have tools to check how the QD observation is affected by the non-Markovianity.

5.2.7 Quantum Darwinism and Non-Markovianity

As in the model studied in Ref. [50] R_δ and f_δ also oscillate in time when the system is non-Markovian, the authors defined a method that quantifies the effect of the non-Markovianity in the time evolution of the QD (see Sec. 5.1). They used the fraction f_δ instead of the redundancy R_δ in their calculations; which is essentially the equivalent, since $f_\delta = 1/R_\delta$. From this, they defined the non-monotonicity of f_δ , \mathcal{N}_f , similarly to the non-Markovianity degree:

$$\mathcal{N}_f = \int_{df_\delta/dt > 0} \frac{df_\delta}{dt} dt. \quad (5.46)$$

Note that, as they are interested in the time evolution of the QD, the integral in this equation is calculated just when df_δ/dt is positive. This expression tells us, basically, how significant is the number of oscillations in the curve f_δ . Further, we can say that \mathcal{N}_f also computes the “quantity of non-Darwinism” in a time interval for a given dynamic. They observed in their model that the curve \mathcal{N}_f is very similar to the curve \mathcal{N} and this shows that, indeed, the time evolution f_δ is different for different degrees of non-Markovianity.

We also calculated \mathcal{N}_f in our model and got qualitatively the same result, see Fig. 21(a). We could observe that \mathcal{N}_f grows with $\bar{\gamma}$ as \mathcal{N} and, the more significant the non-Markovianity degree is, the larger is the quantity \mathcal{N}_f . This result can be expected intuitively since as non-Markovianity grows, more oscillations in the redundancy and f_δ will be present. Then, if we integrate the values of f_δ just when it is growing, the non-monotonicity will increase with the oscillation frequency and, therefore, with $\bar{\gamma}$.

Although this analogy is consistent with that particular model, we can not generalize that the non-Markovianity hinders the QD. In a time interval $\Delta t > T$, the quantity of time that QD decreases is the same as the quantity of time that QD increases. When the excitations are flowing from the system to the environment, the redundancy grows. When the excitations are flowing back to the system, the redundancy decreases. Nevertheless, even in the moments of excitations (and information) backflow, we can say that there exists some redundancy in the system and, therefore, some degree of quantum Darwinism. Hence, we present here a new point of view on this analysis. We believe that a more sensitive figure of merit would be the *averaged* relative redundancy $R_r(\bar{\gamma})$ for a certain period $\Delta t = t_{\max} - t_{\min}$, that is,

$$\bar{R}_r(\bar{\gamma}) = \frac{1}{\Delta t} \int_{t_{\min}}^{t_{\max}} R_r(t, \bar{\gamma}) dt. \quad (5.47)$$

This quantity, instead of calculating the amount of “non-Darwinism”, calculates the averaged quantity of redundant information about the system spread in the environment. In simple words, $\bar{R}_r(\bar{\gamma})$ tells us the probability of finding the system in a “Darwinistic” regime in a time instant, $t_r \in \Delta t$, chosen randomly.

We calculated this quantity for different values of $\bar{\gamma}$ in a time window $\Gamma\Delta t = 10$. We plotted \bar{R}_r in function of $\bar{\gamma}$ in Fig. 21(b). Observe that the averaged redundancy is practically constant with $\bar{\gamma}$, which implies that, for any random instant of time, the probability of finding quantum Darwinism in the Markovian case is nearly the same in the case as high non-Markovianity. Putting it in another way, even if the amount of quantum Darwinism is non-monotonic in time in non-Markovian dynamics, *on average*, it is the same as in the Markovian case.

Since the non-Markovianity of the main oscillator dynamics depends only on $\bar{\gamma}$, the asymptotic state of the environment keeps a record of the non-Markovianity. From the BPH perspective, in the asymptotic regime $\Gamma t \gg 1$, all excitations initially in the

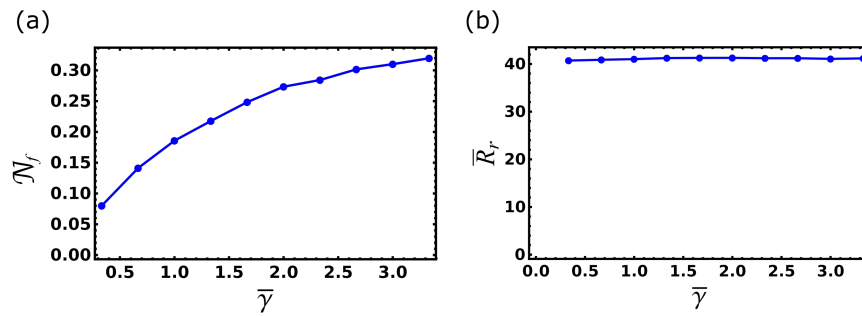


Figure 21 – (a) Non-monotonicity \mathcal{N}_f , and (b) averaged relative redundancy R_r versus $\bar{\gamma}$, with $\bar{\gamma}$ going from 10γ to 100γ ; the time interval of the integration is $\Gamma\Delta t = 10$.

main oscillator go to the environment. Even when there are no more correlations, the environment also keeps a record of the preferred state of the system. However, the record of the preferred observable is essentially “independent” of $\bar{\gamma}$. Then, from this perspective, we conclude that leastwise in this model, we do not have evidence that does exist some correlation between the non-Markovianity degree and the observation (or the probability of detecting) QD; contrariwise, the averaged quantity of QD is pretty much the same for any non-Markovianity degree.

6 Quantum Darwinism in Ultracold Gases

We have focused on non-correlated subenvironments, which are well explored in the literature through theoretical and numerical studies. The environment of the model used in our work in Sec. 5 is non-correlated and is applicable experimentally; we can say that this model is realistic. However, most of the subenvironments in nature become strongly correlated between themselves, and preparing such a setup is quite tricky. Understanding how information about the system spreads in an environment composed of correlated subsystems could enable the application of Quantum Darwinism in other realistic models. In this sense, cold atoms setups are promising frameworks since they have available technologies for experimental implementations.

In search of more realistic models, we came across an exciting work of orthogonality catastrophe [90] performed by T. Busch and his team. They studied the phenomenon in a Fermi sea coupled to a two-level atom and showed that, under some conditions, such coupling makes the Fermi sea states orthogonal. The orthogonality increases quickly with the number of fermions even for very weak interaction between the atom and the Fermi sea. Anderson predicted this effect by studying electrons subject to a potential V [91], and as demonstrated in Ref. [90], it is also valid when the fermions are interacting with an impurity. This work drew our attention, leading us to ask if quantum Darwinism and orthogonality catastrophe can be related.

Working experimentally with fermions is hard, but there is a trick: bosons in a gas can behave as fermions under some specific conditions. This gas, known as the *Tonks Girardeau gas* [92], can be experimentally implemented with cold atoms. It was shown that orthogonality catastrophe is also valid in Tonks-Girardeau limit [93], which makes experiments of orthogonality catastrophe more feasible.

The goals of this chapter are to study quantum Darwinism in a model of ultracold gas and investigate if quantum Darwinism and orthogonality catastrophe are related to each other. We begin introducing Anderson's work in Sec. 6.1 and then, we present the work of orthogonality catastrophe in a Fermi sea coupled to an atom in Sec. 6.2. In Sec. 6.3 we present our work in progress where we use the model of Ref. [90] to investigate quantum Darwinism and in Sec. 6.4 we finish giving motivation to using ultracold atoms in quantum Darwinism studies.

6.1 Anderson Orthogonality Catastrophe

P. W. Anderson introduced the concept of orthogonality catastrophe in a paper published in 1967 [91]. He showed that this is an intrinsic effect in fermionic many-body systems.

In Anderson's work, the system is a non-interacting Fermi gas in the ground state. For simplicity and with no loss of generality, he considered the gas composed by N fermions in a spherical box with radius R and only $l = 0$ scattering states. The idea is to perturb the state of the Fermi gas by suddenly applying a potential V and comparing it with the non-perturbed state.

The spherically symmetrical Bessel functions give the unperturbed states $\phi_n(r)$ of the n -th energy level of a particle, that is

$$\phi_n(r) = \frac{k_n}{(2\pi R^3)^{\frac{1}{2}}} \frac{\sin(k_n r)}{k_n r}, \quad (6.1)$$

with $k_n = n\pi/R$ and $E_n = \hbar^2 k_n^2 / 2m$. By subjecting the fermions to a potential V , the phase states shifts by a quantity $\delta(E_n)$, and the perturbed states $\psi_n(r)$ are given by

$$\psi_n(r) \simeq \frac{k_n}{(2\pi R^3)^{\frac{1}{2}}} \frac{\sin(k_n r - \delta(E_n)) - [1 - r/R]}{k_n r}. \quad (6.2)$$

Consider the two group of states, unperturbed $\{\phi_n(r)\}$ and perturbed $\{\psi_n(r)\}$. The overlap between any pair $(\phi_i(r), \psi_j(r))$ with $i, j \in \{1, \dots, N\}$ is given by

$$A_{i,j} = 4\pi \int_0^R r^2 \phi_i(r) \psi_j(r) dr \simeq \frac{\sin \delta(E_j)}{\pi(i-j) + \delta(E_j)}. \quad (6.3)$$

From this result, we can construct a square matrix A with the values $A_{i,j}$. The overlap $S_{\phi\psi}$ between the unperturbed $|\Phi(r_1, \dots, r_N)\rangle$ and perturbed $|\Psi(r_1, \dots, r_N)\rangle$ global state of the Fermi gas is given by

$$S_{\phi\psi} = \det |A|. \quad (6.4)$$

The main factor changing the fermions states when the potential is turned on is the phase $\delta(E_n)$ gained by each particle. When the fermions are localized in the sphere surface the gained phases are minimal. Then, by setting $\delta = \delta_n(E, r = R)$ for all n , Ref. [91] shows that the overlap is given by

$$S_{\phi\psi} \lesssim \exp \left[\frac{-\sin^2 \delta}{3\pi^2} \right]. \quad (6.5)$$

Therefore, for N and/or δ sufficiently large $S_{\phi\psi}$ goes to zero quickly what means that $|\Phi(r_1, \dots, r_N)\rangle$ and $|\Psi(r_1, \dots, r_N)\rangle$ become orthogonal. As the phase shift is caused by the potential V , it is expected that its intensity makes the Fermi gas states orthogonal. However, it is impressive that taking the limit $N \rightarrow \infty$, the states become orthogonal even for $V \rightarrow 0$.

The exponential in Eq. (6.5) comes from the approximation

$$\frac{1}{\pi^2} \sum_{\substack{i < n_F \\ j > n_F}} \frac{\sin^2 \delta}{(i - j + \delta)^2} \simeq \frac{-\sin^2 \delta}{\pi^2} \ln M, \quad (6.6)$$

where n_F is the Fermi level and M is the radius, R , in atomic units. Note, the phase shift of each fermion contributes exponentially to the final state of the gas. Even when they are small, if N is large enough, the joint effect on the final state is huge.

6.2 Orthogonality Catastrophe in Ultracold Fermi Gases

In the original article on orthogonality catastrophe, the quenching is caused exclusively by a potential V [91]. Goold et al. present in Ref. [90] a model where the system states are quenched through the interaction with a single particle impurity.

6.2.1 The model

The model consists of a non-interacting, spin-polarized Fermi sea in a one-dimensional harmonic trap coupled with a two-level atom. This model is quite practical since the many-body state of the Fermi sea is given by the overlap of individual particles facilitating some calculations. To maintain consistency with the notation used in all previous chapters and avoid miscomprehensions, we shall refer to the impurity as *the system* and the Fermi sea to as *the environment*. With the atom neutral and highly localized, its free Hamiltonian is given by

$$H_S = \frac{\hbar\Omega}{2} (|e\rangle\langle e| - |g\rangle\langle g|), \quad (6.7)$$

where Ω is the frequency related to the energy difference $\Delta E = \hbar\Omega$ between the states $|e\rangle$ and $|g\rangle$. The Hamiltonian of the Fermi sea is

$$H_E = \int \Psi^\dagger(x) \left(-\frac{\hbar^2}{2m} \frac{d^2}{dx^2} + \frac{1}{2} m\omega^2 x^2 \right) \Psi(x) dx, \quad (6.8)$$

where $\Psi^\dagger(x)$ and $\Psi(x)$ are the fermionic creator and annihilator operators, respectively.

Assume that $|e\rangle$ has a proper s -wave scattering length, and $|g\rangle$ does not interact with the environment. Considering that the system is confined in a point $x = d$ by a strong enough potential, the kinetic energy can be neglected. Thus, the interaction Hamiltonian is given by

$$H_I = \kappa \int \Psi^\dagger(x) \delta(x - d) \Psi(x) dx, \quad (6.9)$$

where κ is the magnitude of the scattering potential; that is related to the phase shift δ of Eq. (6.5). Where the total Hamiltonian is

$$H = H_S + H_E + H_I. \quad (6.10)$$

The system state is initially in a superposition of $|g\rangle$ and $|e\rangle$ with equal probabilities and the Fermi sea in the fundamental state of the Harmonic oscillator:

$$|\xi(0)\rangle = \frac{1}{\sqrt{2}} (|g\rangle + |e\rangle) \otimes |\phi\rangle, \quad (6.11)$$

where ϕ is the initial state of the Fermi sea. As the global system is closed, its evolution is described by the unitary operator $U = e^{-i(H_E+H_I)t}$, where $H_I|e\rangle \approx |e\rangle$. Then we get

$$|\xi(t)\rangle = \frac{1}{\sqrt{2}} (U|g\rangle \otimes |\phi\rangle + U|e\rangle \otimes |\phi\rangle) \quad (6.12)$$

$$= \frac{1}{\sqrt{2}} (e^{-iH_E t} |g\rangle \otimes |\phi\rangle + e^{-i(H_E+H_I)t} |e\rangle \otimes |\phi\rangle) \quad (6.13)$$

$$= \frac{1}{\sqrt{2}} (|g\rangle \otimes |\Phi_g(t)\rangle + |e\rangle \otimes |\Psi_e(t)\rangle), \quad (6.14)$$

with

$$|\Phi_g(t)\rangle = e^{-iH_F t} |g\rangle \otimes |\phi\rangle \quad (6.15)$$

$$\text{and} \quad (6.16)$$

$$|\Psi_e(t)\rangle = e^{-i(H_F+H_I)t}. \quad (6.17)$$

At a given time t , the reduced density matrix of the Fermi Sea is

$$\rho_E = \text{tr}_S (|\xi(t)\rangle \langle \xi(t)|) = \frac{1}{2} (|\Phi_g(t)\rangle \langle \Phi_g(t)| + |\Psi_e(t)\rangle \langle \Psi_e(t)|), \quad (6.18)$$

and the reduced density matrix of the system is

$$\begin{aligned} \rho_S &= \text{tr}_E (|\xi(t)\rangle \langle \xi(t)|) \\ &= \frac{1}{2} (|g\rangle \langle g| + \langle \Psi_e(t)|\Phi_g(t)\rangle |g\rangle \langle e| + \langle \Phi_g(t)|\Psi_e(t)\rangle |e\rangle \langle g| + |e\rangle \langle e|). \end{aligned} \quad (6.19)$$

As the system interacts with the environment, it loses coherence, and the off-diagonal terms of ρ_S decrease quickly. The coherence of the system is, therefore, proportional to

$$\langle \Phi_g(t)|\Psi_e(t)\rangle = \nu. \quad (6.20)$$

The quantity $L(t) = |\nu(t)|^2$ is known as *Loschmidt echo* and is frequently used to quantify decoherence in many-body subenvironments [94, 95]. If $|\Phi_g(t)\rangle$ and $|\Psi_e(t)\rangle$ are orthogonal, the state of Eq. (6.14) becomes maximally entangled. Then, there is a clear connection between Anderson's orthogonality catastrophe and entanglement.

6.2.2 Overlaps

Now, let us analyze the Fermi Sea separately. As the Fermi sea is localized by a harmonic trap and is in the ground state, each non-perturbed particle occupies one of the

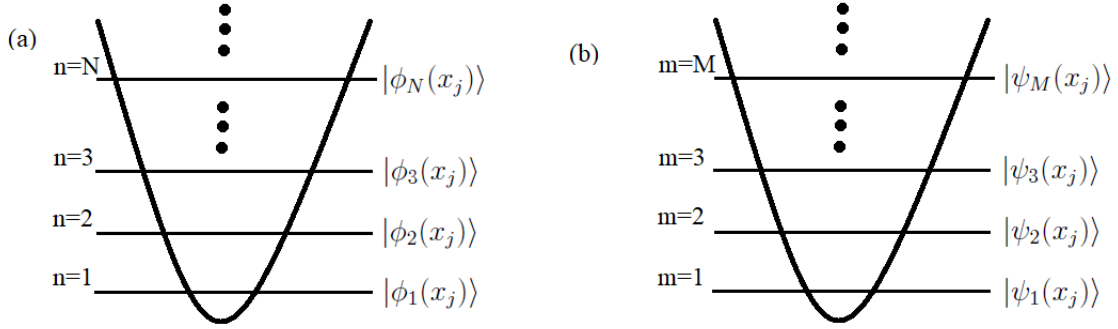


Figure 22 – Quantum harmonic oscillator levels $\{n\}$ that a particle j can occupy without interaction $|\phi_n(x_j)\rangle$ and with interaction $|\psi_n(x_j)\rangle$.

harmonic oscillators' lowest levels (see Fig. 22(a)). The wave function to each fermion at each level is given by the Bessel functions

$$|\phi_n(x_j)\rangle \equiv \phi_n(k_j, x_j) = \frac{\sin(k_j x_j)}{k_j x_j}, \quad (6.21)$$

where n is the level occupied by the j -th particle whose coordinate and wavenumber are x_j and k_j , respectively. Since k_j is directly related to n we drop it off in the ket. The state of the Fermi sea is given by the Slater determinant of the individual states $|\phi_n(k_j, x_j)\rangle$

$$|\Phi(x_1, \dots, x_N)\rangle = \frac{1}{N!} \sum_P \text{sgn}(P) |\phi\rangle_{P(1)}(x_1) \cdots |\phi\rangle_{P(N)}(x_N), \quad (6.22)$$

where N is the total number of fermions and P is the permutations over the possible occupied states. The state $|\Psi(x_1, \dots, x_N)\rangle$ of the perturbed Fermi (Eq. (6.17)) sea is taken similarly. Note that the interaction with the atom shifts the Fermi sea from the ground state. Thus, the number of the maximal level occupied M can be larger than N (see Fig. 22(b)).

The overlap $\langle \Psi(x_1, \dots, x_N) | \Phi(x_1, \dots, x_N) \rangle$ is given by

$$\nu = \langle \Psi(x_1, \dots, x_N) | \Phi(x_1, \dots, x_N) \rangle \quad (6.23)$$

$$= \sum_{PP'} \text{sign}(P) \text{sign}(P') \prod_i \Delta_{P(i), P'(i)}, \quad (6.24)$$

where $\Delta_{m,n} = \langle \phi_m(x) | \psi_n(x) \rangle = \int \psi_n^*(x) \phi_m(x) dx$ is the overlap between two fermions states, with $m = P(i)$ and $n = P'(i)$.

The single particles overlap $\langle \phi_m(x) | \psi_n(x) \rangle$ forms the matrix Δ

$$\Delta = \begin{bmatrix} \langle \phi_1(x) | \psi_1(x) \rangle & \cdots & \langle \phi_1(x) | \psi_N(x) \rangle \\ \vdots & \ddots & \vdots \\ \langle \phi_N(x) | \psi_1(x) \rangle & \cdots & \langle \phi_N(x) | \psi_N(x) \rangle \end{bmatrix}. \quad (6.25)$$

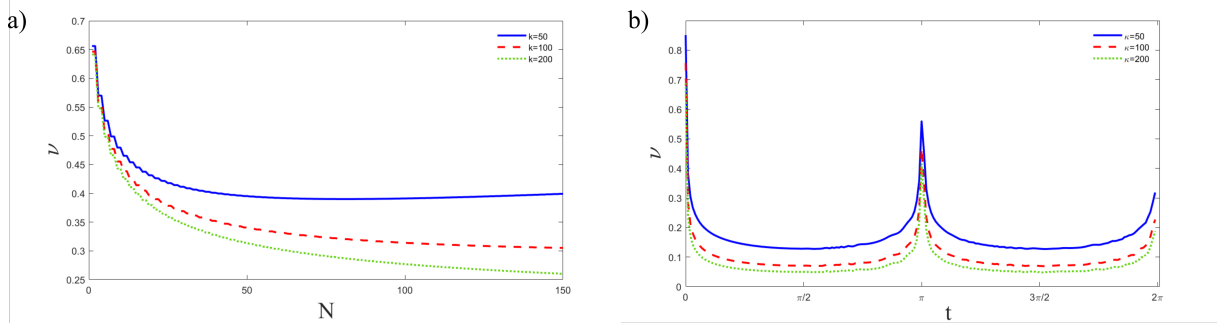


Figure 23 – a) ν in function of the number of particles N at $t = \pi/2$ and with $\kappa = 50$ (blue-solid line), $\kappa = 100$ (red-dashed line), and $\kappa = 200$ (green-dotted line). b) ν in function of t for $N = 150$ and with $\kappa = 50$ (blue-solid line), $\kappa = 100$ (red-dashed line), and $\kappa = 200$ (green-dotted line)

When there is no particle occupying a certain level n its wavefunction is $\psi_n(x) = 0$. As the number of levels occupied can be different for the perturbed and unperturbed Fermi sea, $\Delta_{m,n} = \langle \phi_m(x) | \psi_n(x) \rangle = 0$ for indexes $m > n$. Then, we can truncate the matrix to the order $N \times N$, and the overlap of Eq. (6.24) becomes

$$\nu = \det \Delta \quad (6.26)$$

6.2.3 Orthogonality Catastrophe and Entanglement

In this model, the atom interacts and perturbs the Fermi sea only when the atom is in $|e\rangle$. Thus, the orthogonality is maximal when the probability P_e to measuring the atom $|e\rangle$ is maximal. For the system and environment in a product state initially and with the dynamics driven by the Hamiltonian of Eq. (6.10), the orthogonality ν oscillates. We calculate the orthogonality varying on time for fixed interaction magnitude κ and the number of particles. The plots in Fig. 23(a) shows the behavior of ν in function of the number of particles N at a fixed $t = \pi/2$, for $\kappa = 50$ (blue-solid line), $\kappa = 100$ (red-dashed line), and $\kappa = 200$ (green-dotted line). We see that the orthogonality increases (and ν decreases) with the number of particles N and with the interaction. Fig. 23(b) displays one oscillation cycle on time of ν . Its minimal value is attained at time values multiple of $\pi/2$, namely when $P_e = 1$.

Goold et al. also connect entanglement and orthogonality catastrophe with von Neumann entropy:

$$S(t) = - \sum_i \lambda_i(t) \log \lambda_i(t), \quad (6.27)$$

where $\{\lambda_i(t)\}$ are the eigenvalues of ρ_E . In this model, $S(t)$ gives the degree of entanglement of the Fermi sea. Fig. 24 shows as a color scheme the von Neumann entropy entropy varying with t and N for $\kappa = 200$ and $\kappa = 50$. We can see that the state becomes maximally entangled at the resonance time $t = C\pi/2$ where C is an integer-positive

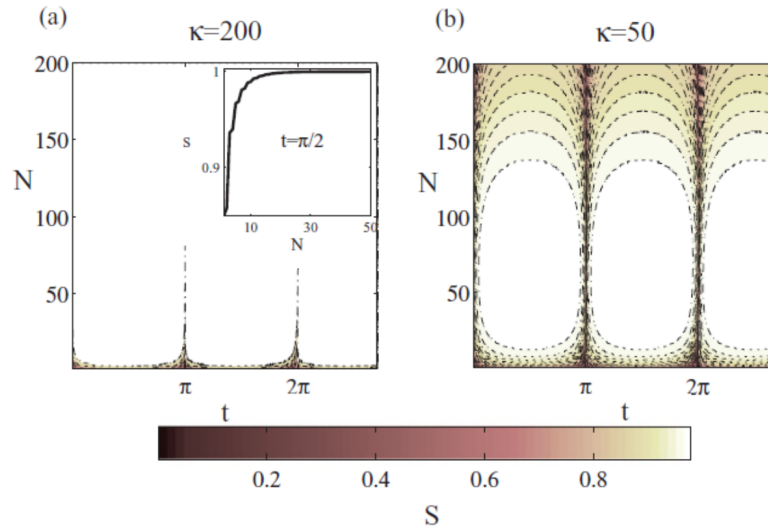


Figure 24 – (Color) Von Neumann entropy S varying with time t in units of the inverse of the trapping frequency (ω^{-1}) for (a) $\kappa = 200$ in units of $l_0/(\hbar\omega)$, and (b) $\kappa = 50$. The inset in (a) shows the Von Neumann entropy varying with N at the time resonance $t = \pi/2$. This image was taken from Ref. [90].

number for both strong ($\kappa = 200$) and weak ($\kappa = 50$) couplings. For strong coupling (see the inset in Fig. 24 (a)), orthogonality catastrophe is observed even for small environments ($N \approx 15$). Furthermore, for large N , the entanglement is close to 1 at any time. For weak coupling (Fig. 24 (b)), the state becomes maximally entangled for large environments and around the resonance, $t = C\pi/2$. These results agree with Anderson's Orthogonality catastrophe and show that it is possible to associate the Fermi sea with a new system (the impurity) without loss of generality. By comparing Figs. 23 and 24 becomes clear that the orthogonality is maximal (and ν is minimal) when the entropy is maximal, indicating that orthogonality catastrophe comes with decoherence.

This work brings a new perspective to orthogonality catastrophe. Now we see that it can be applied to quantum information. Also, the measurement of large systems such as a Fermi sea can be tricky experimentally, thus associating the entire many-body system to a single particle can be very useful.

6.2.4 Tonks-Girardeau Gas

Tonks-Girardeau Gas is a kind of many-body bosonic system that can be mapped into a Fermi sea. This mapping enables the investigation of Orthogonality catastrophe in a bosonic environment. T. Busch and his team performed such analysis where they studied two strongly interacting bosons coupled to an impurity atom, all trapped by a harmonic potential Ref. [93]. By analyzing the Loschmidt echo and the entanglement degree, they show that orthogonality catastrophe can be observed in bosons, even for small systems.

Tonks-Girardeau gas is formed by strongly repulsive bosons where each boson behaves as a *hard-core*. Consider a bosonic many-body system trapped in a nearly one-dimensional trajectory with Hamiltonian

$$H = \sum_{n=1}^N \left[-\frac{\hbar^2}{2m} \frac{d^2}{dx_n^2} + V(x_n) \right] + g_{1D} \sum_{i<j} \delta(|x_i - x_j|), \quad (6.28)$$

where N is the number of bosons, V is the trapping potential and $g_{1D} > 0$ is the interaction intensity. When $g_{1D} \rightarrow \infty$, the system reaches the Tonks-Girardeau limit. In this case, the repulsion between the bosons is so strong that only one particle can occupy the same level. This phenomenon is analogous to Pauli's exclusion principle for fermions. Therefore, the behavior of a Tonks-Girardeau gas is similar to the Fermi sea presented previously.

A Tonks-Girardeau gas can be mapped mathematically into a similar fermionic system. M. Girardeau showed this in 1960 by the Fermi-Bose mapping theorem [92, 96, 97]. To do so, we first replace the last term in Eq. (6.28) with the boundary condition

$$|\psi_B\rangle(x_1, \dots, x_n) = 0 \quad \text{if} \quad |x_i - x_j| = 0, \quad (6.29)$$

for $i \neq j$ and $1 \leq i \leq j \leq N$. When we calculate the Slater determinant of a Fermi sea (Eq. (6.22)), such constraint is implicit. Since the boson wave functions are symmetric while fermions are antisymmetric, we need to correct the symmetrization. Thus, we can apply the symmetrizer operator (S) in the Fermi sea state to obtain $|\Psi_B\rangle$ (see Appendix B),

$$S(x_1, \dots, x_n) = \prod_{1 \leq i < j \leq N} \text{sgn}(x_i - x_j). \quad (6.30)$$

Therefore we get

$$|\Psi_B\rangle(x_1, \dots, x_n) = S(x_1, \dots, x_n) |\Psi_F\rangle(x_1, \dots, x_n), \quad (6.31)$$

where $|\Psi_F\rangle(x_1, \dots, x_n)$ is the Fermi sea global state. And for the ground state Eq. (6.31) simplifies to

$$|\Psi_B\rangle(x_1, \dots, x_n) = | |\Psi_F\rangle(x_1, \dots, x_n) | \quad (6.32)$$

The first Tonks-Girardeau experimental application was performed by I. Bloch and his team in 2004 [98]. They used a Bose-Einstein condensate with approximately 3×10^4 Rydberg atoms trapped in a 2D optical lattice. In the same year, the D.S. Weiss team [99] used trapped Rubidium atoms, but they used a 1D lattice.

Therefore, Tonks-Girardeau gas fulfills the conditions in which we aim to investigate quantum Darwinism, it forms a strongly correlated environment and is realizable experimentally.

6.3 Quantum Darwinism in a Fermi sea

As shown in Sec. 6.1, orthogonality catastrophe is a consequence of the small contributions with a phase shift $\delta(E_n)$ given by each particle of a fermionic environment. We also see that the system and the environment interact, leading the system to lose coherence; and as shown in Chap. 2, the decoherence process highlights the preferred basis of the system. Therefore, the environment can acquire information about the system (See Sec. 2.2).

The way how this information is distributed into the environment has significant consequences. When it is spread redundantly, one can observe quantum Darwinism, where a small fragment of the Fermi Sea contains almost all information about the system available in the whole environment. With T. Busch and T. Fogarty, we are investigating quantum Darwinism in the model of Ref. [90].

6.3.1 Preliminary Results

By using the BPH approach (Chap. 3) and the results presented in Sec. 6.2.3, we could determine the preferential basis. The measure-and-prepare map that describes the preferential observable is

$$\Lambda_F(\rho) \approx \sum_i \text{Tr}(M_i \rho) \sigma_{i,E}. \quad (6.33)$$

The map in Eq. (6.33) applied to ρ_S is the partial trace of the system's degree of freedom of the density matrix given by Eq. (6.14),

$$\Lambda_F^t(\rho_S) = \text{Tr}_{S,E-F}(|\psi(t)\rangle \langle \psi(t)|) \quad (6.34)$$

$$= \text{Tr}(|g\rangle \langle g| \rho_S) \rho_e(t)^{[F]} + \text{Tr}(|e\rangle \langle e| \rho_S) \rho_g(t)^{[F]}, \quad (6.35)$$

with $\rho_g(t)^{[F]} = \text{Tr}_{E-F} |\Phi_g(t)\rangle \langle \Phi_g(t)|$, $\rho_e(t)^{[F]} = \text{Tr}_{E-F} |\Psi_e(t)\rangle \langle \Psi_e(t)|$ and $F \ll N/2$ is a small fragment of the environment. From Eq. 6.35, one concludes that the preferential basis is $\{|g\rangle, |e\rangle\}$ and the preferential observable is energy. The information about the system's preferential observable is spread redundantly when the fidelity between $\rho_e(t)^{[F]}$ and $\rho_g(t)^{[F]}$ is close to zero; indicating that these states are orthogonal.

We calculated the overlap between $\rho_g(t)^{[F]}$ and $\rho_e(t)^{[F]}$ for a single fermion and found that redundancy and orthogonality are minimal. This is expected due to the nature of the problem. As shown in Sec. 6.1, the phase shift caused by the interaction in a single fermion is very small, which means that its state change is small. Thus, a single fermion gives essentially no information about the system. Does this imply that there is no quantum Darwinism at all in this model? Not yet. As we increase the fraction size, the correlations of $\rho_g(t)^{[F]}$ and $\rho_e(t)^{[F]}$ can (or not) increase the information about the system redundantly.

The particles of the Fermi Sea do not interact directly, but their wave function is strongly correlated. Consequently, the reduced density matrices of the environment fractions are quite complex. Thus, we are currently focused on improving our numerical and analytical calculations to find the redundant information for fractions $1 \leq F \leq N/2$.

6.4 Quantum Darwinism in Ultracold Atoms

Most of the environments in nature are huge and can be strongly correlated. Therefore, the Fermi Sea and Tonks-Girardeau can help in studying quantum Darwinism in more realistic systems. Ultracold atoms are well theoretically and experimentally studied, and there is a large number of works in literature. As quantum Darwinism's observation requires well-controlled systems, cold atoms could be an excellent tool to perform experiments of quantum Darwinism.

Thus, after computing quantum Darwinism in a Fermi sea, we shall investigate it in quantum a Tonks-Girardeau Gas through the Fermi-Bose mapping theorem. This study can make possible an experimental study in quantum Darwinism in highly correlated and large environments.

7 Conclusions and Future Perspectives

In this thesis, we presented the concept of quantum Darwinism and our works in this area. In my Ph.D. We discussed the relationship between quantum Darwinism and two, quantum non-Markovianity, and orthogonality catastrophe.

7.1 Quantum Darwinism and Non-Markovianity

In chap. 3, we analyze quantum Darwinism in a system under non-Markovian dynamics. The recent work presented in Ref. [42] stated that non-Markovian dynamics hinder quantum Darwinism. We showed that this effect is not general through a model of quantum harmonic oscillators in coherent states.

This model is well known in the literature, and we adapted it to our necessities. The analytical calculations of the system dynamics are in Appendices C and D. We computed the quantum Darwinism quantifiers numerically with some approximations detailed in Chap. 3.

We identified that the usual quantum Darwinism quantifier, redundancy R_δ , and \mathcal{N}_f used in Ref. [42] take into account neither the “information back-flow” oscillations nor the quantity of information that the whole environment has about the system. We thus propose a more suitable way to quantify quantum Darwinism, the averaged redundancy. It is noticeable that when we use the averaged redundancy in this model, quantum Darwinism can be observed in both PIP and BPH approaches (introduced in Chap. 3), for Markovian and non-Markovian dynamics.

7.2 Quantum Darwinism in Ultracold Gases

In Chap. 6, we present our in-progress work where we are investigating quantum Darwinism in a system inserted in a strongly correlated environment. The model of this work is a two-level atom whose environment is a Fermi sea.

We found analytically one of the necessary conditions for the observation of quantum Darwinism, and at this moment, we are working to improve our numerical calculations to identify the others.

Albeit quantum Darwinism is broadly studied, there are only a few quantities of works with more realistic models and experimental works. Therefore, models of Tonks Girardeau gas can be advantageous since they can be applied in cold atoms experiments. The observation of quantum Darwinism in this model can enable the application of such

studies in a bosonic model through the Tonks Girardeau by the mapping (introduced in Sec. 6.2.4) that can be implemented experimentally.

7.3 Future Perspectives

We aim to finish the studies of quantum Darwinism in a Fermi sea and find out if it can be related to orthogonality catastrophe, as mentioned in Chap. 6. Thus, we will study quantum Darwinism in Tonks Girardeau gas and propose an experimental realization.

There are many possibilities for applying quantum Darwinism studies, such as in the Tonks-Girardeau experiment in Ref. [98], where the cold atoms and the impurity are trapped in an optical lattice. Another possibility is in quantum electrodynamic cavities (QEDC). Ref. [100] proposes a model of polaritons that moves freely in an array of resonant optical cavities that form a strongly interacting many-body system. This model could also be used to investigate quantum Darwinism.

Quantum Darwinism is a promising concept with many possible implications. However, it is essential to improve some studies to understand it better. Therefore, we need to understand it more generally to be able to apply it in more realistic systems.

Bibliography

- [1] Schrödinger, Erwin: *Der stetige übergang von der mikro-zur makromechanik*. Naturwissenschaften, 14(28):664–666, 1926. Citado 2 vezes nas páginas 13 and 100.
- [2] Schrödinger, E: *Die gegenwärtige situation in der quantenmechanik die naturwissenschaften 23 807-812; 823-828; 844-849 [a 207d] transl.: The present situation in quantum mechanics, translator: John d. trimmer*. Proc. of the Ame. Philosophical Society, 124:323–38, 1935. Citado 2 vezes nas páginas 13 and 100.
- [3] Schrödinger, Erwin: *Discussion of probability relations between separated systems*. Em *Mathematical Proceedings of the Cambridge Philosophical Society*, volume 31, páginas 555–563. Cambridge University Press, 1935. Citado 2 vezes nas páginas 13 and 100.
- [4] Heisenberg, Werner: *The actual content of quantum theoretical kinematics and mechanics*. 1983. Citado 2 vezes nas páginas 13 and 100.
- [5] Bohr, Niels: *The quantum postulate and the recent development of atomic theory*, 1928. Citado 3 vezes nas páginas 13, 21, and 100.
- [6] Bohr, Niels: *Discussions with einstein on epistemological problems in atomic physics albert einstein: Philosopher-scientist*. Library of Living Philosophers, 7, 1949. Citado 3 vezes nas páginas 13, 21, and 100.
- [7] Wheeler, John Archibald e Wojciech Hubert Zurek: *Quantum theory and measurement*. Princeton University Press, 2014. Citado 2 vezes nas páginas 13 and 100.
- [8] Breuer, Heinz Peter, Francesco Petruccione *et al.*: *The theory of open quantum systems*. Oxford University Press on Demand, 2002. Citado 4 vezes nas páginas 14, 17, 50, and 115.
- [9] Boulant, N, Joseph Emerson, TF Havel, DG Cory e S Furuta: *Incoherent noise and quantum information processing*. The Journal of chemical physics, 121(7):2955–2961, 2004. Citado na página 14.
- [10] Viola, Lorenza, Evan M Fortunato, Marco A Pravia, Emanuel Knill, Raymond Laflamme e David G Cory: *Experimental realization of noiseless subsystems for quantum information processing*. Science, 293(5537):2059–2063, 2001. Citado na página 14.

- [11] Suter, Dieter e Gonzalo A Álvarez: *Colloquium: Protecting quantum information against environmental noise*. Reviews of Modern Physics, 88(4):041001, 2016. Citado na página 14.
- [12] Schrödinger, Erwin: *The interpretation of quantum mechanics: Dublin seminars (1949-1955) and other unpublished essays*. Ox Bow Pr, 1995. Citado na página 17.
- [13] Zeh, H Dieter: *On the interpretation of measurement in quantum theory*. Foundations of Physics, 1(1):69–76, 1970. Citado 2 vezes nas páginas 17 and 23.
- [14] Zurek, Wojciech H: *Pointer basis of quantum apparatus: Into what mixture does the wave packet collapse?* Physical review D, 24(6):1516, 1981. Citado 3 vezes nas páginas 17, 20, and 23.
- [15] Zurek, Wojciech H: *Environment-induced superselection rules*. Physical review D, 26(8):1862, 1982. Citado 4 vezes nas páginas 17, 20, 23, and 25.
- [16] Zurek, Wojciech H: *Decoherence and the transition from quantum to classical—revisited*. arXiv preprint quant-ph/0306072, 2003. Citado na página 17.
- [17] Schlosshauer, Maximilian: *Quantum decoherence*. Physics Reports, 831:1–57, Oct 2019, ISSN 0370-1573. <http://dx.doi.org/10.1016/j.physrep.2019.10.001>. Citado 3 vezes nas páginas 17, 20, and 38.
- [18] Schlosshauer, Maximilian A: *Decoherence: and the quantum-to-classical transition*. Springer Science & Business Media, 2007. Citado 2 vezes nas páginas 17 and 18.
- [19] Zurek, Wojciech H: *Decoherence and the transition from quantum to classical—revisited*. Los Alamos Science, 27:86–109, 2002. Citado na página 17.
- [20] Hornberger, Klaus, Stefan Gerlich, Philipp Haslinger, Stefan Nimmrichter e Markus Arndt: *Colloquium: Quantum interference of clusters and molecules*. Reviews of Modern Physics, 84(1):157, 2012. Citado na página 18.
- [21] Leggett, Anthony J: *Testing the limits of quantum mechanics: motivation, state of play, prospects*. Journal of Physics: Condensed Matter, 14(15):R415, 2002. Citado na página 18.
- [22] Leibfried, Dietrich, Rainer Blatt, Christopher Monroe e David Wineland: *Quantum dynamics of single trapped ions*. Reviews of Modern Physics, 75(1):281, 2003. Citado na página 18.
- [23] Häffner, Hartmut, Christian F Roos e Rainer Blatt: *Quantum computing with trapped ions*. Physics reports, 469(4):155–203, 2008. Citado na página 18.

- [24] Brune, Michel, E Hagley, J Dreyer, X Maitre, Abdelhamid Maali, Ch Wunderlich, JM Raimond e S Haroche: *Observing the progressive decoherence of the “meter” in a quantum measurement*. Physical Review Letters, 77(24):4887, 1996. Citado na página 18.
- [25] Hornberger, Klaus: *Introduction to decoherence theory*. Em *Entanglement and decoherence*, páginas 221–276. Springer, 2009. Citado na página 19.
- [26] Zurek, Wojciech Hubert: *Decoherence, einselection, and the quantum origins of the classical*. Reviews of modern physics, 75(3):715, 2003. Citado 3 vezes nas páginas 20, 35, and 36.
- [27] Paz, Juan Pablo e Wojciech Hubert Zurek: *Quantum limit of decoherence: Environment induced superselection of energy eigenstates*. Physical Review Letters, 82(26):5181, 1999. Citado na página 21.
- [28] Zurek, Wojciech H: *Preferred states, predictability, classicality and the environment-induced decoherence*. Progress of Theoretical Physics, 89(2):281–312, 1993. Citado na página 21.
- [29] Zurek, Wojciech H, Salman Habib e Juan Pablo Paz: *Coherent states via decoherence*. Physical Review Letters, 70(9):1187, 1993. Citado na página 21.
- [30] Zurek, Wojciech H: *Decoherence, einselection and the existential interpretation (the rough guide)*. Philosophical Transactions of the Royal Society of London. Series A: Mathematical, Physical and Engineering Sciences, 356(1743):1793–1821, 1998. Citado 2 vezes nas páginas 21 and 25.
- [31] Wheeler, John Archibald: *Mathematical foundations of quantum theory*. Em *Proceedings of the New Orleans Conference on the Mathematical Foundations of Quantum Theory, Academic, New York*, 1978. Citado na página 21.
- [32] Everett III, Hugh: *“relative state” formulation of quantum mechanics*. Reviews of modern physics, 29(3):454, 1957. Citado na página 21.
- [33] NEUMANN, Johann von e Robert T BEYER: *Mathematische Grundlagen der Quantenmechanik. Mathematical Foundations of Quantum Mechanics... Translated... by Robert T. Beyer*. Princeton University Press, 1955. Citado na página 22.
- [34] Zurek, Wojciech Hubert: *Information transfer in quantum measurements: Irreversibility and amplification*. Em *Quantum Optics, Experimental Gravity, and Measurement Theory*, páginas 87–116. Springer, 1983. Citado 3 vezes nas páginas 23, 25, and 28.
- [35] Zurek, Wojciech Hubert: *Quantum darwinism*. Nature physics, 5(3):181–188, 2009. Citado 2 vezes nas páginas 25 and 28.

- [36] Zurek, Wojciech H: *Einselection and decoherence from an information theory perspective*. Annalen der Physik, 9(11-12):855–864, 2000. Citado na página 25.
- [37] Zurek, Wojciech H: *Quantum darwinism and envariance*. arXiv preprint quant-ph/0308163, 2003. Citado na página 25.
- [38] Cover, Thomas M e Joy A Thomas: *Elements of information theory*. John Wiley & Sons, 2012. Citado 2 vezes nas páginas 26 and 54.
- [39] Blume-Kohout, Robin e Wojciech H Zurek: *A simple example of “quantum darwinism”: Redundant information storage in many-spin environments*. Foundations of Physics, 35(11):1857–1876, 2005. Citado 3 vezes nas páginas 29, 30, and 32.
- [40] Oliveira, SM, AL de Paula Jr e RC Drumond: *Quantum darwinism and non-markovianity in a model of quantum harmonic oscillators*. Physical Review A, 100(5):052110, 2019. Citado 3 vezes nas páginas 30, 55, and 126.
- [41] Brandao, Fernando GSL, Marco Piani e Paweł Horodecki: *Generic emergence of classical features in quantum darwinism*. Nature communications, 6:7908, 2015. Citado 3 vezes nas páginas 30, 31, and 32.
- [42] Blume-Kohout, Robin e Wojciech H Zurek: *Quantum darwinism in quantum brownian motion*. Physical review letters, 101(24):240405, 2008. Citado 6 vezes nas páginas 35, 36, 37, 56, 58, and 87.
- [43] Zwolak, Michael, HT Quan e Wojciech H Zurek: *Quantum darwinism in a mixed environment*. Physical review letters, 103(11):110402, 2009. Citado 3 vezes nas páginas 35, 38, and 41.
- [44] Hu, Bei Lok, Juan Pablo Paz e Yuhong Zhang: *Quantum brownian motion in a general environment: Exact master equation with nonlocal dissipation and colored noise*. Physical Review D, 45(8):2843, 1992. Citado 2 vezes nas páginas 35 and 36.
- [45] Lindblad, Göran: *Brownian motion of quantum harmonic oscillators: Existence of a subdynamics*. Journal of Mathematical Physics, 39(5):2763–2780, 1998. Citado na página 35.
- [46] Unruh, WG e Wojciech H Zurek: *Reduction of a wave packet in quantum brownian motion*. Physical Review D, 40(4):1071, 1989. Citado na página 35.
- [47] Gröblacher, S, A Trubarov, N Prigge, GD Cole, M Aspelmeyer e J Eisert: *Observation of non-markovian micromechanical brownian motion*. Nature communications, 6(1):1–6, 2015. Citado na página 35.

- [48] Munday, Jeremy N, Davide Iannuzzi e Federico Capasso: *Quantum electrodynamical torques in the presence of brownian motion*. New Journal of Physics, 8(10):244, 2006. Citado na página 35.
- [49] Weiss, Ulrich: *Quantum dissipative systems*, volume 13. World scientific, 2012. Citado 2 vezes nas páginas 36 and 57.
- [50] Galve, Fernando, Roberta Zambrini e Sabrina Maniscalco: *Non-markovianity hinders quantum darwinism*. Scientific reports, 6:19607, 2016. Citado 8 vezes nas páginas 38, 55, 56, 58, 59, 60, 73, and 74.
- [51] Parzen, E: *Stochastic processes. society for industrial and applied mathematics*. Journal of Annals of Mathematical Statistics, 65(5):1585–1591, 1999. Citado na página 44.
- [52] Van Kampen, NG: *Stochastic processes in physics and chemistry, 3rd edn amsterdam*. The Netherlands: Elsevier, 2007. Citado na página 44.
- [53] Rivas, Ángel, Susana F Huelga e Martin B Plenio: *Quantum non-markovianity: characterization, quantification and detection*. Reports on Progress in Physics, 77(9):094001, 2014. Citado 3 vezes nas páginas 45, 48, and 52.
- [54] Fuchs, Christopher A e Jeroen Van De Graaf: *Cryptographic distinguishability measures for quantum-mechanical states*. IEEE Transactions on Information Theory, 45(4):1216–1227, 1999. Citado na página 45.
- [55] Nielsen, Michael A e Isaac Chuang: *Quantum computation and quantum information*, 2002. Citado 7 vezes nas páginas 45, 100, 101, 107, 108, 113, and 117.
- [56] Alicki, Robert e Karl Lendi: *Quantum dynamical semigroups and applications*, volume 717. Springer, 2007. Citado na página 46.
- [57] Fagnola, Franco: *Quantum markov semigroups and quantum flows*. Proyecciones, 18(3):1–144, 1999. Citado na página 46.
- [58] Breuer, Heinz Peter, Elsi Mari Laine e Jyrki Piilo: *Measure for the degree of non-markovian behavior of quantum processes in open systems*. Physical review letters, 103(21):210401, 2009. Citado 4 vezes nas páginas 46, 51, 53, and 60.
- [59] Chruściński, Dariusz e Andrzej Kossakowski: *Markovianity criteria for quantum evolution*. Journal of Physics B: Atomic, Molecular and Optical Physics, 45(15):154002, 2012. Citado 3 vezes nas páginas 47, 48, and 52.
- [60] Lindblad, Goran: *On the generators of quantum dynamical semigroups*. Communications in Mathematical Physics, 48(2):119–130, 1976. Citado na página 47.

- [61] Gorini, Vittorio, Andrzej Kossakowski e Ennackal Chandy George Sudarshan: *Completely positive dynamical semigroups of n -level systems*. Journal of Mathematical Physics, 17(5):821–825, 1976. Citado na página 47.
- [62] Rivas, Angel e Susana F Huelga: *Open quantum systems*, volume 13. Springer, 2012. Citado na página 48.
- [63] Helstrom, CW: *Quantum detection and estimation theory*, 123 academic press. New York, 1976. Citado na página 48.
- [64] Kossakowski, Andrzej: *On quantum statistical mechanics of non-hamiltonian systems*. Reports on Mathematical Physics, 3(4):247–274, 1972. Citado na página 48.
- [65] Kossakowski, Andrzej *et al.*: *On necessary and sufficient conditions for a generator of a quantum dynamical semi-group*. 1972. Citado na página 48.
- [66] Davies, Edward Brian: *Quantum theory of open systems*. Academic Press, 1976. Citado na página 50.
- [67] Wolf, Michael M e J Ignacio Cirac: *Dividing quantum channels*. Communications in Mathematical Physics, 279(1):147–168, 2008. Citado na página 50.
- [68] Chruściński, Dariusz, Andrzej Kossakowski e Ángel Rivas: *Measures of non-markovianity: Divisibility versus backflow of information*. Physical Review A, 83(5):052128, 2011. Citado 2 vezes nas páginas 50 and 51.
- [69] Rivas, Ángel, Susana F Huelga e Martin B Plenio: *Entanglement and non-markovianity of quantum evolutions*. Physical review letters, 105(5):050403, 2010. Citado 2 vezes nas páginas 50 and 52.
- [70] Hall, Michael JW, James D Cresser, Li Li e Erika Andersson: *Canonical form of master equations and characterization of non-markovianity*. Physical Review A, 89(4):042120, 2014. Citado na página 50.
- [71] Chruściński, Dariusz e Sabrina Maniscalco: *Degree of non-markovianity of quantum evolution*. Physical review letters, 112(12):120404, 2014. Citado na página 50.
- [72] Franco, R Lo, Bruno Bellomo, Erika Andersson e Giuseppe Compagno: *Revival of quantum correlations without system-environment back-action*. Physical Review A, 85(3):032318, 2012. Citado na página 51.
- [73] Plenio, Martin B e Shashank S Virmani: *An introduction to entanglement theory*. Em *Quantum Information and Coherence*, páginas 173–209. Springer, 2014. Citado 2 vezes nas páginas 52 and 109.

- [74] Luo, Shunlong, Shuangshuang Fu e Hongting Song: *Quantifying non-markovianity via correlations*. Physical Review A, 86(4):044101, 2012. Citado na página 52.
- [75] Lindblad, Göran: *Completely positive maps and entropy inequalities*. Communications in Mathematical Physics, 40(2):147–151, 1975. Citado na página 53.
- [76] Uhlmann, Armin: *Relative entropy and the wigner-yanase-dyson-lieb concavity in an interpolation theory*. Communications in Mathematical Physics, 54(1):21–32, 1977. Citado na página 53.
- [77] Lu, Xiao Ming, Xiaoguang Wang e CP Sun: *Quantum fisher information flow and non-markovian processes of open systems*. Physical Review A, 82(4):042103, 2010. Citado na página 53.
- [78] Bylicka, Bogna, D Chruściński e Sci Maniscalco: *Non-markovianity and reservoir memory of quantum channels: a quantum information theory perspective*. Scientific reports, 4(1):1–7, 2014. Citado na página 53.
- [79] Lorenzo, Salvatore, Francesco Plastina e Mauro Paternostro: *Geometrical characterization of non-markovianity*. Physical Review A, 88(2):020102, 2013. Citado na página 53.
- [80] Laine, Elsi Mari, Jyrki Piilo e Heinz Peter Breuer: *Measure for the non-markovianity of quantum processes*. Physical Review A, 81(6):062115, 2010. Citado na página 53.
- [81] Jozsa, Richard e Benjamin Schumacher: *A new proof of the quantum noiseless coding theorem*. Journal of Modern Optics, 41(12):2343–2349, 1994. Citado na página 54.
- [82] Jozsa, Richard: *Fidelity for mixed quantum states*. Journal of modern optics, 41(12):2315–2323, 1994. Citado na página 54.
- [83] Wang, Li, Jinchuan Hou e Kan He: *Fidelity, sub-fidelity, super-fidelity and their preservers*. International Journal of Quantum Information, 13(03):1550027, 2015. Citado na página 54.
- [84] Vasile, Ruggero, Sabrina Maniscalco, Matteo GA Paris, Heinz Peter Breuer e Jyrki Piilo: *Quantifying non-markovianity of continuous-variable gaussian dynamical maps*. Physical Review A, 84(5):052118, 2011. Citado 3 vezes nas páginas 54, 55, and 58.
- [85] Rubin, Robert J: *Momentum autocorrelation functions and energy transport in harmonic crystals containing isotopic defects*. Physical Review, 131(3):964, 1963. Citado na página 57.
- [86] Scully, Marlan O e M Suhail Zubairy: *Quantum optics*. Cambridge university press, 1997. Citado 2 vezes nas páginas 61 and 121.

- [87] Paula Jr, AL de, JGG de Oliveira Jr, JG Peixoto de Faria, Dagoberto S Freitas e MC Nemes: *Entanglement dynamics of many-body systems: Analytical results*. Physical Review A, 89(2):022303, 2014. Citado na página 61.
- [88] Santos, Jader P, Alberto L de Paula Jr, Raphael Drumond, Gabriel T Landi e Mauro Paternostro: *Irreversibility at zero temperature from the perspective of the environment*. Physical Review A, 97(5):050101, 2018. Citado 2 vezes nas páginas 61 and 126.
- [89] Liu, Yufeng, Jinyan Zeng *et al.*: *Coherent states of a time-dependent forced harmonic oscillator and their aharonov-anandan phase*. Science in China Series A: Mathematics, 43(6):661–665, 2000. Citado na página 62.
- [90] Goold, John, Thomás Fogarty, N Lo Gullo, Mauro Paternostro e Th Busch: *Orthogonality catastrophe as a consequence of qubit embedding in an ultracold fermi gas*. Physical Review A, 84(6):063632, 2011. Citado 4 vezes nas páginas 77, 79, 83, and 85.
- [91] Anderson, Philip W: *Infrared catastrophe in fermi gases with local scattering potentials*. Physical Review Letters, 18(24):1049, 1967. Citado 3 vezes nas páginas 77, 78, and 79.
- [92] Girardeau, MD, Ewan M Wright e JM Triscari: *Ground-state properties of a one-dimensional system of hard-core bosons in a harmonic trap*. Physical Review A, 63(3):033601, 2001. Citado 2 vezes nas páginas 77 and 84.
- [93] Campbell, Steve, Miguel Ángel García-March, Thomás Fogarty e Thomas Busch: *Quenching small quantum gases: Genesis of the orthogonality catastrophe*. Physical Review A, 90(1):013617, 2014. Citado 2 vezes nas páginas 77 and 83.
- [94] Cucchietti, Fernando M, Diego AR Dalvit, Juan P Paz e Wojciech H Zurek: *Decoherence and the loschmidt echo*. Physical review letters, 91(21):210403, 2003. Citado na página 80.
- [95] Quan, HT, Zhi Song, Xu F Liu, Paolo Zanardi e Chang Pu Sun: *Decay of loschmidt echo enhanced by quantum criticality*. Physical review letters, 96(14):140604, 2006. Citado na página 80.
- [96] Girardeau, Marvin: *Relationship between systems of impenetrable bosons and fermions in one dimension*. Journal of Mathematical Physics, 1(6):516–523, 1960. Citado na página 84.
- [97] Deuretzbacher, Frank, Kai Bongs, Klaus Sengstock e Daniela Pfannkuche: *Evolution from a bose-einstein condensate to a tonks-girardeau gas: An exact diagonalization study*. Physical Review A, 75(1):013614, 2007. Citado na página 84.

- [98] Paredes, Belén, Artur Widera, Valentin Murg, Olaf Mandel, Simon Fölling, Ignacio Cirac, Gora V Shlyapnikov, Theodor W Hänsch e Immanuel Bloch: *Tonks–girardeau gas of ultracold atoms in an optical lattice*. *Nature*, 429(6989):277–281, 2004. Citado 2 vezes nas páginas 84 and 88.
- [99] Kinoshita, Toshiya, Trevor Wenger e David S Weiss: *Observation of a one-dimensional tonks-girardeau gas*. *Science*, 305(5687):1125–1128, 2004. Citado na página 84.
- [100] Hartmann, Michael J, Fernando GSL Brandao e Martin B Plenio: *Quantum many-body phenomena in coupled cavity arrays*. *Laser & Photonics Reviews*, 2(6):527–556, 2008. Citado na página 88.
- [101] Ballentine, Leslie E: *Quantum mechanics: a modern development*. World Scientific Publishing Company, 2014. Citado 2 vezes nas páginas 100 and 101.
- [102] Sakurai, JJ e Addison Wesley Longman: *Quantum mechanics*. Addison-Wesley, 1976. Citado 2 vezes nas páginas 100 and 101.
- [103] Cohen-Tannoudji, C., B. Diu e F. Laloe: *Quantum Mechanics*. Número v. 1 em *Quantum Mechanics*. Wiley, 1991, ISBN 9780471164333. <https://books.google.com.br/books?id=iHcpAQAAMAAJ>. Citado 7 vezes nas páginas 100, 121, 123, 124, 127, 131, and 132.
- [104] Koch, PM, L Moorman, BE Sauer, EJ Galvez, KAH van Leeuwen e D Richards: *Experiments in quantum chaos: microwave ionization of hydrogen atoms*. *Physica Scripta*, 1989(T26):51, 1989. Citado na página 100.
- [105] Davisson, CJ: *Germer (1927), lh*. *Phys. Rev*, 30:707, 1927. Citado na página 100.
- [106] Tonomura, Akiro, J Endo, T Matsuda, T Kawasaki e H Ezawa: *Demonstration of single-electron buildup of an interference pattern*. *American Journal of Physics*, 57(2):117–120, 1989. Citado na página 100.
- [107] Horodecki, Ryszard, Paweł Horodecki, Michał Horodecki e Karol Horodecki: *Quantum entanglement*. *Reviews of modern physics*, 81(2):865, 2009. Citado na página 109.
- [108] Vedral, Vlatko, Martin B Plenio, Michael A Rippin e Peter L Knight: *Quantifying entanglement*. *Physical Review Letters*, 78(12):2275, 1997. Citado na página 109.
- [109] Plenio, Martin B e Vlatko Vedral: *Teleportation, entanglement and thermodynamics in the quantum world*. *Contemporary physics*, 39(6):431–446, 1998. Citado na página 109.
- [110] Giedke, G, B Kraus, M Lewenstein e JI Cirac: *Entanglement criteria for all bipartite gaussian states*. *Physical review letters*, 87(16):167904, 2001. Citado na página 109.

- [111] Peebles Jr, Peyton Z: *Probability, random variables, and random signal principles*. McGraw Hill Book Company, 1987. Citado na página 116.
- [112] Heisenberg, Werner: *Über den anschaulichen inhalt der quantentheoretischen kinematik und mechanik*. Em *Original Scientific Papers Wissenschaftliche Originalarbeiten*, páginas 478–504. Springer, 1985. Citado na página 117.
- [113] Sen, Debashis: *The uncertainty relations in quantum mechanics*. Current Science, páginas 203–218, 2014. Citado na página 117.
- [114] Yuen, Horace P: *Two-photon coherent states of the radiation field*. Physical Review A, 13(6):2226, 1976. Citado na página 126.
- [115] Perelomov, Askold: *Generalized coherent states and their applications*. Springer Science & Business Media, 2012. Citado na página 126.
- [116] Arecchi, FT, Eric Courtens, Robert Gilmore e Harry Thomas: *Atomic coherent states in quantum optics*. Physical Review A, 6(6):2211, 1972. Citado na página 126.
- [117] Zurek, Wojciech H, Salman Habib e Juan Pablo Paz: *Coherent states via decoherence*. Physical Review Letters, 70(9):1187, 1993. Citado na página 126.
- [118] Cohen-Tannoudji, Claude, Bernard Diu, Frank Laloe e Bernard Dui: *Quantum mechanics (2 vol. set)*, 2006. Citado 3 vezes nas páginas 127, 128, and 133.
- [119] Lévy-Leblond, Jean Marc: *Nonrelativistic particles and wave equations*. Communications in Mathematical Physics, 6:286–311, 1967. Citado na página 128.
- [120] Zeeman, Pieter: *Over den invloed eener magnetisatie op den aard van het door een stof uitgezonden licht*. Koninklijke Akademie van Wetenschappen te Amsterdam, 1896. Citado na página 129.
- [121] Aspect, Alain, Philippe Grangier e Gérard Roger: *Experimental realization of einstein-podolsky-rosen-bohm gedankenexperiment: a new violation of bell's inequalities*. Physical review letters, 49(2):91, 1982. Citado na página 129.
- [122] Ter Haar, Dirk: *Elements of statistical mechanics*. Elsevier, 1995. Citado na página 133.

Appendix

APPENDIX A – The Foundations of Quantum Mechanics

This appendix recalls the quantum mechanics foundations. Even starting from the same postulates, one can develop distinct immediate consequences. [55, 101–103]. Therefore, it is essential to mention that this chapter has Ref. [55] as the primary source of concepts description and examples.

The basis of a physical theory is composed of two parts: the physical concepts and the mathematical formalism. We can define the physical concepts from empirical observations. For example, a simple object can be classified by a set of parameters such as localization in space, velocity, mass, energy, and many others. However, to understand the connection (if it exists) between these parameters and their dynamics a second tool is needed, the mathematical formalism. With the combination of these two parts, we can better understand the physical nature by describing and predicting behaviors.

Two physical concepts that are worth defining are the system and its state. A *physical system* is an element of nature that exists objectively, and that we can somehow detect, like, for example, a car, a ball, a molecule, an atom, or a photon. The state of a *physical system* is a set of dynamical variables that describes it, as mass, position, velocity, spin, polarization, between others. Such conditions, individually or in groups, are named *observables* of the system; that is, they are parameters that we can observe direct or indirectly.

The link between physical concepts and mathematical formalism in classical physics is usually intuitive and straightforward. However, in quantum mechanics, this linking can be tricky. The mathematical description of quantum states is more complicated than classical ones, giving rise to several philosophic discussions [1–7].

When described by classical physics, some dynamical variables should take a continuum of values, but the results of experiments show only discrete values. For example, according to classical mechanics and electromagnetism, an electron should emit radiation in a frequency varying continuously while it loses energy and moves in a spiral movement toward the nucleus. Nevertheless, experimental observations show that the energy levels that such electrons can occupy are discrete [104]. Thus, the radiation emitted is proportional to the difference in energy between these levels. Some early experiments, like those in Refs. [105, 106] showed evidence of another important phenomenon, the diffraction of electrons. Beyond quantization, other phenomena such as quantum coherence and entanglement make some systems peculiar, and quantum theory helps understand them.

A.1 Linear Algebra and some Quantum Notation

Linear algebra describes linear equations and linear operations in vector spaces. A quantum system state can be described by a vector or, more generally, an operator and its evolution by linear operators that take a physical state into another physical state. Therefore, it is crucial to understand the basic concepts of linear algebra to describe quantum systems and their evolution. Refs. [55, 101, 102] present a useful review of linear algebra concepts that are essential in quantum mechanics.

Now, we shall recall some concepts of linear algebra and introduce some quantum notation.

A.1.1 Vectors

Usually, the complex conjugate of a matrix A is represented by A^* , its transpose by A^T , and its Hermitian conjugate by $A^\dagger = (A^T)^*$. It is also important to mention that linear algebra is a tool, and our primary interest is in quantum mechanics. Thus, we shall work with linear algebra in the standard quantum mechanics notation, also known as Dirac's notation. Consider a system state that is represented by a $(n \times 1)$ vector $v_{n \times 1}$. We denote the state $v_{n \times 1}$ as $|\psi\rangle$ using the Dirac's notation, where

$$|\psi\rangle = \begin{pmatrix} a_1 \\ a_2 \\ \vdots \\ a_n \end{pmatrix} = v. \quad (\text{A.1})$$

The entire $|\psi\rangle$ is named *ket* and represents only vectors. The vector dual to $|\psi\rangle$ is its transpose conjugate represented by the *bra* $\langle\psi|$.

A.1.2 Basis

A vector in a space vector can be written in terms of other vectors in the same space V . For example, let $v = |v\rangle$ be a vector given by

$$|v\rangle = \begin{pmatrix} a_1 \\ a_2 \end{pmatrix}. \quad (\text{A.2})$$

We can write v as $|v\rangle = a_1 |v_1\rangle + a_2 |v_2\rangle$ where

$$|v_1\rangle \equiv \begin{pmatrix} 1 \\ 0 \end{pmatrix} \quad \text{and} \quad |v_2\rangle \equiv \begin{pmatrix} 0 \\ 1 \end{pmatrix}. \quad (\text{A.3})$$

However, we can also write $|v\rangle$ as

$$|v\rangle = \frac{a_1 + a_2}{\sqrt{2}} |u_1\rangle + \frac{a_1 - a_2}{\sqrt{2}} |u_2\rangle, \quad (\text{A.4})$$

where

$$|v_1\rangle \equiv \frac{1}{\sqrt{2}} \begin{pmatrix} 1 \\ 1 \end{pmatrix} \quad \text{and} \quad |v_2\rangle \equiv \frac{1}{\sqrt{2}} \begin{pmatrix} 1 \\ -1 \end{pmatrix}. \quad (\text{A.5})$$

The set of vectors in Eqs. (A.3) and (A.5) are sets of *linearly independent* vectors. A set of vectors $|v_1\rangle \cdots |v_n\rangle$ is called *linearly dependent* if there exists a set of complex numbers a_1, \cdots, a_n such that

$$a_1 |v_1\rangle \cdots a_n |v_n\rangle = 0. \quad (\text{A.6})$$

Otherwise, it is called *linearly independent*. In a set of linearly dependent vectors, one vector can always be written in terms of the others, and linearly independent vectors never can be associated in this way. In the above example, the sets $\{v_1, v_2\}$ are examples of linearly independent vectors. These sets of linearly independent vectors form a *basis* in the space vector V and the number of elements of this basis is the dimension of V .

A.1.3 Linear Operators

Linear operators can represent the evolution and operations performed in quantum states. A *linear operator* A is a function that takes a matrix M in the space vector V in another matrix \tilde{M} in the space vector W , $A : V \rightarrow W$. In the case of a vector $|v\rangle = \sum_{i=1}^n a_i |v_i\rangle$, one can write

$$A |v\rangle = A \left(\sum_{i=1}^n a_i |v_i\rangle \right) = \left(\sum_{i=1}^n a_i A |v_i\rangle \right) = |w\rangle. \quad (\text{A.7})$$

An operator A defined in V takes the vector $|v\rangle$ in V to another vector $|w\rangle$ in the same space V , $A : V \rightarrow V$. The *identity operator* I takes a vector on itself, $I |v\rangle = |v\rangle$, and the *zero operator* maps any $|v\rangle$ to the zero vector, $0 |v\rangle \equiv 0$.

A.1.4 Inner Products, Outer Products, and Tensor Products

The inner product is an operation that associates two vectors to a scalar number. For two vectors $|u\rangle$ and $|v\rangle$, their inner product is given by $(|u\rangle^T)^* |v\rangle = \langle u|v\rangle$. The *norm* of a vector $|v\rangle$ is defined as

$$\| |v\rangle \| \equiv \sqrt{\langle v|v\rangle}, \quad (\text{A.8})$$

and we say that $|v\rangle$ is *normalized* if $\| |v\rangle \| = 1$. Two vectors $|u\rangle$ and $|v\rangle$ are *orthogonal* when $\langle u|v\rangle = 0$, and, if normalized, are identical when $\langle u|v\rangle = 1$.

The *outer product* associates two matrices to another matrix. The outer product of the matrices M_1 and M_2 is given by $M_1(M_2^T)^*$. For example, the outer product between the vectors $|v\rangle$ and $|w\rangle$ is given by

$$|v\rangle \left(|w\rangle^T \right)^* = |v\rangle \langle w|. \quad (\text{A.9})$$

In quantum mechanics formalism, some quantum operators can be described as an outer product. Such operators take a quantum state $|v\rangle$ in another valid quantum state $|w'\rangle$,

$$(|w\rangle\langle v|)|v'\rangle = |w\rangle\langle v|v'\rangle = \langle v|v'\rangle|w\rangle = |w'\rangle. \quad (\text{A.10})$$

Therefore, we can define the identity operator as

$$I \equiv \sum_i |i\rangle\langle i|. \quad (\text{A.11})$$

The *tensor product* defines a space vector composed of smaller space vectors. For example, V and W 's space vectors can be associated with a larger space vector given by $V \otimes W$, where \otimes is the tensor product symbol. The tensor product between two vectors $|v\rangle$ and $|w\rangle$ is given by $|v\rangle \otimes |w\rangle$.

A.1.5 Eigenvectors and Eigenvalues

An *eigenvector* of an operator A is a nonzero vector $|v\rangle$ such that $A|v\rangle = v|v\rangle$, where $v \in \mathbb{C}$ is a scalar named *eigenvalue*. To find the eigenvectors and eigenvalues of an operator, one can use the *characteristic function*

$$c(\lambda) = \det |A - \lambda I|, \quad (\text{A.12})$$

where I is the identity operator. The solution of the *characteristic equation*

$$c(\lambda) = 0 \rightarrow \det |A - \lambda I| = 0, \quad (\text{A.13})$$

gives the eigenvalues and eigenvectors of A .

A.1.6 Eigenspaces

With the characteristic function of Eq. (A.13) one can find the eigenvectors and eigenvalues of a given matrix A . Thus, we can define the set E composed of all vectors v that satisfy

$$E = \{v : \det (A - \lambda I) v = 0\}. \quad (\text{A.14})$$

E is the set of all possible eigenvectors of A with eigenvalues λ that forms the eigenspace of A .

A.2 Quantum states and Their Evolution

Postulate 1: Any isolated physical system can be associated with a Hilbert space known as *state space*. The system state is completely described by a unit matrix, also known as *state operator*, in the state space.

This postulate defines the mathematical tool that shall be used in quantum mechanics. The system states are described by unit matrices belonging to Hilbert space.

In a vector space, the linear combination of two or more state matrices generates another matrix state. Since quantum systems are described with vector states, a combination of two or more quantum states is also a valid quantum state. A quantum state $|\psi\rangle$ can be described as a combination of n other quantum states

$$|\psi\rangle = \sum_{i=1}^n a_i |\psi_i\rangle, \quad (\text{A.15})$$

where $|a_1|^2 + \dots + |a_n|^2 = 1$ for a normalized $|\psi\rangle$. This concept is known as the superposition principle. For example, consider a system that lives in a two-dimensional space state known as a *qubit*. If $|0\rangle$ and $|1\rangle$ are two possible orthogonal states of the system, then

$$|\psi\rangle = \frac{1}{\sqrt{2}} (a|1\rangle + b|0\rangle), \quad (\text{A.16})$$

$a, b \in \mathbb{C}$ and $|a|^2 + |b|^2 = 1$, is also a possible state. This fact is known as the *superposition principle* of quantum states, and the condition $|a|^2 + |b|^2 = 1$ comes from $\langle\psi|\psi\rangle = 1$ and guarantees that $|\psi\rangle$ is a unitary vector.

Let us now define unitary operations and closed quantum systems. A quantum operator takes a quantum system to another quantum system and can describe quantum operations and quantum evolutions. A quantum operator U is *unitary* when $U^\dagger U = I$, where I is the identity operator. *Closed* quantum systems are isolated systems that do not interact with no other system. From these definitions, we can transcribe the second postulate of quantum mechanics.

Postulate 2: The state's evolution of a closed quantum system is always unitary; this means that the evolution from the state $|\psi\rangle$ to the state $|\psi'\rangle$ of a closed quantum system can be described by a unitary operator

$$|\psi'\rangle = U |\psi\rangle. \quad (\text{A.17})$$

Once the state vector of Eq. (A.15) is normalized, the squared coefficients $|a_i|^2$ give the probability of the state being in the state $|\psi_i\rangle$. Therefore, the description of quantum evolutions with unitary operators guarantees this probabilistic character of quantum states.

If we know the Hamiltonian H of the system, this unitary operation becomes the Schrödinger equation and gives the time evolution.

Postulate 2': The time evolution of a closed quantum system can be always described by the *Schrödinger equation*,

$$i\hbar \frac{d|\psi(t)\rangle}{dt} = H(|\psi(t)\rangle), \quad (\text{A.18})$$

where \hbar is the *Planck's constant* and the Hamiltonian is a Hermitian operator.

A.3 Measurement of Quantum systems

As in classical cases, one needs to measure a quantum system to know its state. Postulate 2 states how to describe the evolution of a closed quantum system. However, measurement performance makes the system no longer closed since the measurement apparatus has to interact with the system in some way.

When a quantum system is subject to a measurement process, there is a set of possible results. Each result can be obtained with a certain probability. The description of this measurement process requires the third postulate.

Postulate 3: Quantum measurements are described by a set of *measurement operators* $\{M_i\}$ acting on the system's space. The index m_i refers to each possible result of the measurement. Consider a system in a particular state $|\psi\rangle$. The probability of the measurement process getting an outcome m_i is given by

$$p(m_i) = \langle\psi|M_i|\psi\rangle. \quad (\text{A.19})$$

The state of the system immediately after the measurement is given by

$$\frac{M_i|\psi\rangle}{\sqrt{\langle\psi|M_i|\psi\rangle}}, \quad (\text{A.20})$$

where the denominator is a normalization fraction. The set of measurement operators obeys the *completeness equation*

$$\sum_i M_i^\dagger M_i = I, \quad (\text{A.21})$$

guaranteeing that all probabilities sum up to one

$$\sum_i p(m_i) = \sum_i \langle\psi|M_i|\psi\rangle = 1. \quad (\text{A.22})$$

Note, as described in Eq. (A.20), the measurement process is described by operators acting on the system, which can change the system state. In some cases, if the system is initially in a superposition, after the measurement, this superposition can be destroyed.

To infer the system state correctly after a measurement process, it is essential to distinguish the possible outcomes. Consider a system in the state

$$|\psi\rangle = a|\psi_1\rangle + b|\psi_2\rangle \quad (\text{A.23})$$

under a measurement process where the possible results are $|\psi_1\rangle$ with probability $|a|^2$ and $|\psi_2\rangle$ with probability $|b|^2$. When $|\psi_1\rangle$ and $|\psi_2\rangle$ are orthogonal, a lamp turns on a blue light if the measurement result is $|\psi_1\rangle$ and a yellow light if the measurement result is $|\psi_2\rangle$. However, if $\langle\psi_1|\psi_2\rangle > 0$, the colors will mix up, and the light will become green (see

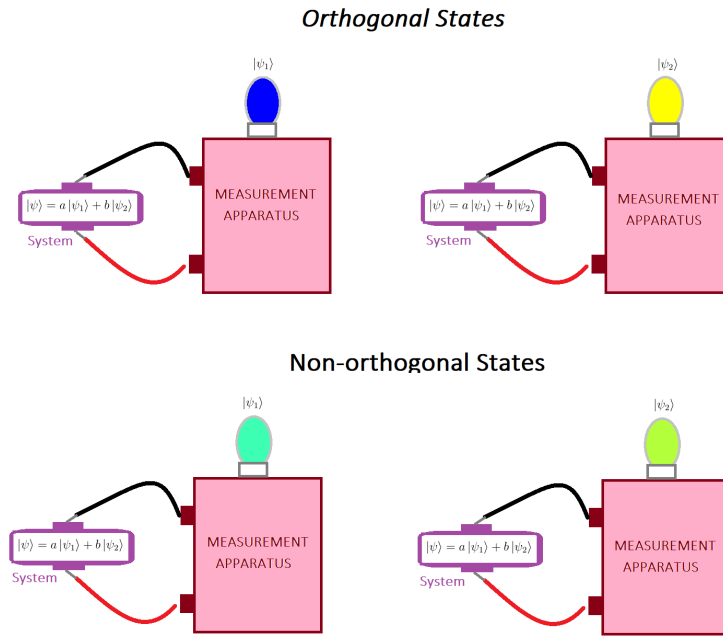


Figure 25 – (Color) $|\psi\rangle$ is an arbitrary superposition state of a two-level system. If the system state is measured in $|\psi_1\rangle$ the apparatus turn on a lamp with a blue light and if the state measured is $|\psi_2\rangle$ the lamp light becomes yellow. When the states are orthogonal the light colors can be clearly distinguished, otherwise the colors mix up and we can not exactly infer the system state.

Fig. 25). The measurement apparatus can not distinguish between the possible states of the system, and the answer is imprecise. Therefore, the orthogonality between the states of the system gives the distinguishability between them, and non-orthogonal states can never be distinguished correctly.

A.3.1 Projective Measurements

Projective measurements is a particular case of the measurement described in postulate 3. Projective measurements are described by Hermitian observables M in the system space with spectral decomposition

$$M = \sum_i P_i, \quad (\text{A.24})$$

where P_i is a projector onto the eigenspace of M with eigenvalue i . Each i is related to a possible outcome of the observable. Thus, the observable P outcomes are represented by projectors M_i applied to a state $|\psi\rangle$. The relation

$$p_M(i) = \langle \psi | P_i | \psi \rangle \quad (\text{A.25})$$

gives the probability of obtaining an outcome i after the measurement. Soon after the measurement, the state of the system becomes $|\psi\rangle$. Soon after the measurement, the state

of the system becomes

$$|\psi\rangle \longrightarrow \frac{P_i |\psi\rangle}{\sqrt{p_M(i)}}. \quad (\text{A.26})$$

Projectors of projective observables must satisfy three conditions: The completeness relation $\sum_i M_i^\dagger M_i = I$, the set of $\{M_i\}$ is composed by Hermitian orthogonal projectors, and $M_i M_i' = \delta_{i,i'} M_i$.

One example is the measurement of the observable Z in a qubit system in the state [55]

$$|\psi\rangle = \frac{1}{\sqrt{2}} (|0\rangle + |1\rangle), \quad (\text{A.27})$$

where

$$Z = \begin{pmatrix} 1 & 0 \\ 0 & -1 \end{pmatrix} = |1\rangle \langle 1| - |0\rangle \langle 0| \quad (\text{A.28})$$

whose eigenvalues of the respective eigenvectors $|0\rangle$ and $|1\rangle$ are $\lambda = 1$ and $\lambda = -1$. The projectors are $P_1 = |1\rangle \langle 1|$ with $\lambda = 1$ and $P_2 = |0\rangle \langle 0|$ with $\lambda = -1$. The probabilities are, therefore,

$$\begin{aligned} p(\lambda = 1) &= \langle \psi | P_1 | \psi \rangle \\ &= \frac{1}{2} (|0\rangle + |1\rangle) |1\rangle \langle 1| (|0\rangle + |1\rangle) = \frac{1}{2} \end{aligned} \quad (\text{A.29})$$

$$\begin{aligned} p(\lambda = -1) &= \langle \psi | P_2 | \psi \rangle \\ &= \frac{1}{2} (|0\rangle + |1\rangle) |0\rangle \langle 0| (|0\rangle + |1\rangle) = \frac{1}{2}. \end{aligned} \quad (\text{A.30})$$

The states after the measurement are

$$\frac{P_1 |\psi\rangle}{\sqrt{p(1)}} = \frac{1}{\sqrt{2}} |1\rangle \quad (\text{A.31})$$

for the outcome related to $\lambda = 1$ and

$$\frac{P_2 |\psi\rangle}{\sqrt{p(-1)}} = \frac{1}{\sqrt{2}} |0\rangle \quad (\text{A.32})$$

for $\lambda = -1$.

POVM

Projective measurement properties are quite useful due to their simplicity; they are largely used in quantum computation studies. However, in general, the measurements do not satisfy all conditions required to be projective, and we need to back to postulate 3.

POVM (Positive Operator-Valued Measure) is a mathematical tool extracted from the measurement definition in postulate 3. Such measurements are useful when we are not interested in the state after the measurement but in the probabilities of outcomes. Define

$$E \equiv M_i^\dagger M_i. \quad (\text{A.33})$$

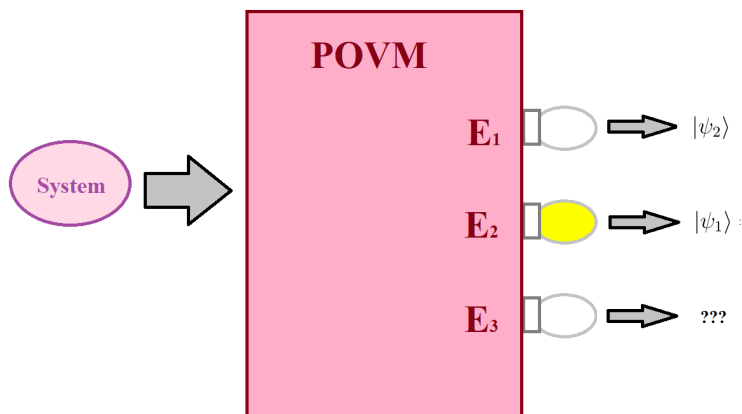


Figure 26 – Schematic illustrating a POVM kind measurement.

Then E is also a positive operator such that $\sum_i E_i = I$ and $p(i) = \langle \psi | E_i | \psi \rangle$. Each E_i is a *POVM element* and the set $\{E_i\}$ forms a POVM.

In the example of Eqs. (A.27) and (A.28) the POVM elements are $E_i = P_i$, since in this case $P_i P_{i'} = \delta_{i,i'} P_i$, and the probabilities are given by $p(i) = \langle \psi | E_i | \psi \rangle = \langle \psi | P_i | \psi \rangle$. In this case, the operators are orthogonal, meaning that it is always possible to distinguish the outcomes. However, this is not general.

Consider the example where a system in a state $|\psi\rangle$ with the two possible outcomes

$$|\psi_1\rangle = |0\rangle \quad (\text{A.34})$$

and

$$|\psi_2\rangle = \frac{1}{\sqrt{2}} (|0\rangle + |1\rangle). \quad (\text{A.35})$$

To perform a measurement to determine the system state one can apply a POVM with the following elements

$$E_1 \equiv \frac{\sqrt{2}}{1 + \sqrt{2}} |1\rangle \langle 1|, \quad (\text{A.36})$$

$$E_2 \equiv \frac{\sqrt{2}}{1 + \sqrt{2}} \frac{(\langle 0| - \langle 1|)(|0\rangle - |1\rangle)}{2}, \quad (\text{A.37})$$

$$E_3 \equiv I - E_1 - E_2, \quad (\text{A.38})$$

where it is easy to check that $\sum_i E_i = I$ [55]. Suppose that the system is measured by a POVM apparatus with three possible outcomes. Each outcome is the result of a POVM element acting on the system's state and turning on a lamp when activated (See Fig 26). If the system state is $|\psi_1\rangle$, the probability of observing E_1 is $p(E_1) = \langle \psi_1 | E_1 | \psi_1 \rangle = 0$. Thus, if the measurement outcome is E_1 the system's state is, for sure, $|\psi_2\rangle$. Likewise, if the state is $|\psi_2\rangle$, the probability of observing the outcome E_2 is null. If the result of the measurement is E_2 , the system's state must be $|\psi_1\rangle$. However, if the result is $|E_0\rangle$,

we can not infer the system state, since both, $\langle \psi_1 | E_3 | \psi_1 \rangle$ and $\langle \psi_2 | E_1 | \psi_2 \rangle$, are nonzero. If the outcomes are E_1 or E_2 , this POVM gives the system's state with precision and says nothing when the outcome is E_3 . POVM measurements are an option to get some information about systems whose possible outcomes are not orthogonal.

A.4 Composite Systems

It is quite rare to find wholly isolated systems in Nature. Systems, interacting or not, can form a larger system named *composite system*. If the composite system is closed, its evolution is governed by the Schrödinger equation and its description by tensor product.

Postulate 4: A set composed by n systems, $S = \{S_1, \dots, S_n\}$ is described by tensor products. Their state space $\mathcal{H}(S)$ is the tensor product of all individual state spaces $\{\mathcal{H}(S_1), \dots, \mathcal{H}(S_n)\}$, that is,

$$\mathcal{H}(S) = \mathcal{H}(S_1) \otimes \dots \otimes \mathcal{H}(S_n). \quad (\text{A.39})$$

If the state of the i -th system S_i is $|\psi_i\rangle$, the joint state $|\Psi\rangle$ of the global system S is given by

$$|\Psi\rangle = |\psi_1\rangle \otimes \dots \otimes |\psi_n\rangle. \quad (\text{A.40})$$

Composite systems can also be in superposition states. For example, consider a system S_A on a basis $\{a_i\}$ and a system S_B on a basis $\{b_i\}$. A possible superposition state $|\Psi\rangle$ for the composite system S_{AB} is

$$|\Psi\rangle \equiv \sum_i C_i |a_i\rangle |b_i\rangle, \quad (\text{A.41})$$

where $C_i \in \mathbb{C}$ are constants such that $\sum_i |C_i|^2 = 1$. In this case, the global state $|\Psi\rangle$ can not be written as a product state of the subsystems S_A and S_B . This superposition is known as *entanglement* [107]. Entanglement can be quantified in different ways [73, 107, 108] and has an important role in quantum mechanics [109, 110].

An example of a composite system is the set measurement M apparatus plus the system S . When the composite system $M + S$ is a closed global system, its evolution is unitary and is described in postulate 4. Let $\{M_i\}$ be the measurement operators on the system S , whose orthonormal basis is $\{|m_i\rangle\}$. If the unitary operator acts only on the space state of M , $U = I_S \otimes U_M$, the initial state of the measurement operator is $|m_0\rangle$, and the system state is $|\psi\rangle$, the evolution is given by

$$U |\psi\rangle |m_0\rangle \equiv \sum_i M_i |\psi\rangle |m_i\rangle. \quad (\text{A.42})$$

From the evolution of $S + M$, we can describe a measurement process. For a projective measurement described by projectors $P_i \equiv I_S \otimes |m_i\rangle\langle m_i|$, the probability to obtain an outcome i is

$$p(i) = \langle \psi | \langle 0 | U^\dagger P_i U | \psi \rangle | 0 \rangle \quad (\text{A.43})$$

$$= \sum_{i', i''} \langle \psi | M_{i'}^\dagger \langle m_{i'} | (I_S \otimes |m_i\rangle\langle m_i|) M_{i''} | \psi \rangle | m_{i''} \rangle. \quad (\text{A.44})$$

As $\{|m_i\rangle\}$ are orthogonal, $\langle m_{i'} | m_{i''} \rangle = \delta_{i', i''}$, the probability $p(i)$ becomes

$$p(i) = \langle \psi | M_i^\dagger M_i | \psi \rangle \quad (\text{A.45})$$

and the post-measurement state of the composite system following Eq. (A.26) becomes

$$\frac{M_i | \psi \rangle | m_i \rangle}{\sqrt{p(m_i)}} \quad (\text{A.46})$$

and the state of S is

$$\frac{M_i | \psi \rangle}{\sqrt{p(m_i)}}. \quad (\text{A.47})$$

In the last, the unitary operator does not act in the system, but it could. Let us consider a unitary evolution described by $U = U_S \otimes U_M$ and a system S with an orthonormal basis $\{|\psi_i\rangle\}$. For S and M with initial states $|\psi\rangle$ and $|m_0\rangle$, respectively, an interesting evolution is given by

$$U | \psi \rangle | m_0 \rangle \equiv \sum_i M_i | \psi_i \rangle | m_i \rangle. \quad (\text{A.48})$$

In this case, the S and M states can no longer be factorized. Now, each state of S and M are correlated by a factor M_i . This phenomenon is known as *entanglement*.

A.5 Density Matrix

We can conveniently use an operator to describe a quantum system. In some situations, the best description of a quantum system is a set of possible states $\{|\psi_k\rangle\}$, each with a probability p_k . This system state can be described through the *density operator*

$$\rho \equiv \sum_k p_k | \psi_k \rangle \langle \psi_k |. \quad (\text{A.49})$$

Also known as *the density matrix*, this operator can describe any quantum state. If there is a description of Eq. (A.49) state with only one element in the sum, this system is said to be in a *pure state*; otherwise, it is in a *mixed state*.

Notation and postulates

Any density matrix holds all postulates:

- Any ρ is associated to a Hilbert space \mathcal{H}
- The evolution of closed systems is always unitary

$$\rho \xrightarrow{U} U\rho U^\dagger \quad (\text{A.50})$$

- The evolution of quantum systems is described by the Schrödinger equation

$$i\hbar \frac{d\rho(t)}{dt} = H\rho(t), \quad (\text{A.51})$$

- The measurement process of a state ρ can be represented by the set of operators $\{M_i\}$.
- The state of composite systems with n subsystems is represented by tensor operators, $\rho_1 \otimes \cdots \otimes \rho_n$.

Therefore, the unitary evolution of a general density matrix is given by

$$\rho = \sum_k p_k |\psi_k\rangle \langle \psi_k| \xrightarrow{U} U\rho U^\dagger = \sum_k p_k U |\psi_k\rangle U^\dagger \langle \psi_k|. \quad (\text{A.52})$$

At this point, it is convenient to introduce a handy mathematical tool, the trace. The *trace of a matrix* is simply the sum of its diagonal elements. For a matrix A with elements $a_{i,j}$, where i is the i -th row and j is the j -th column, the trace is defined as

$$\text{tr}A \equiv \sum_i a_{ii}. \quad (\text{A.53})$$

Trace operations are *cyclic* $\text{tr}(AB) = \text{tr}(BA)$ and linear $\text{tr}(A+B) = \text{tr}(A) + \text{tr}(B)$.

Consider the identity matrix $I = \sum_i |i\rangle \langle i|$, where $\{|i\rangle\}$ is an orthonormal basis. Suppose A is an arbitrary operator acting in a system $\rho = |\psi\rangle \langle \psi|$. Applying the trace properties, we have

$$\text{tr}(A|\psi\rangle \langle \psi|) = \sum_i \langle i| (A|\psi\rangle \langle \psi|) |i\rangle \quad (\text{A.54})$$

$$= \sum_i \langle i|A|\psi\rangle \langle \psi|i\rangle \quad (\text{A.55})$$

$$= \langle \psi|A|\psi\rangle. \quad (\text{A.56})$$

Further, we can verify from the cyclic property that trace of density matrices (or any other operator) are invariant under unitary transformations

$$\text{tr}(U\rho U^\dagger) = \text{tr}(U^\dagger U\rho) = \text{tr}\rho. \quad (\text{A.57})$$

The measurement processes of mixed states can be described in a similar way to pure states. The difference is that we shall take to account an ensemble of pure states. Since ρ represents an ensemble of states $|\psi_k\rangle$, one needs to define which state k is being measured and all possible outcomes m_i . Consider the measurement process described by the operators set $\{M_i\}$ with possible outcomes $\{m_i\}$. If the system state in the moment of the measurement is $|\psi_k\rangle$, then the probability of obtaining the result m_i for a given k is

$$p(m_i|k) = \langle \psi_k | M_i^\dagger M_i | \psi_k \rangle. \quad (\text{A.58})$$

Observe that $p(m_i|k)$ using the cyclic property of trace we get

$$p(m_i|k) = \text{tr} \left(M_i^\dagger M_i | \psi_k \rangle \langle \psi_k | \right). \quad (\text{A.59})$$

Thus, from trace definition in Eq. (A.53), the probability to get the outcome m_i given all possible $|\psi_k\rangle$ is

$$p(m_i) = \sum_k p_k p(m_i|k). \quad (\text{A.60})$$

$$= \sum_k p_k \text{tr} \left(M_i^\dagger M_i | \psi_k \rangle \langle \psi_k | \right) \quad (\text{A.61})$$

$$= \text{tr} \left(M_i^\dagger M_i \rho \right). \quad (\text{A.62})$$

The density operator after the measurement is obtained in a similar way and is given by

$$\frac{M_i \rho M_i^\dagger}{\text{tr} \left(M_i^\dagger M_i \rho \right)} \quad (\text{A.63})$$

A.5.1 Density Matrix Properties

As mentioned previously, the density matrix is a general form to describe quantum systems that can not be represented by a single state vector $|\psi\rangle$, and it holds all quantum mechanics postulates. Thus, it is interesting to describe the density matrix in a way more general than an ensemble of vector states. From this, we present some general properties.

First, we connect the ensemble of the state's interpretation to general characteristics. Suppose we have a given operator ρ . It represents an ensemble of quantum states $\{p_i, |\psi_i\rangle\}$ only if some conditions are satisfied.

Property 1: ρ is a density operator only if it has trace one. Consider the ensemble $\rho = \sum_i p_i |\psi_i\rangle \langle \psi_i|$, thus

$$\text{tr}(\rho) = \text{tr} \left(\sum_i p_i |\psi_i\rangle \langle \psi_i| \right) \quad (\text{A.64})$$

$$= \sum_i p_i \text{tr}(|\psi_i\rangle \langle \psi_i|) \quad (\text{A.65})$$

$$= \sum_i p_i = 1. \quad (\text{A.66})$$

As $\text{tr}(|\psi_1\rangle\langle\psi_1|)$ and the probabilities p_i sum up to one, the trace of $|\rho\rangle$ is one.

Property 2: ρ is a positive operator. Consider an arbitrary vector in state space $|\phi\rangle$, thus

$$\langle\phi|\rho|\phi\rangle = \langle\phi|\sum_i p_i |\psi_1\rangle\langle\psi_1|\phi\rangle \quad (\text{A.67})$$

$$= \sum_i p_i \langle\phi|\psi_1\rangle\langle\psi_1|\phi\rangle \quad (\text{A.68})$$

$$= \sum_i p_i |\langle\phi|\psi_1\rangle|^2 \geq 0. \quad (\text{A.69})$$

Since $|\langle\phi|\psi_1\rangle|^2$ must be positive and the $p_i \geq 0$ for any state vector $|\phi\rangle$, the *positivity* of ρ must be satisfied.

Property 3: If ρ satisfies property 2, it must have a spectral decomposition (see Ref. [55] for more details of spectral decomposition). That is, there exist orthogonal vectors $|i\rangle$ and real non-negative eigenvalues λ_i such that

$$\rho = \sum_i \lambda_i |i\rangle\langle i|. \quad (\text{A.70})$$

The set $\{|i\rangle\}$ forms an orthonormal basis whose eigenvalues are $\{\lambda_i\}$. Therefore, $\sum_i \lambda_i = 1$ and $0 \leq \lambda \leq 1$.

Property 4: A density matrix ρ represent a pure state only if

$$\rho^2 = \rho. \quad (\text{A.71})$$

Consider the following spectral decomposition $\rho = \sum_i \lambda_i |i\rangle\langle i|$. One can write

$$\begin{aligned} \rho^2 &= \left(\sum_i \lambda_i |i\rangle\langle i| \right) \left(\sum_j \lambda_j |j\rangle\langle j| \right) \quad (\text{A.72}) \\ &= \sum_{i,j} \lambda_i \lambda_j |i\rangle\langle i| |j\rangle\langle j| \\ &= \sum_{i,j} \lambda_i \lambda_j |i\rangle\langle j| \langle j| \langle i| \\ &= \sum_{i,j} \lambda_i \lambda_j |i\rangle\langle j| \delta_{i|j} \\ &= \sum_i \lambda_i^2 |i\rangle\langle i|. \quad (\text{A.73}) \end{aligned}$$

Thus, $\rho^2 = \rho$ only when $\lambda^2 = \lambda$, that is, only if $\lambda = 1$. A consequence of this property is that $\text{tr}(\rho^2) = 1$ only if ρ represents a pure state; otherwise, $\text{tr}(\rho^2) \leq 1$. The trace of ρ^2 is given by

$$\text{tr}(\rho^2) = \sum_i \lambda_i^2. \quad (\text{A.74})$$

Since $0 \leq \lambda \leq 1$, $\sum_i \lambda_i^2 = 1$ only for pure states. For non-pure states, $\lambda_i < 1$ for all i and, therefore, $\text{tr}(\rho^2) < 1$.

A.5.2 Composite Systems and Reduced Density Matrix

As in single systems, the density matrix can also represent composite systems. Consider a composite system composed of two systems, S_A and S_B in the pure state

$$|\Psi_{AB}\rangle = c_1 |\alpha_1, \beta_1\rangle + c_2 |\alpha_2, \beta_2\rangle, \quad (\text{A.75})$$

where $|\alpha_1\rangle$ and $|\alpha_2\rangle$ are related to S_A and $|\beta_1\rangle$ and $|\beta_2\rangle$ to S_B . Its density matrix is given by

$$\rho_{AB} = |\Psi\rangle \langle\Psi| \quad (\text{A.76})$$

$$= |c_1|^2 |\alpha_1, \beta_1\rangle \langle\alpha_1, \beta_1| + |c_2|^2 |\alpha_2, \beta_2\rangle \langle\alpha_2, \beta_2| + c_1 c_2^* |\alpha_1, \beta_1\rangle \langle\alpha_2, \beta_2| + c_1^* c_2 |\alpha_2, \beta_2\rangle \langle\alpha_1, \beta_1|. \quad (\text{A.77})$$

The density matrix of non-pure states can also be represented as an ensemble of pure states $|\alpha_i, \beta_i\rangle$ with probability p_i

$$\rho = \sum_i p_i |\alpha_i, \beta_i\rangle \langle\alpha_i, \beta_i|. \quad (\text{A.78})$$

The description of composite systems with density matrices, even for pure states, is very convenient for finding the states of the subsystems; This is achieved by *taking the partial trace* of the subsystem that we are not interested in, that is

$$\rho_A \equiv \text{tr}_B (\rho_{AB}). \quad (\text{A.79})$$

The matrix ρ_A is known as *the reduced density matrix* for the system S_A . Consider the matrix $\rho = |\alpha_1, \beta_1\rangle \langle\alpha_2, \beta_2|$. Defining $\rho = |\alpha_1\rangle \langle\alpha_2| \otimes |\beta_1\rangle \langle\beta_2|$, the partial trace of ρ for $|\alpha_1\rangle \langle\alpha_2|$ is defined as

$$\text{tr}_B (|\alpha_1\rangle \langle\alpha_2| \otimes |\beta_1\rangle \langle\beta_2|) = |\alpha_1\rangle \langle\alpha_2| \text{tr}_B (|\beta_1\rangle \langle\beta_2|). \quad (\text{A.80})$$

The partial trace $\rho_A \equiv \text{tr}_B (\rho_{AB})$ is also a density matrix where all degrees of freedom of the subsystem S_B was discarded remaining only the state of S_A .

This tool is crucial in studies of open quantum systems. When an open quantum system interacts with other systems for some time interval $\Delta t = t_f - t_i$, its evolution can not be described by a unitary operator and, therefore, we can not use the Schrödinger equation to describe its final state. In this case, an option is to evolve the global state of all systems and to trace out the systems of non-interest after the interaction time.

A state represented by Eq. (A.80) is a product state of the two systems, meaning that the states of the subsystems can be factorized. However, this is not always the case. Suppose the state of a composed system is

$$|\psi\rangle = \frac{1}{\sqrt{2}} (|00\rangle + |11\rangle) \quad (\text{A.81})$$

whose density matrix is

$$\rho = \frac{1}{2} (|00\rangle \langle 00| + |11\rangle \langle 11| + |11\rangle \langle 00| + |00\rangle \langle 11|). \quad (\text{A.82})$$

By using the cyclic trace property, the reduced state of one subsystem S_1 is

$$\rho_1 = \text{tr}(\rho) \quad (\text{A.83})$$

$$= \frac{1}{2} \text{tr} (|00\rangle \langle 00| + |11\rangle \langle 11| + |11\rangle \langle 00| + |00\rangle \langle 11|) \quad (\text{A.84})$$

$$= \frac{1}{2} (|0\rangle \langle 0| \langle 0|0\rangle + |1\rangle \langle 1| \langle 1|1\rangle + |1\rangle \langle 0| \langle 0|1\rangle + |0\rangle \langle 1| \langle 1|0\rangle) \quad (\text{A.85})$$

$$= \frac{1}{2} (|0\rangle \langle 0| + |1\rangle \langle 1|). \quad (\text{A.86})$$

Note, the global system ρ can be represented by a single state vector $|\psi\rangle$, the reduced state ρ_1 is not pure. It is easy to check that $\rho^2 = \rho$ and $\rho_1^2 \neq \rho_1$.

It is important to mention that it is more convenient to describe the evaluation of open quantum systems through master equations in some situations. These master equations give the state of S at any time t and are obtained through the Liouville-von Neumann differential equation (see Ref. [8]).

Another interesting tool is the *Schmidt decomposition* that describes the global density matrix ρ_{AB} in such a way that reduced density matrices ρ_A and ρ_B with the same eigenvalues. Consider a composite system in a state $|\psi\rangle$. Then there exists orthonormal basis $\{|i_A\rangle\}$ related to the subsystem S_A and $\{|i_B\rangle\}$ related to the subsystem S_B such that

$$\rho_{AB} = \sum_i \lambda_i |i_A, i_B\rangle, \quad (\text{A.87})$$

where $\lambda_i \geq 0$, $\lambda_i \in \mathbb{R}$ and $\sum_i \lambda_i = 1$. The coefficients λ_i are known as the *Schmidt coefficients*. The set $\{|i_A, i_B\rangle\}$ forms a basis for ρ_{AB} where the eigenvalues, also known as *Schmidt coefficients*, are $\{\lambda_i\}$.

The partial trace over the Schmidt decomposition for S_A and S_B gives $\rho_A = \sum_i \lambda_i^2 |i_A\rangle \langle i_A|$ and $\rho_B = \sum_i \lambda_i^2 |i_B\rangle \langle i_B|$, respectively. Thus, the eigenvalues of both reduced density matrices are identical. Schmidt decomposition is quite useful since the eigenvalues are essential for many concepts of quantum theory.

APPENDIX B – Some Fundamental Concepts of Quantum Mechanics

This chapter recalls the main concepts used in the works described in this thesis. The first is the uncertainty principle in Sec. B.1. In Sec. B.2 we introduce conceptually an important class of quantum states: the coherent states. Then, we recall momentum angular in quantum systems in Sec B.3 and identical particles in Sec B.4.

B.1 Uncertainty Principle

As shown in Sec. A.3, a projective measurement M can be described by a set of projectors $\{P_i\}$ acting on the system state where each projector represents a possible outcome. In general, the same state is prepared and measured experimentally several times to define the M and $\{P_i\}$. Then, the calculation of the probabilities in Eq. (A.19) is quite opportune; this enables the computation of interesting quantities as average value and standard deviation of a particular measurement.

B.1.1 Average Value and Standard Deviation

Following the probability theory [111], the average value of a measurement M of a system in the state $|\psi\rangle$ is given by

$$Av(M) = \sum_i m_i p(m_i) \quad (\text{B.1})$$

$$= \sum_i m_i \langle \psi | P_i | \psi \rangle \quad (\text{B.2})$$

$$= \langle \psi | \sum_i m_i P_i | \psi \rangle = \langle \psi | M | \psi \rangle, \quad (\text{B.3})$$

that can be written as

$$\langle M \rangle \equiv \langle \psi | M | \psi \rangle. \quad (\text{B.4})$$

Since the last notation is frequently used, we shall work with it.

Another important quantity is the standard deviation $\Delta(M)$, that is given by

$$(\Delta M)^2 = \langle (M - \langle M \rangle)^2 \rangle. \quad (\text{B.5})$$

The standard deviation of a measurement sequence quantifies how much the results obtained deviate from the average value. It is crucial to determine the precision and reliability of a measure.

B.1.2 Heisenberg Uncertainty Principle

The application of average value and standard deviation concepts give rise to an elegant result introduced in 1927 by Werner Heisenberg [112, 113] known as the Heisenberg Uncertainty Principle. However, before describing the principle, let us define some mathematical concepts.

Commutator: The *commutator* of two squared matrices A and B gives the difference between the matrix multiplication AB and BA , that is,

$$[A, B] \equiv AB - BA. \quad (\text{B.6})$$

If $[A, B] = 0$ we say that the matrices A and B commute, otherwise it does not commute.

Anti-Commutator: The *anti-commutator* of A and B is given by

$$\{A, B\} \equiv AB + BA, \quad (\text{B.7})$$

and the matrices A and B anti-commutes if $\{A, B\} = 0$

Cauchy-Schwarz inequality: Consider two vectors in the Hilbert space $|u\rangle$ and $|v\rangle$. The Cauchy-Schwarz inequality affirms that

$$|\langle u|v\rangle|^2 \leq \langle u|u\rangle \langle v|v\rangle, \quad (\text{B.8})$$

where the equality happens only if $|u\rangle$ and $|v\rangle$ are related for some scalar z , that is

$$|v\rangle = z|u\rangle \quad \text{or} \quad |u\rangle = z|v\rangle. \quad (\text{B.9})$$

The demonstration of this inequality is very well described in Ref. [55].

Consider two Hermitian operators A and B that can act on a system in the state $|\psi\rangle$. Suppose that the averaged value for AB and $|\psi\rangle$ is

$$\langle AB \rangle = \langle \psi|AB|\psi \rangle = x + iy, \quad (\text{B.10})$$

for $x, y \in \mathbb{R}$. The average value of the commutator and anti-commutator between A and B are

$$\langle \psi|[A, B]|\psi \rangle = 2iy \quad (\text{B.11})$$

$$\langle \psi|\{A, B\}|\psi \rangle = 2x. \quad (\text{B.12})$$

Thus,

$$|\langle \psi|[A, B]|\psi \rangle|^2 + |\langle \psi|\{A, B\}|\psi \rangle|^2 = 4|\langle \psi|AB|\psi \rangle|^2. \quad (\text{B.13})$$

An operator O acting on a vector $|\psi\rangle$ generates another vector, $O|\psi\rangle = |\psi'\rangle$. By applying the Cauchy-Schwarz inequality to $\langle \psi|AB|\psi \rangle$ we get

$$|\langle \psi|AB|\psi \rangle|^2 \leq \langle \psi|A^2|\psi \rangle \langle \psi|B^2|\psi \rangle. \quad (\text{B.14})$$

Joining Eqs. (B.13) and (B.14), we get the following relation

$$|\langle \psi | [A, B] | \psi \rangle|^2 \leq 4 \langle \psi | A^2 | \psi \rangle \langle \psi | B^2 | \psi \rangle. \quad (\text{B.15})$$

As A and B are Hermitian, they can represent the standard deviation of observables. Then, suppose $A = C - \langle C \rangle$ and $B = D - \langle D \rangle$ and substitute in Eq. (B.15). The result is the *uncertainty Heisenberg principle*:

$$\Delta(C)\Delta(D) \geq \frac{|\langle \psi | [C, D] | \psi \rangle|}{2} \quad (\text{B.16})$$

This result lets clear what the commutator between two observables says. Note that the uncertainty is zero only if $[C, D] = 0$. In this case, it does not matter the order at which C and D are applied to $|\psi\rangle$; the result is the same. When $[C, D] \geq 0$, there is an uncertainty C and D are measured simultaneously. As we mentioned in Sec. A.4, a measurement apparatus can behave as a quantum system and interact with the main system, changing its states. Therefore, the Heisenberg principle in Eq. B.16 is a consequence of possible disturbances caused by measurements in quantum systems.

A nice example is the application of the Pauli operators in a qubit state. The *Matrices operators* are 2×2 matrices given by:

$$\begin{aligned} \sigma_0 \equiv I &\equiv \begin{pmatrix} 1 & 0 \\ 0 & 1 \end{pmatrix} & \sigma_1 \equiv \sigma_x &\equiv \begin{pmatrix} 0 & 1 \\ 1 & 0 \end{pmatrix} \\ \sigma_2 \equiv \sigma_y &\equiv \begin{pmatrix} 0 & -i \\ i & 0 \end{pmatrix} & \sigma_3 \equiv \sigma_z &\equiv \begin{pmatrix} 1 & 0 \\ 0 & -1 \end{pmatrix}. \end{aligned} \quad (\text{B.17})$$

It is easy to check that these matrices have the following commutation relation:

$$[\sigma_i, \sigma_j] = 2i \sum_{k=1}^3 \epsilon_{ijk} \sigma_k, \quad (\text{B.18})$$

where $\epsilon_{123} = \epsilon_{231} = \epsilon_{312} = 1$, $\epsilon_{321} = \epsilon_{213} = \epsilon_{132} = -1$, and $\epsilon_{ijk} = 0$ otherwise. Suppose that $|\psi\rangle = |0\rangle$. The uncertainty is given by

$$\Delta(\sigma_i)\Delta(\sigma_j) \geq \left| i \langle \psi | \sum_{k=1}^3 \epsilon_{ijk} \sigma_k | \psi \rangle \right|. \quad (\text{B.19})$$

The only situation where the uncertainty is non-zero is when $i = 1 = x$ and $j = 1 = y$, at which

$$\Delta(\sigma_x)\Delta(\sigma_y) \geq |i \langle \psi | \sigma_z | \psi \rangle| = \left| i \begin{pmatrix} 0 & 1 \\ 0 & -1 \end{pmatrix} \begin{pmatrix} 1 & 0 \\ 0 & -1 \end{pmatrix} \begin{pmatrix} 0 \\ 1 \end{pmatrix} \right| = 1. \quad (\text{B.20})$$

Otherwise, it is always zero.

B.2 Coherent states

Coherent states are those that, when subject to a suitable harmonic potential, the uncertainty is minimal at any time. The wave function of this state $|\psi\rangle$ is the closest to a classical field and is frequently referred to as “classical” states. The description of coherent states is compatible with the ground state wave function of the displaced simple harmonic oscillator. Then, we shall recall some properties of quantum harmonic oscillators.

We can define coherent states from electromagnetic radiation or states of quantum harmonic oscillators with the same result. Albeit both approaches are complete individually, together, they provide an understanding of coherent states in a complementary way. From the electromagnetic approach, one can deduce how to prepare a coherent state while the quantum harmonic oscillator approaches make their properties more intuitive from the quantum mechanics point of view. Therefore we will introduce both approaches.

In this section, we concentrate on the physics behind the concepts. Thus for more details about the calculations, check the references quoted in the text. To start, let us recall the quantum harmonic oscillator concept.

B.2.1 Quantum Harmonic Oscillators

The motion equation of a classical particle subject to a harmonic potential energy $V(x)$, where $x = x(t)$ is the particle position, is given by

$$m \frac{dx^2}{dt} = - \frac{dV(x)}{dx} = -kx. \quad (\text{B.21})$$

Where k is a positive constant.

With the initial conditions, one can compute the general solution of this differential equation. For $x(0) = 0$ and $\dot{x} = 0$, we get

$$x = A \cos(\omega t - \phi), \quad (\text{B.22})$$

$$\ddot{x} = \frac{p}{m} = -A\omega \sin(\omega t - \phi) \quad (\text{B.23})$$

where $\omega = \sqrt{\frac{k}{m}}$, A is the amplitude, and ϕ the phase. The kinetic energy is $T = \frac{p^2}{2m}$, where $p = m \frac{dx}{dt}$ is the momentum. Thus, the total energy is

$$E = T + V = \frac{p^2}{2m} + \frac{1}{2}m\omega^2 x^2. \quad (\text{B.24})$$

In quantum harmonic oscillators, X and P are operators whose commutation relation is

$$[X, P] = i\hbar, \quad (\text{B.25})$$

$$H = \frac{P^2}{2m} + \frac{1}{2}m\omega^2 X^2. \quad (\text{B.26})$$

As this Hamiltonian is time-independent when applied to a quantum state $|\psi\rangle$ gives

$$H |\psi_i\rangle = E_i |\psi_i\rangle. \quad (\text{B.27})$$

Note that X and P have dimensions. To facilitate, we shall use dimensionless operators defined as

$$\hat{X} \equiv \sqrt{\frac{m\omega}{\hbar}} X \quad (\text{B.28})$$

$$\hat{P} \equiv \sqrt{\frac{1}{m\omega\hbar}} P, \quad (\text{B.29})$$

and with $H = \hbar\omega\hat{H}$, the dimensionless Hamiltonian is

$$\hat{H} = \frac{1}{2} (\hat{X}^2 + \hat{P}^2) \quad (\text{B.30})$$

From this, the commutation relation becomes

$$[\hat{X}, \hat{P}] = i, \quad (\text{B.31})$$

Defining the *creation* a^\dagger and *annihilation* a operators,

$$\begin{aligned} a &\equiv \sqrt{\frac{1}{2}} (\hat{X} + i\hat{P}) \\ a^\dagger &\equiv \sqrt{\frac{1}{2}} (\hat{X} - i\hat{P}), \end{aligned} \quad (\text{B.32})$$

we get

$$[a, a^\dagger] = 1. \quad (\text{B.33})$$

By defining the operator

$$N \equiv a^\dagger a, \quad (\text{B.34})$$

we get

$$\hat{H} = a^\dagger a + \frac{1}{2} = aa^\dagger - \frac{1}{2} = N + \frac{1}{2}. \quad (\text{B.35})$$

When $|\psi\rangle = |n\rangle$ is an eigenvalue of the Hamiltonian we get

$$N |n\rangle = n |n\rangle \quad (\text{B.36})$$

and Eq. (B.27) becomes

$$\hat{H} |n\rangle = \left(N + \frac{1}{2}\right) |n\rangle \quad (\text{B.37})$$

$$= \left(n + \frac{1}{2}\right) |n\rangle. \quad (\text{B.38})$$

The eigenvalues n can be interpreted as the number of excitations of quantum harmonic oscillators and, the basis $\{|n\rangle\}$ is known as the *Fock basis*. The names “creation” (a) and “annihilation” (a^\dagger) operators can be understood intuitively from the following properties

$$a^\dagger |n\rangle = \sqrt{n+1} |n+1\rangle \quad (\text{B.39})$$

$$a |n\rangle = \sqrt{n} |n-1\rangle. \quad (\text{B.40})$$

In this respect, the creation (annihilation) operator can create (destroy) excitations when applied to a system state. It is worth highlighting that the objective of this section is to recall the quantum harmonic oscillator concept; to see these results in detail, please check Ref. [103].

B.2.2 Radiation of a Classical Current

Coherent states are the result of radiation emitted by a classical current, with current density $\mathbf{J}(\mathbf{r}, t)$ is not an operator. Consider the case where $\mathbf{J}(\mathbf{r}, t)$ is coupled to the potential vector operator $\mathbf{A}(\mathbf{r}, t)$ [86], whose interaction Hamiltonian is given by

$$H_I = \int \mathbf{J}(\mathbf{r}, t) \cdot \mathbf{A}(\mathbf{r}, t). \quad (\text{B.41})$$

The state $|\psi(t)\rangle$ of this composed system evolves according to the Schrödinger equation

$$\hbar \frac{d}{dt} |\psi(t)\rangle = -iH_I, \quad (\text{B.42})$$

such that

$$|\psi(t)\rangle = \exp \left[-\frac{i}{\hbar} \int_0^t H_I(t') dt' \right] |0\rangle \quad (\text{B.43})$$

In particular, the exponential above is given by

$$\exp \left[-\frac{i}{\hbar} \int_0^t H_I(t') dt' \right] = \prod_{\mathbf{k}} \exp \left(\alpha_{\mathbf{k}} a_{\mathbf{k}}^\dagger - \alpha_{\mathbf{k}}^* a_{\mathbf{k}} \right), \quad (\text{B.44})$$

where $\alpha_{\mathbf{k}} \in \mathbb{C}$ is a time-dependent amplitude and \mathbf{k} is the possible modes of the electromagnetic wave (for more details, please check Ref. [86]). If the initial state is the vacuum state, $|\psi(0)\rangle = 0$, Eq. B.43 becomes

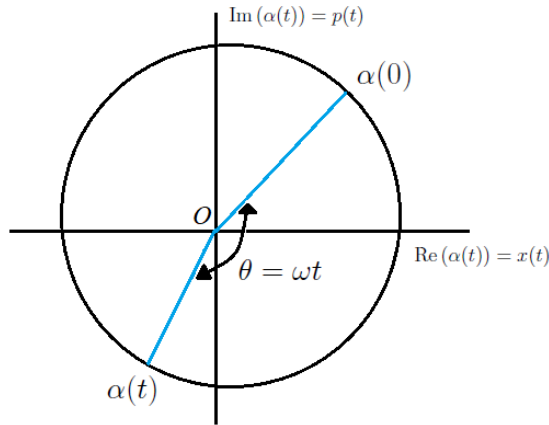
$$|\psi(t)\rangle = \prod_{\mathbf{k}} \exp \left(\alpha_{\mathbf{k}} a_{\mathbf{k}}^\dagger - \alpha_{\mathbf{k}}^* a_{\mathbf{k}} \right) |0\rangle. \quad (\text{B.45})$$

The state $|\psi(t)\rangle$ of Eq. (B.45) is named *coherent state* and can be written as a tensor product of single-mode coherent state $|\alpha_{\mathbf{K}}\rangle$

$$|\psi(t)\rangle \equiv |\{\alpha_{\mathbf{k}}\}\rangle \equiv \bigotimes_{\mathbf{K}} |\alpha_{\mathbf{k}}\rangle, \quad (\text{B.46})$$

that for a single mode becomes

$$|\alpha\rangle = e^{\alpha a^\dagger - \alpha^* a}. \quad (\text{B.47})$$

Figure 27 – Coherent state α in the complex plane.

B.2.3 Coherent States of Quantum Harmonic Oscillator

Coherent states are those more close to a classical state. A quantum harmonic oscillator state satisfies this condition when its position $x(t)$ and momentum $p(t)$ can be measured at a time instant t with minimum uncertainty.

Consider a classic harmonic oscillator state denoted as $\alpha(t)$. We can describe it in terms of $x(t)$ and $p(t)$ as

$$\alpha(t) = \frac{1}{\sqrt{2}} [x(t) + ip(t)], \quad (\text{B.48})$$

where $\hat{X}(t)$ and $\hat{P}(t)$ are given by Eqs. (B.22) and (B.23), respectively. By integrating Eq. B.48 we get

$$\frac{d}{dt}\alpha(t) = -i\omega\alpha(t). \quad (\text{B.49})$$

The solution of this equation is

$$\alpha(t) = \alpha(0)e^{-i\omega t}, \quad (\text{B.50})$$

where

$$\alpha(0) = \frac{1}{\sqrt{2}} [x(0) + ip(0)]. \quad (\text{B.51})$$

For simplicity we define $\alpha(0) \equiv \alpha_0$

The state $\alpha(t)$ is a complex number $a + bi$ with $a, b \in \mathbb{R}$ where $a = x(t)/\sqrt{2}$ and $b = p(t)/\sqrt{2}$. By plotting in the complex plane (see Fig. 27), $\alpha(t)$ describes a circle with radius $O\alpha_0$, centered in the origin O , and angular velocity ω . The real axis is given by $x(t)/\sqrt{2}$ while $p(t)/\sqrt{2}$ gives the complex plane. For this kind of state, the radius is constant, and the angle between α and α_0 is $\theta = \omega t$. Furthermore, with no dissipation, the total energy E (Eq. (B.24)) is also constant.

The state of a quantum harmonic oscillator is considered *classic* or *quasi-classic* when the average values $\langle \hat{X} \rangle$, $\langle \hat{P} \rangle$ and $\langle H \rangle$, given by Eqs. (B.28) to (B.30), are

$$\langle \hat{X} \rangle \approx x(t) \quad \langle \hat{P} \rangle \approx p(t), \quad \text{and} \quad \langle H \rangle \approx E. \quad (\text{B.52})$$

For the arbitrary state $|\psi(t)\rangle$, the the evolution of the operation $\langle a \rangle(t) = \langle \psi(t)|a|\psi(t)\rangle$ is given by

$$i\hbar \frac{d}{dt} \langle a \rangle(t) = \langle [a, H] \rangle \quad (\text{B.53})$$

where $[a, H] = \hbar\omega a$ (see Ref. [103]). From this, the solutions for $\langle a \rangle(t)$ and $\langle a^\dagger \rangle(t)$ are

$$\langle a \rangle(t) = \langle a \rangle(0) e^{i\omega t} \quad (\text{B.54})$$

$$\langle a^\dagger \rangle(t) = \langle a^\dagger \rangle(0) e^{i\omega t}. \quad (\text{B.55})$$

Observe that Eqs. (B.54) and (B.55) are quite similar to the solution of classical $\alpha(t)$ in Eq. (B.50). This analogy leads to the relations

$$\langle \hat{X} \rangle = \frac{1}{\sqrt{2}} \left[\langle a \rangle(0) e^{-i\omega t} + \langle a^\dagger \rangle(0) e^{i\omega t} \right] \quad (\text{B.56})$$

$$\langle \hat{P} \rangle = -\frac{i}{\sqrt{2}} \left[\langle a \rangle(0) e^{-i\omega t} - \langle a^\dagger \rangle(0) e^{i\omega t} \right]. \quad (\text{B.57})$$

As defined in Eq. B.53, quasi-classic states must satisfy some conditions. By comparing Eqs. (B.54) and (B.55) the relations $\langle \hat{X} \rangle \approx x(t)$ $\langle \hat{P} \rangle \approx p(t)$ are valid when

$$\langle a \rangle(0) = \alpha_0, \quad (\text{B.58})$$

and the condition

$$\langle \psi | \alpha | \psi \rangle = \alpha_0, \quad (\text{B.59})$$

must be satisfied for a normalized state vector $|\psi\rangle$. The condition

$$\langle H \rangle = \frac{\hbar\omega}{2} \left(\langle a^\dagger a \rangle(0) + 1 \right) \approx E(t) \quad (\text{B.60})$$

is satisfied when

$$\langle a^\dagger a \rangle(0) = \langle \psi | a^\dagger a | \psi \rangle = |\alpha_0|^2. \quad (\text{B.61})$$

The probability of finding of finding n modes of a quantum harmonic oscillator is given by the Poisson distribution. Consider the Fock state $|n\rangle$, thus $P(n)$ is

$$p(n) = \langle n | \alpha \rangle \langle \alpha | n \rangle = \frac{|\alpha|^{2n} e^{-\langle n \rangle}}{n!} = \frac{\langle n \rangle^n e^{-\langle n \rangle}}{n!}, \quad (\text{B.62})$$

as $\langle n \rangle = |\alpha|^2$.

B.2.4 Properties of Coherent states

Coherent states are eigenvalues of the annihilation operator a : Consider an operator $b(\alpha_0)$ defined as

$$b(\alpha_0) \equiv a - \alpha_0. \quad (\text{B.63})$$

Then, we get

$$b^\dagger(\alpha_0)b(\alpha_0) = a^\dagger a + \alpha_0^* \alpha_0 - \alpha_0 a^\dagger + \alpha_0^* a. \quad (\text{B.64})$$

By expanding the quantity $\langle \psi(0) | b^\dagger(\alpha_0)b(\alpha_0) | \psi(0) \rangle$ in terms of the operators a^\dagger and a , and applying Eqs. (B.59) and (B.61) it becomes

$$\langle \psi(0) | b^\dagger(\alpha_0)b(\alpha_0) | \psi(0) \rangle = \alpha_0^* \alpha_0 + \alpha_0^* \alpha_0 - \alpha_0 \alpha_0^* - \alpha_0^* \alpha_0 = 0. \quad (\text{B.65})$$

This means that $b(\alpha_0) | \psi(0) \rangle = 0$ and then

$$a | \psi(0) \rangle = [b(\alpha_0) + \alpha] | \psi(0) \rangle = \alpha_0 | \psi(0) \rangle. \quad (\text{B.66})$$

The results of Eq. (B.66) show that coherent states are eigenvectors of the annihilation operator a with eigenvalue α_0 . For convenience, we shall use the conventional notation of coherent states where $| \psi(0) \rangle \equiv | \alpha \rangle$ and $\alpha_0 \equiv \alpha$, where

$$a | \alpha \rangle = \alpha | \alpha \rangle. \quad (\text{B.67})$$

Coherent states in the Fock basis: We can also write coherent states in the Fock basis $\{ | n \rangle \}$ (see Ref. [103]). By expanding $| \alpha \rangle$ using the fock states $| n \rangle$ we obtain

$$| \alpha \rangle = e^{-\frac{|\alpha|^2}{2}} \sum_n \frac{\alpha^n}{\sqrt{n!}} | n \rangle. \quad (\text{B.68})$$

Coherent states are dislocated fundamental states of quantum harmonic oscillators: From Eq. (B.40), one can show that $| n \rangle = [(a^\dagger)^n / \sqrt{n!}] | 0 \rangle$. Then, Eq. (B.68) becomes

$$| \alpha \rangle = e^{-\frac{|\alpha|^2}{2}} e^{\alpha a^\dagger} | 0 \rangle. \quad (\text{B.69})$$

As $\exp(\alpha^* a) | 0 \rangle = 0$ we can rewrite the last equation as

$$| \alpha \rangle = D(\alpha) | 0 \rangle, \quad (\text{B.70})$$

where

$$D(\alpha) = e^{-\frac{|\alpha|^2}{2}} e^{\alpha a^\dagger} e^{-\alpha^* a}. \quad (\text{B.71})$$

If two operators obey the relation

$$[[A, B], A] = [[A, B], B] = 0, \quad (\text{B.72})$$

the relation

$$e^{A+B} = e^{[A,B]/2} e^A e^B \quad (\text{B.73})$$

is valid. Thus, from defining $A = \alpha a^\dagger$ and $B = -\alpha^* a$, we get

$$D(\alpha) = e^{\alpha a^\dagger - \alpha^* a}. \quad (\text{B.74})$$

Note that this approach gives a result completely compatible with Eq. (B.47).

The Operator $D(\alpha)$ is unitary behaves as a displacement operator when acting on a and a^\dagger ,

$$D^{-1}(\alpha) a D(\alpha) = a + \alpha \quad (\text{B.75})$$

$$D^{-1}(\alpha) a^\dagger D(\alpha) = a^\dagger + \alpha^*. \quad (\text{B.76})$$

Therefore $D(\alpha)$ is frequently referred to as the *displacement operator*.

A coherent state is a result of a displacement operator applied in a vacuum state of the harmonic oscillator; that is, it is a displaced vacuum state.

The uncertainty in position and momentum of coherent states is minimum at any time: As shown in Eq. (B.31), the position and momentum operator of quantum harmonic oscillators do not commute, meaning that the order that they are applied matters. That is, for an arbitrary state vector $|\psi\rangle$,

$$PX |\psi\rangle \neq |\psi\rangle. \quad (\text{B.77})$$

This generates uncertainty. The uncertainty of a quantum harmonic oscillator in an arbitrary state is given by

$$\Delta(X)\Delta(P) \geq \frac{1}{2}. \quad (\text{B.78})$$

We expect that the quantum harmonic oscillator state closest to a classical state has the smallest possible uncertainty.

Therefore, let us calculate the uncertainty of a coherent state. By using Eqs. (B.67) and (B.32), the average value $\Delta(X)$ and $\Delta(P)$ are given by

$$\langle \hat{X} \rangle = \langle \alpha | \hat{X} | \alpha \rangle = \sqrt{2} \operatorname{Re}(\alpha) \quad (\text{B.79})$$

$$\langle \hat{P} \rangle = \langle \alpha | \hat{P} | \alpha \rangle = \sqrt{2} \operatorname{Im}(\alpha). \quad (\text{B.80})$$

Similarly,

$$\langle \hat{X}^2 \rangle = \langle \alpha | \hat{X}^2 | \alpha \rangle = \frac{1}{2} [4 \operatorname{Re}(\alpha)^2 + 1] \quad (\text{B.81})$$

$$\langle \hat{P}^2 \rangle = \langle \alpha | \hat{P}^2 | \alpha \rangle = \frac{1}{2} [1 - 4 \operatorname{Im}(\alpha)^2]. \quad (\text{B.82})$$

From Eq. B.5 the standard deviations are

$$\Delta\hat{X} = \frac{1}{\sqrt{2}} \quad (\text{B.83})$$

$$\Delta\hat{P} = \frac{1}{\sqrt{2}}, \quad (\text{B.84})$$

and therefore the uncertainty of coherent states are

$$\Delta X \Delta P = \frac{1}{\hbar} \Delta\hat{X} \Delta\hat{P} = \frac{1}{2}. \quad (\text{B.85})$$

The equality signal comes from the fact that the uncertainty of coherent states does not depend on α , taking the same value at any time t . This means that the uncertainty of coherent states is minimum making them quasi-classical states.

The scalar product between two coherent states, $|\alpha\rangle$ and $|\alpha'\rangle$: Unlike Fock states, two different coherent states are not orthogonal. To verify we can calculate their intern product with Eq. B.47,

$$\langle\alpha|\alpha'\rangle = e^{\frac{1}{2}(-|\alpha|^2 + \alpha'\alpha^* + \alpha'^*\alpha - |\alpha'^2|)}. \quad (\text{B.86})$$

However, $|\alpha\rangle$ and $|\alpha'\rangle$ are approximately orthogonal if $\alpha - \alpha' \gg 1$ and the their overlap is

$$|\langle\alpha|\alpha'\rangle|^2 = e^{-|\alpha - \alpha'|^2}. \quad (\text{B.87})$$

From these facts, any coherent states can be written in terms of another by using the following expansion:

$$|\alpha\rangle = \frac{1}{\pi} \int d^2\alpha' |\alpha'\rangle \langle\alpha'|\alpha\rangle = \frac{1}{\pi} \int d^2\alpha' |\alpha'\rangle e^{\frac{1}{2}(-|\alpha|^2 + \alpha'\alpha^* + \alpha'^*\alpha - |\alpha'^2|)}. \quad (\text{B.88})$$

and are said to form an *overcomplete* set.

The fact that coherent states can be prepared experimentally from classical currents, as shown in Sec. B.2.2, is a great advantage, and their properties them suitable for various studies of quantum systems. This concept is largely used in different fields of quantum theory, and several excellent results were found [40, 88, 114–117]. In Chap. 5, we present a work where coherent states were used to investigate quantum Darwinism and non-Markovianity.

B.3 Angular Momentum

Momentum is an important concept in physics that gives a quantity related to the mass and velocity of some particle or set of particles. In classical physics, *linear momentum* \vec{P} is a vector quantity related to the linear motion of a particle and is given by the product between its mass m and velocity \vec{v} , that is, $\vec{p} = m\vec{v}$. *Angular momentum* $\vec{\mathcal{L}}$ is related to

the rotational motion of a particle and is given by the cross product $\vec{\mathcal{L}} = \vec{r} \times \vec{p}$, where \vec{r} is the position vector. Both linear and angular momentum carry interesting properties when combined with conservation law and other basic concepts, allowing the dynamical description of physical systems. For example, the angular momentum of an isolated system is a *constant of motion*.

Analog to the classical case, linear and angular momentum can be defined for quantum systems with similar properties. The linear and angular momentum of a quantum system is associated with an operator of an observable. Linear momentum operators are usually denoted by \mathbf{p} and are related to the velocity of a quantum system. Angular momentum is composed of two parts: Orbital and spin angular momentum. *Orbital angular momentum* \mathbf{L} always has a classical counterpart, while *spin angular momentum* \mathbf{S} is intrinsic of elementary particles. These two angular momenta together form the *total angular momentum* \mathbf{J} of quantum a system such that

$$\mathbf{J} = \mathbf{S} + \mathbf{L}. \quad (\text{B.89})$$

Such operators have important properties that are largely used in investigations of quantum mechanics. We describe the most basic of these properties in the following subsections. For more details and deductions, please check Refs. [103,118].

B.3.1 Orbital Angular Momentum

Analog to the classical angular momentum, \mathbf{L} can be written in terms of the angular momentum with operator \mathbf{P} and the particle position with position operator \mathbf{X} , that is,

$$\mathbf{L} = \mathbf{X} \times \mathbf{P}. \quad (\text{B.90})$$

The observable \mathbf{L} can be decomposed in three observables L_x , L_y , and L_z , where x , y , and z are the directions of a three-dimensional Cartesian space. These components are associated with the quantized angular momentum $\vec{\mathcal{L}}$ in the x , y , and z directions of a spinless particle. By using the commutation relations between \mathbf{X} and \mathbf{P} (Eq. B.25), the commutation operation between L_x , L_y , and L_z are given by

$$[L_i, L_j] = i\hbar \sum_{k=1}^3 \epsilon_{ijk} L_k, \quad (\text{B.91})$$

where $x \equiv 1$, $y \equiv 2$, and $z \equiv 3$, $\epsilon_{123} = \epsilon_{231} = \epsilon_{312} = 1$, $\epsilon_{321} = \epsilon_{213} = \epsilon_{132} = -1$, and $\epsilon_{ijk} = 0$ otherwise. Another relevant operator is

$$\mathbf{L}^2 \equiv L_x^2 + L_y^2 + L_z^2. \quad (\text{B.92})$$

For a system composed of N particles with no spin, $\mathbf{S} = 0$, the total angular momentum is given by

$$\mathbf{L} = \sum_{i=1}^N \mathbf{L}_i, \quad (\text{B.93})$$

with \mathbf{L}_i given by Eq. (B.90).

By applying L_z and \mathbf{L}^2 to their eigenvectors $|l, m\rangle$ we get

$$L_z |l, m\rangle = \hbar m |l, m\rangle \quad (\text{B.94})$$

$$\mathbf{L}^2 |l, m\rangle = \hbar^2 l(l+1) |l, m\rangle, \quad (\text{B.95})$$

where $l = 0, 1/2, 1, 3/2, \dots$ and $m = -l, -l+1, \dots, l-1, l, \dots$. The discrete quantities l and m come from the schrödinger equation solutions for a quantum state in spherical coordinates, $|\psi\rangle = |l, m\rangle$ (see Ref. [118]). Therefore, these operators represent the quantized orbital linear momentum L of a particle or a set of particles.

B.3.2 Spin Angular Momentum

As mentioned before, spin is an intrinsic property of elementary particles, and this is confirmed by Lorentz or Galilean group analysis [119]. A notable example of spin is the electron spin. The experimental observation of electron spin was essential for understanding this concept.

The algebraic theory of spins follows the same steps as the orbital angular momentum. The spin \mathbf{S} can also be decomposed in the x , y , and z directions satisfying the commutation relation

$$[S_i, S_j] = i\hbar \sum_{k=1}^3 \epsilon_{ijk} S_k, \quad (\text{B.96})$$

and with

$$\mathbf{S}^2 \equiv S_x^2 + S_y^2 + S_z^2. \quad (\text{B.97})$$

Furthermore, the eigenvectors of \mathbf{S}^2 and S_z must to satisfy

$$S_z |s, m\rangle = \hbar m |s, m\rangle \quad (\text{B.98})$$

$$\mathbf{S}^2 |s, m\rangle = \hbar^2 s(s+1) |s, m\rangle. \quad (\text{B.99})$$

One can also associate \mathbf{S}^2 and S_z to the operators

$$S_{\pm} \equiv S_x \pm iS_y \quad (\text{B.100})$$

and obtain

$$S_{\pm} |s, m\rangle = \hbar \sqrt{s(s+1) - m(m \pm 1)} |s, (m \pm 1)\rangle, \quad (\text{B.101})$$

where $s = 0, 1/2, 1, 3/2, \dots$ and $m = -s, -s+1, \dots, s-1, s, \dots$

B.3.3 Spin 1/2

The case $s = 1/2$ is quite important since it can be the first step to understanding higher spins' formalism. Electrons are good examples of spin 1/2 particles since they

were used in the first experimental studies of spins like the Zeeman effect [120] and the Stern-Gerlach experiment [121].

Spin 1/2 operators have only two possible eigenstates

$$|\uparrow\rangle \equiv |s = \frac{1}{2}, m = \frac{1}{2}\rangle \quad (\text{B.102})$$

$$\text{and} \quad (\text{B.103})$$

$$|\downarrow\rangle \equiv |s = \frac{1}{2}, m = -\frac{1}{2}\rangle, \quad (\text{B.104})$$

where $|\uparrow\rangle$ and $|\downarrow\rangle$ are known as *spin up* and *spin down*.

From Eqs. (B.98) to (B.100) one can deduce

$$\mathbf{S}^2 = \frac{3}{4}\hbar^2\sigma_0, \quad (\text{B.105})$$

$$S_z = \frac{1}{2}\hbar\sigma_z, \quad (\text{B.106})$$

$$S_x = \frac{1}{2}\hbar\sigma_x, \quad (\text{B.107})$$

$$S_y = \frac{1}{2}\hbar\sigma_y, \quad (\text{B.108})$$

where σ_0 , σ_x , σ_y , and σ_z are the Pauli's matrices given in Eq. (B.17).

An interesting fact is that the operators S_+ and S_- can flip the states on the basis $\{|\uparrow\rangle, |\downarrow\rangle\}$. Define

$$|\uparrow\rangle \equiv \begin{pmatrix} 1 \\ 0 \end{pmatrix} \quad (\text{B.109})$$

$$|\downarrow\rangle \equiv \begin{pmatrix} 0 \\ 1 \end{pmatrix} \quad (\text{B.110})$$

$$\cdot \quad (\text{B.111})$$

Thus, by applying S_+ to $|\downarrow\rangle$ and S_- to $|\uparrow\rangle$ we get

$$S_+ |\downarrow\rangle = \begin{pmatrix} 0 & 1 \\ 0 & 0 \end{pmatrix} \begin{pmatrix} 0 \\ 1 \end{pmatrix} = \hbar \begin{pmatrix} 1 \\ 0 \end{pmatrix} = \hbar |\uparrow\rangle, \quad (\text{B.112})$$

$$S_- |\uparrow\rangle = \begin{pmatrix} 0 & 0 \\ 1 & 0 \end{pmatrix} \begin{pmatrix} 1 \\ 0 \end{pmatrix} = \hbar \begin{pmatrix} 0 \\ 1 \end{pmatrix} = \hbar |\downarrow\rangle. \quad (\text{B.113})$$

B.3.4 Addition of Spin Angular Momentum

Elementary particles, such as electrons, protons, neutrons, etc., have spin 1/2. The total spin of a system composed of two spin 1/2 particle is the sum of individual spins,

$$\mathbf{S} \equiv \mathbf{S}_1 + \mathbf{S}_2, \quad (\text{B.114})$$

with

$$\mathbf{S}_1 = \mathbf{S}^{[1]} \otimes I_2 \quad (\text{B.115})$$

$$\mathbf{S}_2 = I_1 \otimes \mathbf{S}^{[2]}. \quad (\text{B.116})$$

That is, $\mathbf{S}_{1(2)}$ acts only on system 1(2).

By applying the component S_z in a state $|s_1, m_1\rangle |s_2, m_2\rangle$, we get

$$S_z |s_1, m_1\rangle |s_2, m_2\rangle = (s_z^{[1]} \otimes I_2 + I_1 \otimes S_z^{[2]}) |s_1, m_1\rangle |s_2, m_2\rangle \quad (\text{B.117})$$

$$= (m_1 + m_2) |s_1, m_1\rangle |s_2, m_2\rangle. \quad (\text{B.118})$$

For each possible state of two spin 1/2 particles, we have

$$|\uparrow\uparrow\rangle : m = 1, |\uparrow\downarrow\rangle : m = 0, |\downarrow\uparrow\rangle : m = 0, \text{ and } |\downarrow\downarrow\rangle : m = -1. \quad (\text{B.119})$$

Since m ranges between $-s$ and s , s has just two possible values $s = \{0, 1\}$. The possible states with $s = 1$ are

$$|11\rangle = |\uparrow\uparrow\rangle \quad (\text{B.120})$$

$$|10\rangle = \frac{1}{\sqrt{2}} (|\uparrow\downarrow\rangle + |\downarrow\uparrow\rangle) \quad (\text{B.121})$$

$$|1-1\rangle = |\downarrow\downarrow\rangle. \quad (\text{B.122})$$

This set of three states is known as *triplet*. For $s = 0$, there is only one possible state

$$|01\rangle = \frac{1}{\sqrt{2}} (|\uparrow\downarrow\rangle - |\downarrow\uparrow\rangle), \quad (\text{B.123})$$

that is known as *singlet*.

Due to their simplicity and experimental applicability, spin systems are quite useful in investigating many quantum properties such as entanglement, decoherence, etc. They are also frequently used in quantum computation and quantum information. In Chap. 3, we present a nice work where spin systems were used to study quantum Darwinism.

B.4 Identical Particles

Identical particles are whose intrinsic properties are precisely the same. That is, such particles have all the same mass, charge, spin, etc. Consequently, it is impossible to distinguish these particles experimentally. We can safely affirm that electrons, protons, and hydrogen atoms are examples of identical particles. However, an electron and a positron are not identical to each other since they have different charges.

In classical mechanics, identical particles can be distinguished by their trajectory since the position and momentum of a particle are well-defined. In quantum mechanics,

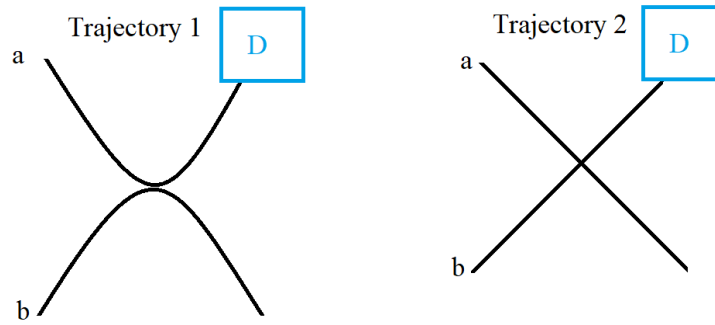


Figure 28 – Two particles a and b that can follow two different trajectories after colliding. The detector D can not distinguish which particle was detected if they are identical.

there is an uncertainty associated with the particle trajectory preventing the distinction of identical particles. Thus, if the wave packet of the particles overlaps, we can never distinguish them accurately. For example, consider that two particles a and b moving in different directions collide, see Fig. 28. After the collision, they can perform two different trajectories, 1 or 2. If they are identical, the detector D can only detect a particle; it can not differentiate which one was detected.

B.4.1 Different State Vectors Associated to a Same Physical State

Some difficulties arise when dealing with identical particles. When they form a composed system, some mathematical descriptions can not distinguish the particles. Different state vectors can describe the same physical system. This difficulty is evident in a system composed of two spin $1/2$ particles. Consider two spin observables \mathbf{S}_1 and \mathbf{S}_2 and the orthonormal basis $\{|e_1, e_2\rangle\}$ where e_1 and e_2 can be \uparrow or \downarrow each one. Consider the state $|\psi\rangle = |e_1, e_2\rangle$ where the composite system is a particle with spin up and another with spin down. The mathematical representation of this state could be

$$|\psi\rangle = |e_1 = \uparrow, e_2 = \downarrow\rangle, \text{ or} \quad (\text{B.124})$$

$$|\psi\rangle = |e_1 = \downarrow, e_2 = \uparrow\rangle. \quad (\text{B.125})$$

Furthermore, by the superposition principle $|\psi\rangle$ also could be

$$|\psi\rangle = \alpha |\uparrow, \downarrow\rangle + \beta |\downarrow, \uparrow\rangle, \quad (\text{B.126})$$

where $|\alpha|^2 + |\beta|^2 = 1$ for any $\alpha, \beta \in \mathbb{C}$. This phenomenon know as *exchange degeneracy*.

Exchange degeneracy is not exclusive to two-level systems. It is general and can create troubles in the applications of the postulates of quantum mechanics (see Chap. A) since the physical predictions can not depend on the Kets chosen [103].

B.4.2 Symmetric and Antisymmetric Wave Functions

The symmetry of a wave function represented by the ket $|\psi\rangle$ in an isomorphic space state has significant consequences in quantum systems. Consider two particles not identical but with the same spin s . As the space is isomorphic, they can be described in the same basis $\{|u_i\rangle\}$. If, for example, particle 1 is a proton and particle 2 an electron-composed system can be described on the basis $\{|u_i^{[1]}, u_j^{[2]}\rangle\}$. The order does not matter in a product state, thus

$$|u_i^{[1]}, u_j^{[2]}\rangle = |u_j^{[2]}, u_i^{[1]}\rangle \quad (\text{B.127})$$

However, for $i \neq j$

$$|u_i^{[1]}, u_j^{[2]}\rangle \neq |u_j^{[1]}, u_i^{[2]}\rangle. \quad (\text{B.128})$$

Since the space of the particle's state are isomorphic, there is a linear operator $P_{2,1}$, such that

$$P_{21} |u_i^{[1]}, u_j^{[2]}\rangle = |u_j^{[1]}, u_i^{[2]}\rangle, \quad (\text{B.129})$$

where P_{21} is Hermitian, since $P_{21} = P_{21}^\dagger$ and $P_{21}^2 = 1$. P_{21} is known as *permutation operator* [103].

As the eigenvalues of P_{12} must be real and their squares are 1, the only possible values are +1 and -1. The wave function is said to be *symmetric* if

$$P_{12} |\psi_S\rangle = |\psi_S\rangle \quad (\text{B.130})$$

and *antisymmetric* if

$$P_{12} |\psi_A\rangle = -|\psi_A\rangle. \quad (\text{B.131})$$

Now, let us define two projectors

$$S = \frac{1}{2}(1 + P_{12}) \quad \text{and} \quad (\text{B.132})$$

$$A = \frac{1}{2}(1 - P_{12}). \quad (\text{B.133})$$

Thus, the following relations are valid

$$S^2 = S; \quad A^2 = A \quad (\text{B.134})$$

$$, S^\dagger = S; \quad A^\dagger = A \quad (\text{B.135})$$

$$, SA = AS = 0, \quad \text{and } S + A = 1. \quad (\text{B.136})$$

When S is applied to an arbitrary state $|\psi\rangle$, the state vector $S|\psi\rangle$ is symmetric while when A is applied, $A|\psi\rangle$ is antisymmetric, that is

$$P_{12}S|\psi\rangle = S|\psi\rangle \quad (\text{B.137})$$

$$P_{12}A|\psi\rangle = -A|\psi\rangle. \quad (\text{B.138})$$

Thus, the projectors A and S are called *symmetrizer* and *antisymmetrizer*.

It is important to mention that the permutation operators, A and S , can also be defined for systems with an arbitrary number of particles, See Ref. [118].

B.4.3 Symmetry of Bosons and Fermions

Bosons are particles with integer spins that follow the *Bose-Einstein* statistics, while *Fermions* are particles with half-integer spins that follow the *Fermi-Dirac* statistics (see Ref. [122]).

Important properties arise when permutation, symmetrization, and antisymmetrization concepts are applied to identical particle states. As shown before, exchange degeneracy can be a problem in dealing with identical particles. One way to overcome this is by symmetrizing the global state if the particles are bosons, that is

$$|\psi\rangle_B = S \left(|u_i^{[1]}, u_j^{[2]}\rangle + |u_j^{[1]}, u_i^{[2]}\rangle \right), \quad (\text{B.139})$$

and antisymmetrizing if they are fermions

$$|\psi\rangle_F = A \left(|u_i^{[1]}, u_j^{[2]}\rangle - |u_j^{[1]}, u_i^{[2]}\rangle \right). \quad (\text{B.140})$$

Therefore, we can say that fermions have *symmetric wave functions* and bosons *antisymmetric wave functions*.

From this, we can deduce the fact that fermions cannot occupy the same state, that is, $j = i$, since

$$|\psi\rangle_F = A \left(|u_i^{[1]}, u_i^{[2]}\rangle - |u_i^{[1]}, u_i^{[2]}\rangle \right) = 0. \quad (\text{B.141})$$

This is known as *the Pauli exclusion principle* and has relevant physical consequences [118].

The symmetrization processes are frequently used in studies of composed quantum systems with identical particles since they make viable physical prediction calculations of identical particles.

APPENDIX C – Dynamics of a Many-Body Quantum Harmonic Oscillators in coherent states

This appendix shows how we computed the state evolution of the many-body system presented in Sec. 5.2. The model consists of a quantum harmonic oscillator, referred to as the system, coupled to N other quantum harmonic oscillators, the environment. All environment oscillators are coupled to the system but do not interact directly between themselves. The Hamiltonian is given by

$$H = \hbar\omega_0 a^\dagger a + \hbar \sum_{k=1}^N \omega_k b_k^\dagger b_k + \hbar \sum_{k=1}^N \gamma_k (a^\dagger b_k + a b_k^\dagger), \quad (\text{C.1})$$

where ω_0 and ω_k are the system oscillator frequency and k -th environment oscillator frequency, respectively; a^\dagger and a are the creation and annihilation operators for the system and b^\dagger and b are the same operators that act only in the k -th environment oscillator; and γ_k is the constant coupling between the system and the k -th environment oscillator.

In this model, the system and all subenvironments are in a coherent state (Sec. B.2). The environment is initially in the vacuum state $|0\rangle = |0\rangle_1 \dots |0\rangle_N$ and the system in a coherent state $|\alpha_0\rangle$. Considering the system and the environment initially decoupled, the global state at $t = 0$ is

$$|\psi(0)\rangle = |\alpha_0\rangle \otimes \prod_{k=1}^N |0_k\rangle, \quad (\text{C.2})$$

and at some time t we get

$$|\psi(t)\rangle = |\alpha(t)\rangle \otimes \prod_{k=1}^N |\lambda_k(t)\rangle. \quad (\text{C.3})$$

The system plus the environment forms a closed system, and as mentioned in Sec. A.2, the dynamics of such a state are given by the Schrödinger equation,

$$H |\psi(t)\rangle = i\hbar \frac{d}{dt} |\psi(t)\rangle. \quad (\text{C.4})$$

Thus, by substituting Eq.(C.3) in the right side of Eq. (C.4) we get

$$\frac{d}{dt} |\psi(t)\rangle = \frac{d}{dt} \left(|\alpha(t)\rangle \otimes \prod_{k=1}^N |\lambda_k(t)\rangle \right) \quad (\text{C.5})$$

$$= \frac{d|\alpha(t)\rangle}{dt} \otimes \prod_{k=1}^N |\lambda_k(t)\rangle + |\alpha(t)\rangle \sum_i \frac{d}{dt} \left(\prod_{k=1}^N |\lambda_k(t)\rangle \right). \quad (\text{C.6})$$

From the definition and properties of coherent states, the time derivative of an arbitrary coherent state $|\beta(t)\rangle$ is

$$\frac{d}{dt} |\beta(t)\rangle = \frac{d}{dt} \left(e^{-\frac{|\beta|^2}{2}} \sum_n \frac{\beta^n}{\sqrt{n!}} |n\rangle \right) \quad (\text{C.7})$$

$$= -\frac{1}{2} \left(\frac{d}{dt} |\beta(t)|^2 \right) |\beta(t)\rangle + \dot{\beta}(t) a^\dagger |\beta(t)\rangle. \quad (\text{C.8})$$

Thus, Eq (C.6) becomes

$$\frac{d}{dt} |\psi(t)\rangle = -\frac{1}{2} \left(\frac{d}{dt} |\alpha(t)|^2 + \sum_k |\lambda_k(t)|^2 \right) |\psi(t)\rangle + \left(\dot{\alpha}(t) a^\dagger + \sum_k \dot{\lambda}_k(t) a^\dagger \right) |\psi(t)\rangle. \quad (\text{C.9})$$

As there are neither external nor dissipative forces, the excitations number is conserved; that is

$$-\frac{1}{2} \left(\frac{d}{dt} |\alpha(t)|^2 + \sum_k |\lambda_k(t)|^2 \right) = 0, \quad (\text{C.10})$$

and we get

$$i\hbar \frac{d}{dt} |\psi(t)\rangle = i\hbar \left(\dot{\beta}(t) a^\dagger |\alpha(t)\rangle + \dot{\beta}(t) a^\dagger |\lambda_k(t)\rangle \right) |\psi(t)\rangle. \quad (\text{C.11})$$

Applying the Hamiltonian to $|\psi(t)\rangle$ as in the left side of Eq. (C.4) we get

$$H |\psi(t)\rangle = \hbar\omega_0 \alpha(t) a^\dagger |\psi(t)\rangle + \sum_k \hbar\omega_k \lambda_k(t) b_k^\dagger |\psi(t)\rangle + \sum_k \gamma_k \left(\lambda_k(t) a^\dagger + \alpha(t) \lambda_k^\dagger \right) |\psi(t)\rangle. \quad (\text{C.12})$$

As from Eq. (C.4), these two last expressions are equal, we get

$$\left(i\dot{\alpha}(t) - \omega_0 \alpha(t) - \sum_k \gamma_k \lambda_k(t) \right) a^\dagger |\psi(t)\rangle + \sum_k \left(i\dot{\lambda}_k(t) - \omega_k \lambda_k(t) - \gamma_k \alpha(t) \right) b_k^\dagger |\psi(t)\rangle = 0. \quad (\text{C.13})$$

As $a^\dagger |\psi(t)\rangle$ and $b_k^\dagger |\psi(t)\rangle$ are linearly independent, the motion equations of $|\alpha(t)\rangle$ and $|\lambda_k(t)\rangle$ are

$$i \frac{d\alpha(t)}{dt} = \omega_0 \alpha(t) + \sum_k \gamma_k \lambda_k(t) \quad (\text{C.14})$$

$$i \frac{d\lambda_k(t)}{dt} = \omega_k \lambda_k(t) + \gamma_k \alpha(t). \quad (\text{C.15})$$

In the interaction picture, these equations become

$$i \frac{d\tilde{\alpha}(t)}{dt} = \sum_k \gamma_k \tilde{\lambda}_k(t) e^{i(\omega_0 - \omega_k)t} \quad (\text{C.16})$$

$$i \frac{d\tilde{\lambda}_k(t)}{dt} = \gamma_k \tilde{\alpha}(t) e^{-i(\omega_0 - \omega_k)t}, \quad (\text{C.17})$$

where $\tilde{\alpha}(t) = \alpha(t) e^{i\omega_0 t}$ and $\tilde{\lambda}_k(t) = \lambda_k(t) e^{i\omega_k t}$. The only difference between these pictures is a global phase that does not affect the system's dynamics.

The way that the system loses excitations for the environment is defined by the coupling. Here we consider constant coupling and a specific kind of non-constant coupling.

C.1 Constant Coupling

For constant coupling, $\gamma_k = \gamma$ for all k . Thus, the motion equations are given by

$$i \frac{d\tilde{\alpha}(t)}{dt} = \sum_k \gamma \tilde{\lambda}_k(t) e^{i\Delta\omega_k t} \quad (\text{C.18})$$

$$i \frac{d\tilde{\lambda}_k(t)}{dt} = \gamma \tilde{\alpha}(t) e^{-i\Delta\omega_k t}, \quad (\text{C.19})$$

where $\Delta\omega_k = \omega_0 - \omega_k$. By integrating Eq. (C.19) and substituting in Eq. (C.18) we get

$$\dot{\tilde{\alpha}}(t) = - \sum_k \gamma^2 \int_0^\infty e^{i\Delta\omega_k(t-t')} \tilde{\alpha}. \quad (\text{C.20})$$

By considering N large enough we can take the continuum limiting to solve Eq. (C.20). In particular, we get

$$\sum_k \longrightarrow \int \rho(\omega) d\omega \quad (\text{C.21})$$

$$\gamma_k \longrightarrow \gamma(\omega), \quad (\text{C.22})$$

where $\rho(\omega)$ is the modes density that gives the number of modes between ω and $\omega + d\omega$ and $\gamma(\omega)$ is a continuum function dependent on ω . Therefore, Eq. (C.20) becomes

$$\dot{\tilde{\alpha}}(t) = - \int_0^t dt' \tilde{\alpha}(t') \int_{\omega_0 - \delta\omega}^{\omega_0 + \delta\omega} d\omega \gamma^2(\omega) \rho(\omega) e^{i\Delta\omega_k(t-t')}. \quad (\text{C.23})$$

This equation is general and is valid for any kind of coupling; the only approximation is the continuum limiting. However, we want to analyze an environment with constant coupling and a constant modes distribution, that is,

$$\gamma^2(\omega) \rho(\omega) = c, \quad (\text{C.24})$$

where c is a constant value. We are interested in the dynamics where the difference $|\omega_0 - \omega_k|$ is not too large; this makes the interaction between the system and the environment relevant. Thus, the integral in the frequency can be taken from $-\infty$ to ∞ without loss of generality and we get

$$\dot{\tilde{\alpha}}(t) = -c \int_0^t dt' \tilde{\alpha}(t') \int_{-\infty}^{\infty} d\omega e^{i\Delta\omega_k(t-t')} \quad (\text{C.25})$$

$$= -2\pi c \int_0^t dt' \delta(t-t') \tilde{\alpha}(t') \quad (\text{C.26})$$

$$= -2\pi c \tilde{\alpha}(t). \quad (\text{C.27})$$

The solution of this differential equation is

$$\tilde{\alpha}(t) = \alpha_0 e^{-\Gamma t}, \quad (\text{C.28})$$

where α_0 is the amplitude of the initial coherent state of the system and $\Gamma = 2\pi c$.

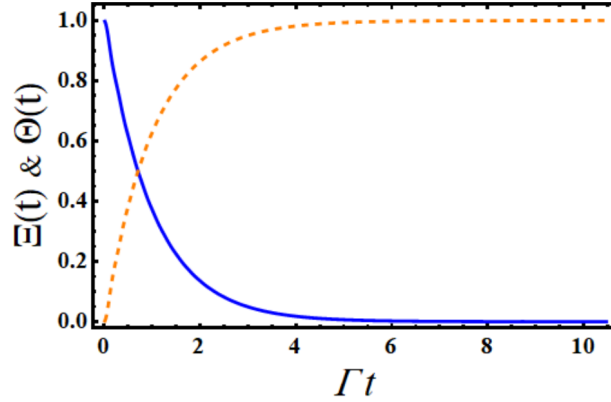


Figure 29 – System and environment excitations $\Xi(t)$ and $\Theta(t)$ in function of Γt for constant coupling.

By substituting Eq. (C.28) in Eq. (C.19) we get

$$\dot{\tilde{\lambda}}(t) = -i\gamma\alpha_0 e^{-(i\Delta\omega_k + \Gamma)t}, \quad (\text{C.29})$$

and therefore

$$\tilde{\lambda}_k(t) = i\alpha_0\gamma \frac{e^{-(\Gamma + i\Delta\omega_k)t} - 1}{\Gamma + i\Delta\omega_k}. \quad (\text{C.30})$$

The quantity $|\alpha(t)|^2$, $|\lambda_k(t)|^2$, and $\sum_{k=1}^N |\lambda_k(t)|^2$ give the system, k -th environment oscillator and entire environment excitations, respectively. We back to use the Schrödinger picture since $|\alpha(t)|^2 = |\tilde{\alpha}(t)|^2$ and $|\lambda(t)|^2 = |\tilde{\lambda}(t)|^2$.

As the total excitation in the global system must be conserved, we have

$$|\alpha_0|^2 = \Xi(t) + \Theta(t), \quad (\text{C.31})$$

where $\Xi(t) = |\alpha(t)|^2$ and $\Theta(t) = \sum_{k=1}^N |\lambda_k(t)|^2$. By analyzing the oscillator's dynamics, one can observe the system excitations being transferred to the environment with an exponential rate Γ . Through exact numerical calculations, we analyzed the dynamic of an environment composed by N oscillators, with $\Gamma = 4\pi\gamma^2 \frac{N}{\Delta\omega} \approx 0.07$ with $\Delta\omega = 1.8$, $\alpha_0 = 3$, $\gamma = 0.1/30$ and $c \approx 0.06$. The plot in Fig. 29 shows that the excitations of the system (blue-solid line) decrease exponentially while the environment excitations (orange-dashed line) increase with the same proportion in total agreement with Eq. C.31.

C.2 Non-Constant coupling: γ and $\bar{\gamma}$

Another interesting case is where only the environment oscillator in resonance with the system (that is, the j -th oscillator whose $\omega_j = \omega_0$) has a different coupling $\bar{\gamma}$, and the rest has the same coupling γ . We shall investigate the case where $\bar{\gamma} \gg \gamma$.

By separating the environment oscillator in resonance with the system, Eqs. (C.18) and (C.19) become

$$\dot{\tilde{\alpha}} = -i\bar{\gamma}\tilde{\lambda}_0(t) - i \sum_k \gamma_k e^{i\Delta\omega_k t} \tilde{\beta}_k(t), \quad (\text{C.32})$$

$$\dot{\tilde{\lambda}}_0(t) = -i\bar{\gamma}\tilde{\alpha}(t) \quad (\text{C.33})$$

$$\dot{\tilde{\lambda}}_k(t) = -i \sum_k \gamma_k e^{i\Delta\omega_k t} \tilde{\alpha}(t), \quad (\text{C.34})$$

where $\lambda_0(t)$ is related to the resonant environment oscillator. By integrating Eq. (C.34) and substituting in Eq. (C.32) we get

$$\dot{\tilde{\alpha}} = -i\bar{\gamma}\tilde{\lambda}_0(t) - \sum_k |\gamma_k|^2 \int_0^t dt' e^{i\Delta\omega_k(t-t')} \tilde{\alpha}(t'). \quad (\text{C.35})$$

By taking the continuum limiting Eq. (C.35) becomes

$$\dot{\tilde{\alpha}} = -i\bar{\gamma}\tilde{\lambda}_0(t) - \int_0^t \int_{\omega_0-\Delta\omega}^{\omega_0+\Delta\omega} dt' d\omega \gamma^2(\omega) \rho(\omega) e^{i\Delta\omega_k(t-t')} \tilde{\alpha}(t'). \quad (\text{C.36})$$

The integral in this equation is related to the non-resonant environment oscillators that have the same coupling. Therefore, once again, we can set $\gamma^2(\omega)\rho(\omega) = c = \text{const.}$ and consider the case where the environment frequencies are concentrated around ω_0 , extending the integral limits to $-\infty$ and ∞ . Thus, we have

$$\dot{\tilde{\alpha}} = -i\bar{\gamma}\tilde{\lambda}_0(t) - c \int_0^t \int_{-\infty}^{\infty} dt' d\omega e^{i\Delta\omega_k(t-t')} \tilde{\alpha}(t'). \quad (\text{C.37})$$

Following the steps of Eqs. (C.25) to (C.27), the differential equation of $\alpha(t)$, $\lambda_0(t)$, and $\lambda_k(t)$ are given by

$$\dot{\alpha} = -i\bar{\gamma}\tilde{\lambda}_0(t) - 2\pi c \tilde{\alpha}(t') \quad (\text{C.38})$$

$$\dot{\tilde{\lambda}}_0 = -i\bar{\gamma}\tilde{\alpha}(t). \quad (\text{C.39})$$

The solution of these differential equations are

$$\tilde{\alpha}(t) = \frac{\alpha_0}{2\Omega} e^{-\pi c t} \left[\pi c \left(e^{-\Omega t} - e^{\Omega t} \right) \Omega \left(e^{-\Omega t} + e^{\Omega t} \right) \right] \quad (\text{C.40})$$

$$\tilde{\lambda}_0(t) = \frac{i\alpha_0\bar{\gamma}}{2\Omega} e^{-\pi c t} \left(e^{-\Omega t} - e^{\Omega t} \right), \quad (\text{C.41})$$

with $\Omega = \sqrt{(\pi c)^2 - \bar{\gamma}^2}$. By substituting these solutions in Eq. (C.34) and solving $\dot{\tilde{\lambda}}_k(t)$ we find

$$\tilde{\lambda}_k(t) = \frac{-i\alpha_0\bar{\gamma}}{2\Omega} \left[\frac{(\pi c + \Omega) \left(1 - e^{-(\pi c + i\Delta\omega + \Omega)t} \right) (\pi c - \Omega) \left(1 - e^{-(\pi c + i\Delta\omega - \Omega)t} \right)}{\pi c + i\Delta\omega + \Omega} \frac{1}{-\pi c - i\Delta\omega + \Omega} \right]. \quad (\text{C.42})$$

Note that for this kind of coupling transfer of excitations will oscillate. By taking the limit $\bar{\gamma} \gg \gamma$, Ω becomes complex, and oscillations can be described in terms of sines and cosines. The excitations of the system will be transferred to the environment with a decay rate Γ with additional oscillating behavior. With the same parameters of Fig. 29 and $\bar{\gamma} = 50\gamma$, we plotted the transfer of excitations in Fig. 30. We can see that even with the total number of excitations conserved, the transfer of excitations oscillates.

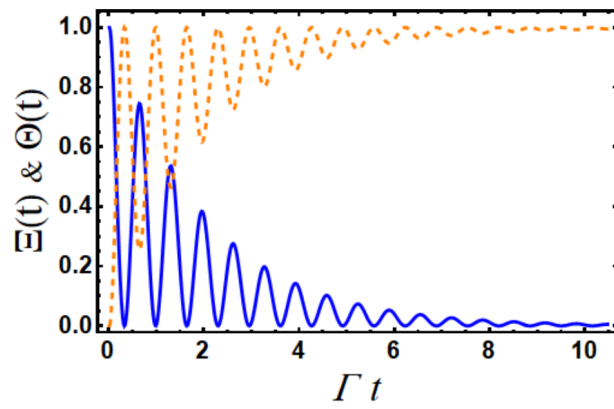


Figure 30 – System and environment excitations $\Xi(t)$ and $\Theta(t)$ in function of Γt for non-constant coupling $\bar{\gamma} = 50\gamma$

APPENDIX D – Many-Body Environment as a Two Level System

A technical problem that arises when dealing with a quantum many-body system is building the density matrix. The larger the number of particles in the system, the more difficult it is to work with the density matrix. Separating a fraction of the system is even more difficult in this case.

Writing the part of the system's interest and complementary part on a qubit basis is an easy trick to fractionate the environment. However, it is necessary to describe the system and all subenvironments on an orthonormal basis.

Consider a two-level system coupled to a many-body environment composed of N particles whose state described as

$$|\Psi\rangle = \frac{1}{\sqrt{2}} (|e, \psi_e\rangle + |g, \psi_g\rangle), \quad (\text{D.1})$$

Where $\{|e\rangle, |g\rangle\}$ are the states of the system and $\{|\psi_e\rangle, |\psi_g\rangle\}$ are the states of the whole environment, and

$$\begin{aligned} |\psi_e\rangle &= |\psi_e^{[1]}, \psi_e^{[2]}, \dots, \psi_e^{[N]}\rangle \\ |\psi_g\rangle &= |\psi_g^{[1]}, \psi_g^{[2]}, \dots, \psi_g^{[N]}\rangle. \end{aligned} \quad (\text{D.2})$$

If we can separate the part of the interest of the complementary part of the environment, we can rewrite the global system as

$$|\Psi\rangle = \frac{1}{\sqrt{2}} (|e, \psi_e^{[I]}, \psi_e^{[c]}\rangle + |g, \psi_g^{[I]}, \psi_g^{[c]}\rangle), \quad (\text{D.3})$$

where $|\psi_e^{[I]}\rangle$ and $|\psi_g^{[I]}\rangle$ are the states of the part of the interest of the environment, and $|\psi_e^{[c]}\rangle$ and $|\psi_g^{[c]}\rangle$ are the states of the complementary part of it.

To get the part of the interest of the environment, we need to trace out the complementary part and the system of the environment. In this case, the density matrix of the global system is

$$\rho = |\Psi\rangle \langle\Psi|, \quad (\text{D.4})$$

and the density matrix of the part of interest in the environment is

$$\begin{aligned} \rho_{f_I} &= \text{Tr}_{S_{f_c}} \rho \\ &= \frac{1}{2} (|\psi_g^{[I]}\rangle \langle\psi_g^{[I]}| + |\psi_e^{[I]}\rangle \langle\psi_e^{[I]}|). \end{aligned} \quad (\text{D.5})$$

To write $|\psi_e^{[I]}\rangle$ and $|\psi_g^{[I]}\rangle$ in an orthonormal basis we need to write them as

$$\begin{aligned} |1'\rangle &= \cos \mu |\psi_e^{[I]}\rangle + e^{i\theta} \sin \mu |\psi_g^{[I]}\rangle \\ |0'\rangle &= -\sin \mu |\psi_e^{[I]}\rangle + e^{i\theta} \cos \mu |\psi_g^{[I]}\rangle, \end{aligned} \quad (\text{D.6})$$

with $\theta \in \mathbb{R}$. To get $\langle \psi_e^{[I]} | \psi_g^{[I]} \rangle = 0$. We need to define

$$\mu = \frac{\pi}{4}, \quad (\text{D.7})$$

and

$$e^{i\theta} = \frac{\langle \psi_e^{[I]} | \psi_g^{[I]} \rangle}{|\langle \psi_e^{[I]} | \psi_g^{[I]} \rangle|}. \quad (\text{D.8})$$

Then we have

$$\begin{aligned} |1'\rangle &= \frac{1}{\sqrt{2}} (|\psi_e^{[I]}\rangle + e^{i\theta} |\psi_g^{[I]}\rangle) \\ |0'\rangle &= \frac{1}{\sqrt{2}} (-|\psi_e^{[I]}\rangle + e^{i\theta} |\psi_g^{[I]}\rangle), \end{aligned} \quad (\text{D.9})$$

and normalizing it, we get

$$\begin{aligned} |1\rangle &= \frac{|1'\rangle}{\sqrt{\langle 1'|1'\rangle}} = \frac{|1'\rangle}{\sqrt{1 + |\langle \psi_g^{[I]} | \psi_e^{[I]} \rangle|}} \\ |0\rangle &= \frac{|0'\rangle}{\sqrt{\langle 0'|0'\rangle}} = \frac{|0'\rangle}{\sqrt{1 - |\langle \psi_g^{[I]} | \psi_e^{[I]} \rangle|}}. \end{aligned} \quad (\text{D.10})$$

In this way, the states $|\psi_{e(g)}^{[I]}\rangle$ can be written as

$$\begin{aligned} |\psi_e^{[I]}\rangle &= S_+ |1\rangle - S_- |0\rangle \\ |\psi_g^{[I]}\rangle &= e^{i\theta} (S_+ |1\rangle + S_- |0\rangle), \end{aligned} \quad (\text{D.11})$$

with

$$S_{\pm} \equiv \sqrt{\frac{1 \pm |\langle \psi_e^{[I]} | \psi_g^{[I]} \rangle|}{2}}. \quad (\text{D.12})$$

To construct the density matrix of the system and interest part on an orthonormal basis, we need first to trace out the complementary part

$$\rho_{sf_I} = \text{tr}_c f_c \rho \quad (\text{D.13})$$

$$= \frac{1}{2} (|g, \psi_g^I\rangle \langle g, \psi_g^I| + |e, \psi_e^I\rangle \langle e, \psi_e^I| + \nu_c |g, \psi_g^I\rangle \langle e, \psi_e^I| + \nu_c^* |e, \psi_e^I\rangle \langle g, \psi_g^I|) \quad (\text{D.14})$$

where $\nu_c = \langle \psi_e^{[c]} | \psi_g^{[c]} \rangle$. Next, describing the states $|\psi_{e(g)}^{[I]}\rangle$ as in (D.11), we get

$$\begin{aligned} \rho &= \frac{1}{2} (S_+^2 |e, 1\rangle \langle e, 1| - S_+ S_- |e, 1\rangle \langle e, 0| + S_+^2 z |e, 1\rangle \langle g, 1| + S_+ S_- z |e, 1\rangle \langle g, 0| \\ &\quad - S_+ S_- |e, 0\rangle \langle e, 1| + S_-^2 |e, 0\rangle \langle e, 0| - S_- S_+ z |e, 0\rangle \langle g, 1| - S_-^2 z |e, 0\rangle \langle g, 0| \\ &\quad S_+^2 z^* |g, 1\rangle \langle e, 1| - S_+ S_- z^* |g, 1\rangle \langle e, 0| + S_+^2 |g, 1\rangle \langle g, 1| + S_+ S_- |g, 1\rangle \langle g, 0| \\ &\quad S_- S_+ z^* |g, 0\rangle \langle e, 1| - S_-^2 z^* |g, 0\rangle \langle e, 0| + S_- S_+ |g, 0\rangle \langle g, 1| + S_-^2 |g, 0\rangle \langle g, 0|), \end{aligned} \quad (\text{D.15})$$

with $z = \nu_c e^{i\theta}$.

With this basis changing, we can get the density matrix of the system and the part of the interest of the environment, and the parameters that we need to know are $|\psi_e^I\rangle$, $|\psi_g^I\rangle$, $|\psi_e^c\rangle$ and $|\psi_g^c\rangle$.